Mechanisms of Fatigue with Aging: Evidence from the Whole-Limb to the Single Cell in Humans

Christopher W. Sundberg
Marquette University

MECHANISMS OF FATIGUE WITH AGING: EVIDENCE FROM THE WHOLE-LIMB TO THE SINGLE CELL IN HUMANS

by

Christopher W. Sundberg, B.S., M.S.

A Dissertation submitted to the Faculty of the Graduate School,
Marquette University,
in Partial Fulfillment of the Requirements for
the Degree of Doctor of Philosophy

Milwaukee, Wisconsin

May 2018

ABSTRACT
MECHANISMS OF FATIGUE WITH AGING: EVIDENCE FROM THE WHOLE-LIMB TO THE SINGLE CELL IN HUMANS

Christopher W. Sundberg, B.S., M.S.

Marquette University, 2018

Aging is accompanied by a loss of muscle mass and increased fatigability of limb muscles making it difficult for old adults to generate the force and power necessary to perform daily activities, such as ascending a flight of stairs. The mechanisms for the age-related increase in fatigability in old and very old adults (≥80 yrs) and whether there are differences between men and women are unknown. The purpose of this dissertation was to determine the mechanisms for the age-related increase in fatigability in men and women by studying fatigue at the level of the whole-limb and within the muscle cells.

Study one compared the fatigability of the knee extensor muscles and determined the mechanisms of fatigue in young, old, and very old men and women elicited by high-velocity exercise. Fatigability of the whole-limb increased across age groups, with no sex differences observed in any age cohort. The age-related increase in power loss was strongly associated with changes in involuntary muscle contractile properties, with minimal contribution from age differences in neural drive. These data suggest the increased fatigability with aging is determined primarily by mechanisms within the muscle for both sexes.

To test whether cross-bridge mechanisms could explain the age-related losses in whole-muscle power and increased fatigability, muscle cells from vastus lateralis biopsies were exposed to conditions mimicking quiescent muscle and fatiguing levels of hydrogen (H^+) and phosphate (P_i). The fatigue-mimicking conditions revealed that H^+ and P_i act synergistically to cause marked reductions in human cross-bridge function. However, other than severe atrophy of fast fibers in old men and women, the effects of the fatigue conditions on cross-bridge function with either severe (study 2) or a range of elevated H^+ and P_i (study 3) did not differ with age. These data suggest that age-related losses in whole-muscle power are due primarily to atrophy of fast fibers, but the age-related increase in fatigability cannot be explained by an increased sensitivity of the cross-bridge to H^+ and P_i. Combined, these studies suggest that interventions targeting the muscle are necessary to mitigate age-related declines in power and increased fatigability in men and women.

ACKNOWLEDGMENTS

Christopher W. Sundberg, B.S., M.S.

There are no words to express the level of appreciation and respect I have for my advisors, Professors Sandra Hunter and Robert Fitts. While your perspectives and scientific approach could not be more different, what unifies you as extraordinary mentors is your passion and love for science, your unwavering devotion to the success of your students, and your willingness to let your students grow and develop their own inquisitive minds. You lead by example and welcome others into your laboratories like we are part of your family. I am especially thankful for your willingness to allow me to pursue projects in both of your labs. There is no doubt that it presented a unique set of challenges, but it provided me with a level of academic training that I believe could not be achieved at any other institution. It goes without saying that without you two I would not be the scientist I am today, and for that, I am forever in your debt.

I would like to thank my committee members, Professor Scott Trappe and Dr. Alexander Ng, for their continued commitment and support throughout this journey. Professor Trappe thank you for your willingness to train a young ambitious graduate student in the muscle biopsy procedure and for the fine hospitality you provided while we visited your lab in Ball State. Dr. Ng thank you for sharing your expertise in spectroscopy with me and always believing in my abilities even when I doubted them. I look forward to working with you both on the projects moving forward.

I am extremely grateful for the Departments of Physical Therapy and Biological Sciences, and for all the members, both past and present, from the Hunter and Fitts labs.

In particular, I would like to thank Bonnie Schlindler-Delap, Drew Kuplic, Jack Senefeld, Jose Delgadillo, Min Kwon, Hamid Hassanlouei, Vianney Rozand, Rita Deering, Lauren Sara, Mitch Adam, and Hugo Pereira from the Hunter lab, and Cassie Nelson, Laura Teigen, Catrina Tegen, Sarea Wang, and Lauren Kelly from the Fitts lab. I would also like to thank Dan Holbus and Tom Dunk for your expertise in designing and fabricating custom equipment, Dr. Robert Prost for sharing your expertise in magnetic resonance imaging and spectroscopy with me, and Dr. Carolyn Smith for assisting with all of the early morning muscle biopsies. This ambitious project and every one of my accomplishments during my time at Marquette were only possible because of all of your hard work and support.

Last but definitely not least, I would like to thank my family, especially my wife, Kelsie, for their loving and enduring support. You made the difficult times seem easy and the triumphant times that much more incredible. The pursuit of a PhD is a daunting task, and you provided me with a level of compassion and generosity that I did not deserve, but will forever remember and appreciate.

TABLE OF CONTENTS

LIST OF TABLES

CHAPTER 2

CHAPTER 3

CHAPTER 4

LIST OF FIGURES

CHAPTER 1

CHAPTER 2

CHAPTER 3

CHAPTER 4

CHAPTER 1

REVIEW OF THE LITERATURE

In the United States, people over the age of 65 make up ~12% of the population but account for astounding 66% of the healthcare budget (Jacobsen *et al.*, 2011). In the next 30 years, the number of old adults is expected to double and make up over 25% of the population – imposing an even greater economic demand on the healthcare system (Jacobsen *et al.*, 2011). According to the Center for Disease Control (2013), a loss of mobility and physical function are the primary determinants for the health and well-being of the old adult population. Thus, discovering the causes for the loss in mobility and ways to mitigate it are at the forefront for improving health and reducing the economic burden on the aging population.

Undoubtedly, a portion of the loss in mobility and physical function occurs due to the age-related loss in muscle mass (Doherty, 2003). However, the age-related loss in muscle strength and power, which are important for mobility, are much greater than would be predicted from the loss in muscle mass alone, suggesting that other factors must play an important role (Reid & Fielding, 2012; Russ *et al.*, 2012; Hepple & Rice, 2016; Hunter *et al.*, 2016). Fatigability of limb muscle, often termed fatigue or muscle fatigue, is one of the factors important for mobility and is characterized by an acute reduction in force and power that occurs in response to prior contractile activity (Debold *et al.*, 2016; Hunter, 2017). Historically, studies on fatigue were conducted through the lens of enhancing athletic performance, but more recently there is recognition that for clinical and aging populations, fatigue can also limit the ability to perform daily activities and

tolerate exercise training (Kent-Braun *et al.*, 2012; Hunter, 2017). Because exercise training is one of the most efficacious remedies to improve healthspan with aging (Seals *et al.*, 2016), and to mitigate the age-related declines in skeletal muscle mass (Law *et al.*, 2016), and mitochondrial, metabolic (Conley *et al.*, 2007; Drake & Yan, 2017), and cardiovascular function (Seals, 2014), identifying the mechanisms of fatigue is important to help design targeted interventions to improve mobility and quality of life in old adults.

The fatigue paradox with aging

A majority of studies on the age-related changes in muscle fatigue have been on isometric contractions and have found that old adults (~60-79 years) are typically *less* fatigable than young adults when performing both maximal (Ditor & Hicks, 2000; Hunter *et al.*, 2008; Callahan *et al.*, 2009) and submaximal isometric contractions (Bilodeau *et al.*, 2001; Kent-Braun *et al.*, 2002; Hunter *et al.*, 2004; Kent-Braun, 2009; Christie *et al.*, 2011; Yoon *et al.*, 2012). Early theories purported that the fatigue resistance during isometric contractions was due, at least in part, to the age-related losses in muscle mass and strength (Kent-Braun *et al.*, 2002; Hunter *et al.*, 2004). Indeed, experiments on young adults have shown that intramuscular pressure increases in proportion to the absolute force produced by the muscle (Sadamoto *et al.*, 1983; Sjogaard *et al.*, 1986; Sjogaard *et al.*, 2004), and can occlude blood flow once the intramuscular pressure exceeds the systolic blood pressure (Barnes, 1980; Sjogaard *et al.*, 1988). Thus, the lower absolute forces produced in old compared to young adults may result in greater perfusion of the muscle with age. Increased muscle perfusion would allow for an augmented delivery of oxygen and substrates to the contracting muscle and a reduced accumulation of metabolic

by-products that have been implicated as important mediators of muscle fatigue (e.g., H^+, P_i, $H_2PO_4^-$). However, this theory was unable to explain the age-related fatigue resistance that continued to persist even when young and old participants were matched for strength (Hunter *et al.*, 2005) or performed isometric contractions under ischemic conditions (Chung *et al.*, 2007; Lanza *et al.*, 2007).

One of the most prominent consequences of human aging is the loss of skeletal muscle mass that occurs due to both the death of motor units and the atrophy of the remaining muscle fibers (Campbell *et al.*, 1973; Lexell *et al.*, 1983; Lexell *et al.*, 1988; Doherty *et al.*, 1993). Although not always observed (Frontera *et al.*, 2000a; D'Antona *et al.*, 2003; Frontera *et al.*, 2008), numerous studies have documented a selective atrophy and decreased proportional area of muscle fibers expressing the fast myosin heavy chain (MHC) II isoform in old compared to young adults (Jakobsson *et al.*, 1990; Klitgaard *et al.*, 1990; Lexell & Taylor, 1991; Coggan *et al.*, 1992; Lexell & Downham, 1992; Hunter *et al.*, 1999; Klein *et al.*, 2003; Trappe *et al.*, 2003). Because fast MHC II fibers have lower oxidative capacity and higher energetic demands than slow MHC I fibers (Schiaffino & Reggiani, 2011), the selective atrophy of fast fibers could theoretically decrease the reliance on glycolysis and increase the relative contribution of oxidative phosphorylation to synthesize ATP in old compared to young adults. The decreased reliance on anaerobic pathways for ATP synthesis would result in a decreased accumulation of metabolic by-products and may explain the age-related fatigue resistance during isometric contractions.

In vivo studies using phosphorus magnetic resonance spectroscopy (^{31}P-MRS) have supported this theory by revealing that during isometric contractions old adults have

an improved energetic cost of contraction and a greater reliance on oxidative metabolism to synthesize ATP compared to young adults (Kent-Braun *et al.*, 2002; Lanza *et al.*, 2005; Lanza *et al.*, 2007; Tevald *et al.*, 2010). The improvement in the energetic cost of contraction with age occurred during both volitional (Kent-Braun *et al.*, 2002; Lanza *et al.*, 2005; Lanza *et al.*, 2007) and electrically-evoked contractions (Tevald *et al.*, 2010) suggesting that the observed differences could not be explained by age-related changes in motor unit recruitment or firing frequencies. Most importantly, the old adults demonstrated a smaller decrease in pH and increase in intracellular $[P_i]$ and $[H_2PO_4^-]$, which was strongly associated with the reductions in force (Kent-Braun *et al.*, 2002; Lanza *et al.*, 2007) and could accurately predict the fatigue resistance with aging (Callahan *et al.*, 2016). Interpreted together, these findings provide compelling evidence that the primary mechanism for the age-related fatigue resistance during isometric contractions is due to a reduced reliance on glycolytic metabolism that results in a blunted accumulation of metabolic by-products in old compared to young adults.

Paradoxically, when old adults perform dynamic contractions, the age-related fatigue resistance is reversed in a velocity dependent manner, with minimal differences observed at slow-to-moderate velocities but an increased fatigability in the old compared with young adults at high-velocities (McNeil & Rice, 2007; Callahan *et al.*, 2009; Dalton *et al.*, 2010; Callahan & Kent-Braun, 2011; Dalton *et al.*, 2012; Yoon *et al.*, 2013; Yoon *et al.*, 2015). The mechanisms for the greater age-related reductions in power during dynamic exercise are unresolved but may be due to changes occurring anywhere along the motor pathway (Fig. 1.1). These mechanisms could range from an inability of the nervous system to adequately drive the muscle (Gandevia, 2001) to impairments in

excitation-contraction coupling and/or cross-bridge function (Fitts, 1994; Allen *et al.*, 2008; Fitts, 2008; Debold *et al.*, 2016).

Recent advances in non-invasive stimulation procedures allow identification of where along the motor pathway the mechanisms of fatigue originate (McNeil *et al.*, 2013; Todd *et al.*, 2016). For example, neural drive from the motor cortex during maximal voluntary contractions can be quantified using the interpolated twitch technique with transcranial magnetic stimulation (TMS) (Todd *et al.*, 2003, 2016). This approach uses a single magnetic pulse delivered over the motor cortex while the participant performs a maximal voluntary isometric contraction (MVC). Any increased force generated by the superimposed stimulus indicates that either not all of the motor units were recruited or the discharge frequencies were not high enough to maximize force summation (Gandevia, 2001). An increase in the amplitude of the superimposed twitch during or immediately following the fatiguing exercise indicates a failure of the nervous system to voluntarily activate the muscle (Gandevia, 2001; Todd *et al.*, 2003, 2016). It has been shown that voluntary neural drive from the motor cortex during and following a fatiguing isometric exercise is reduced and more variable with aging for some muscle groups (Hunter *et al.* 2016). Whether reduced voluntary neural drive from the motor cortex contributes to the age-related increase in fatigability with high-velocity contractions is not known. Additionally, by integrating TMS with measures of surface electromyography (EMG) and electrically-evoked contractions of the motor nerve, we can further localize the origin of fatigue to changes in the excitability of the corticospinal tract (Hunter *et al.*, 2008; Kennedy *et al.*, 2016), neuromuscular propagation (Fuglevand *et al.*, 1993), and/or the contractile properties within the muscle (Fitts, 1994; Kent-Braun *et al.*, 2012). No studies

have integrated these stimulation techniques together to identify the mechanisms for the age-related increased fatigability during high-velocity contractions.

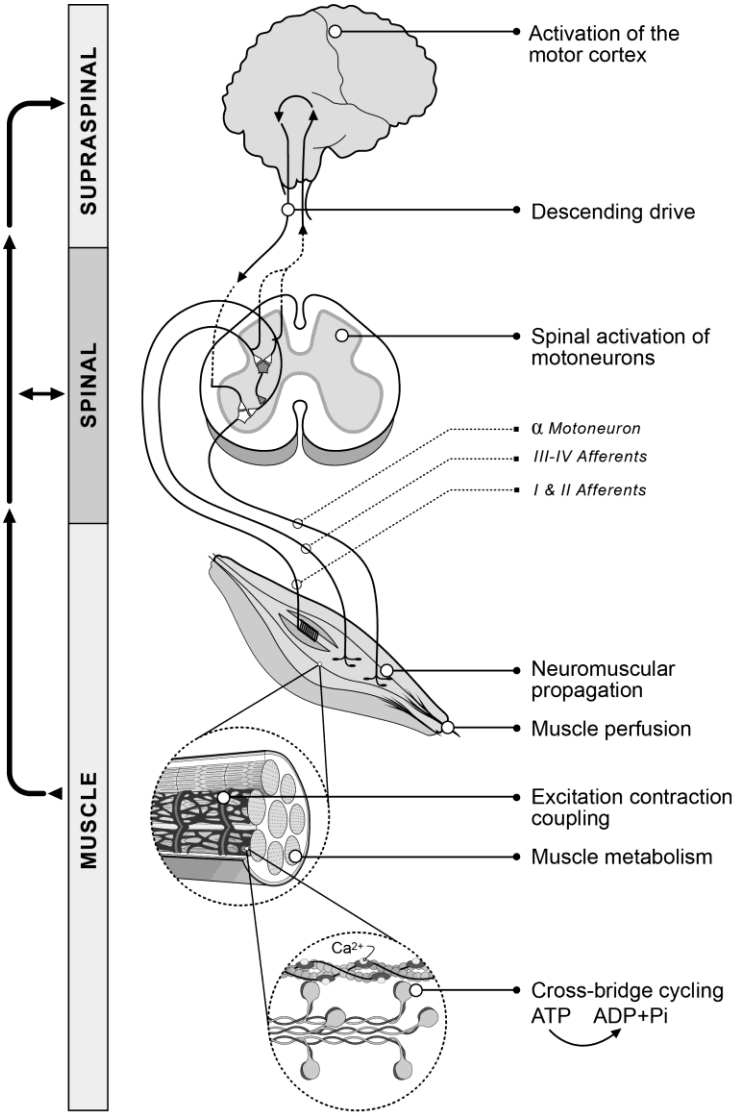

Figure 1.1. Schematic of the potential sites of fatigue along the motor pathway. During volitional contractions, skeletal muscle is activated via signals that originate in the motor cortex of the cerebrum and are transmitted to the α-motoneurons within the ventral horn of the spinal cord. The output of the polydendritic α-motoneuron is determined by the ensemble synaptic input from tens of thousands of both sensory and descending neural pathways. The propagation of the action potential to the neuromuscular junction and into the t-tubule induces a series of cellular responses causing conformational changes in the regulatory proteins of the sarcomere that allow the interaction of myosin and actin to initiate the power stroke. The age-related increased fatigability during dynamic contractions may be due to changes occurring at any location in this complex physiological pathway, which can be probed with non-invasive stimulation procedures. The figure was reprinted from Hunter (2017).

The number of very old adults (i.e., ≥80 yrs of age) is expected to increase over 3-fold by the year 2050 and is currently the fastest growing age demographic globally (United Nations, 2017). Despite this rapid growth, studies on very old adults remain limited and reveal that compared to older adults just 10 yrs younger, very old adults show a blunted hypertrophic response to resistance exercise training (Slivka *et al.*, 2008; Raue *et al.*, 2009), increased instability of neuromuscular transmission (Hepple & Rice, 2016), and an increased prevalence of denervated fibers and fibers coexpressing multiple MHC isoforms (Purves-Smith *et al.*, 2014; Spendiff *et al.*, 2016). Ultimately these age-related changes in the very old adults manifest as an accelerated loss in muscle power and impaired mobility (Reid & Fielding, 2012), and for the ankle dorsiflexor muscles is exacerbated by the increase in fatigability (McNeil & Rice, 2007; Justice *et al.*, 2014). For example, the power loss elicited by high-velocity contractions of the dorsiflexor muscles was greater in a group of very old men (84 yrs) compared to young men (26 yrs), but showed minimal differences between the old (64 yrs) and young men (McNeil & Rice, 2007). Whether this age-related progression in fatigability is observed in a larger muscle group, such as the knee extensor muscles, and/or differs between men and women is not known.

Women currently account for ~54% of the global population in individuals aged ≥60 yrs and ~61% of the population in those aged ≥80 yrs (United Nations, 2017). Despite the large prevalence of women in the aging population, studies aimed at identifying the mechanisms for the age-related increase in fatigability during high-velocity contractions have been conducted only on men and reported that the increased power loss is due primarily to mechanisms within the muscle (McNeil & Rice, 2007;

Dalton *et al.*, 2010, 2012). It is unknown whether the mechanisms for the increased fatigability observed in older women (Callahan & Kent-Braun, 2011; Senefeld *et al.*, 2017) are similar to those observed in older men. However, evidence from cross-sectional studies report that age-related muscle atrophy and the decline in neuromuscular function of the knee extensor muscles are typically more pronounced in old women (Trappe *et al.*, 2003; Kosek *et al.*, 2006; Miller *et al.*, 2013), suggesting that the mechanisms for the age-related increase in fatigability may differ in women compared with men. Understanding the mechanisms of fatigue in the knee extensors of old and very old men and women is important because 1) the knee extensors are more susceptible to age-related losses in function compared with other limb muscles (Hunter *et al.*, 2000; Lanza *et al.*, 2003; Candow & Chilibeck, 2005), 2) the knee extensors of old adults experience fatigue-induced power loss when performing daily activities (Petrella *et al.*, 2005; Foulis *et al.*, 2017), and 3) knee extensor power output and fatigability are associated with functional performance with aging (Bassey *et al.*, 1992; Senefeld *et al.*, 2017).

Thus, the purpose of the first study in this dissertation (chapter 2) was to quantify the fatigability of the knee extensor muscles and identify the mechanisms of fatigue in young (≤35 yr), old (60-79 yr) and very old (≥80 yr) men and women elicited by high-velocity concentric contractions. The primary hypotheses were that 1) the reductions in mechanical power during the fatiguing exercise would progressively increase with age (i.e., fatigability in young < old < very old), but there would be no sex differences in any of the age cohorts, and 2) the increased fatigability in the old and very old men and women would be due primarily to mechanisms originating within the muscle.

Mechanisms of fatigue within the muscle

The leading mechanisms purported to be responsible for the exercise-induced reductions in mechanical power within the muscle are an accumulation of metabolic by-products (i.e., H^+, P_i, $H_2PO_4^-$) that act to both directly inhibit cross-bridge function and to impair excitation-contraction coupling (Fitts, 1994; Allen *et al.*, 2008; Fitts, 2008; Debold *et al.*, 2016). In contrast to the improved energetic cost of contraction observed with aging during isometric contractions (Kent-Braun *et al.*, 2002; Lanza *et al.*, 2005; Lanza *et al.*, 2007; Tevald *et al.*, 2010), the opposite is observed when older adults perform dynamic contractions (Layec *et al.*, 2013; Layec *et al.*, 2014, 2015). For example, there is evidence for an ~37% increase in the ATP cost of contraction during a dynamic plantar flexor exercise in old (~74 yrs) compared to young (~22 yrs) men and women (Layec *et al.*, 2015). The greater ATP demand for a given amount of mechanical power output should theoretically lead to a greater accumulation of metabolic by-products in old compared to young adults, which would explain the age-related increase in fatigability. However, despite the increased energetic cost of generating power with age, the decrease in pH and increase in intracellular [P_i] during the dynamic exercise did not differ or was blunted in the old compared to young adults (Layec *et al.*, 2013; Layec *et al.*, 2014, 2015). These findings suggest that an alternative mechanism within the muscle must be responsible for the increase in fatigability with age. Thus, the purpose of the second (chapter 3) and third studies (chapter 4) of this dissertation was to determine whether cross-bridge mechanisms could explain the age-related increase in fatigability during high-velocity exercise.

Contemporary cross-bridge theory suggests that the chemomechanical transduction of the actin-myosin interaction is partitioned into ~6 structural transitions that make up the full power stroke of the cross-bridge cycle (Geeves *et al.*, 2005; Caremani *et al.*, 2013, 2015; Debold *et al.*, 2016). Displayed in figure 1.2 is a schematic modified from Geeves *et al.* (2005) that depicts the transition steps of the cycle in saturating Ca^{2+}. Briefly, starting in the rigor complex, ATP binds to the catalytic site on myosin and dissociates myosin from actin (step 1). The hydrolysis of ATP reprimes and cocks the myosin head which attaches to actin in a weakly bound state with the hydrolysis by-products still attached in the catalytic site (step 2). In the conventional power stroke, the weakly bound cross-bridge transitions to the strongly bound state through unknown mechanisms (step 3). Inorganic phosphate (P_i) is released from the catalytic site initiating the power stroke where myosin pivots at the light chain domain (step 4). The power stroke continues with an isomerization step where ADP is still attached in the catalytic site (step 5), that is then followed by the release of ADP (step 6). Age-related impairments in any of the steps of the cross-bridge cycle may be responsible for the increased fatigability during dynamic exercise.

In the following paragraphs, the mechanisms of fatigue at the level of the cross-bridge will be reviewed. The focus will specifically be on the data showing the individual and combined effects of elevated concentrations of P_i and H^+, because 1) the reductions in voluntary isometric force during a fatiguing contraction in young and old adults is strongly correlated with the accumulation of these ions (Lanza *et al.*, 2007), and 2) these ions have the most evidence that they cause fatigue by impairing specific steps of the cross-bridge cycle (Fig. 1.2) (Fitts, 1994, 2008; Debold *et al.*, 2016). It is important to

note however, that these ions also affect Ca^{2+} regulation and that other compounds accumulate during intense contractile activity (e.g., ADP, Mg^{2+}, oxidative free radicals, extracellular K^{+}), which are also implicated in fatigue (Fitts, 1994; Allen *et al.*, 2008; Kent-Braun *et al.*, 2012). The following review of the literature focuses primarily on evidence from the chemically skinned fiber preparation, because 1) this preparation can

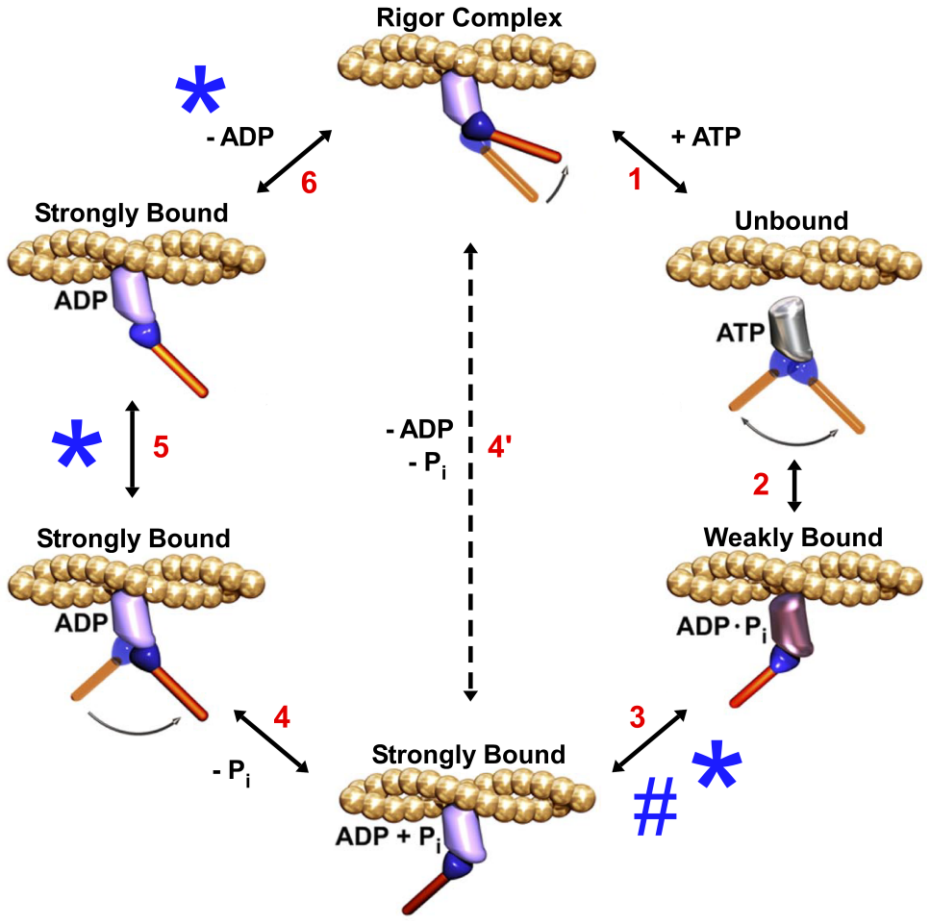

Figure 1.2. Schematic of the cross-bridge cycle and the steps affected by H^{+} and P_i. The conventional cross-bridge cycle is labeled with steps 1-6 starting with the rigor complex. Elevated H^{+} is thought to 1) decrease peak isometric force (P_o) by inhibiting the forward rate constant of the low- to high-force transition (step 3) and 2) slow shortening velocity by inhibiting the ADP isomerization step (step 5) and/or the release of ADP (step 6). Elevated P_i is thought to decrease P_o and contractile economy by forcing the cross-bridge through an unconventional power stroke where myosin detaches early in the low- to high-force transition (step 3) and rapidly releases P_i and ADP (step 4'). Steps affected by H^{+} and P_i are denoted by * and $^{\#}$, respectively. The figure was modified from Geeves *et al.* (2005).

be used in studies on human skeletal muscle, and 2) the preparation permits precise control over the intracellular milieu to systematically study both the individual and collective effects of metabolic by-products while leaving the contractile proteins in the intact sarcomeric state. A majority of this section has been published in a manuscript I coauthored with Professor Robert Fitts and colleagues (Debold *et al.*, 2016).

Effects of intracellular acidosis, H^+

During intense contractile activity, high rates of ATP hydrolysis and increased glycolytic flux generate hydrogen ions (H^+) that causes a reduction in intracellular pH (Robergs *et al.*, 2004). In quiescent human skeletal muscle, intramuscular pH remains at ~7.0 but declines precipitously to between 6.5 and 6.2 during intense volitional contractions (Hermansen & Osnes, 1972; Wilson *et al.*, 1988; Cady *et al.*, 1989; Burnley *et al.*, 2010). These values however, were measured via ^{31}P-MRS or from muscle biopsy samples and represents the spatial average of a heterogeneous mixture of muscle fiber types. Thus, because ATP hydrolysis rates are known to differ considerably between fiber types (Schluter & Fitts, 1994; Schiaffino & Reggiani, 2011), more severe acidic states within individual fibers, particularly fast MHC IIa or IIx fibers, is highly likely. In saturating concentrations of free Ca^{2+}, pH of 6.2 was shown to reduce peak isometric force of rat and rabbit fibers by 4-18% at 30°C (Pate *et al.*, 1995; Knuth *et al.*, 2006) (Fig. 1.3A). This reduction is similar to the 10% decline observed in isolated living mouse fibers at 32°C (Westerblad *et al.*, 1997), but considerably lower than the ~30% reduction observed in skinned rat fibers at 15°C (Knuth *et al.*, 2006). The observation that acidosis depresses peak isometric force even under saturating Ca^{2+} conditions

indicates that the hydrogen ion is acting directly on the cycling cross-bridge. While the precise mechanism remains unresolved, it has been suggested that acidosis reduces peak isometric force by inhibiting the forward rate constant of the low- to high-force state of the cross-bridge cycle (step 3 in Fig. 1.2), which would reduce the force per cross-bridge (Metzger & Moss, 1987, 1990b).

The mitigated effects of pH on peak isometric force at near *in vivo* temperatures compared to colder temperatures has caused considerable debate over the relative importance of acidosis in the fatigue process (Fitts, 2016; Westerblad, 2016). However, the depressive effects of acidosis on cross-bridge function during fatigue extend beyond the direct effects of H^+ on peak isometric force in saturating Ca^{2+}. For example, acidosis also decreases the sensitivity of the myofilaments to Ca^{2+} due, at least in part, to H^+ competitively inhibiting the binding of Ca^{2+} to troponin C (Palmer & Kentish, 1994; Parsons *et al.*, 1997).The reduced myofibrillar Ca^{2+} sensitivity manifests as a rightward shift in the force-calcium relationship and considerably larger reductions in peak isometric force in rat fibers contracting in pH 6.2 and submaximal Ca^{2+} conditions (Nelson & Fitts, 2014). Additionally, acidosis depresses the rate of tension development (k_{tr}) in skinned fibers under submaximal Ca^{2+} conditions as reflected by a reduced k_{tr} following a slack re-extension maneuver at 15°C (Metzger & Moss, 1990b). Given that the myoplasmic free Ca^{2+} is reduced during high-intensity fatiguing contractions (Fitts, 1994; Allen *et al.*, 2008; Allen *et al.*, 2011), the H^+-induced decrements in cross-bridge function under submaximal Ca^{2+} conditions are likely more representative of what occurs during fatigue *in vivo*.

From a human performance and aging perspective, the most important question to consider is how these metabolites influence the ability of the cross-bridge to shorten under submaximal loads and to generate power. In addition to the effect H^+ has on peak isometric force, intracellular acidosis has been shown to reduce both the loaded and unloaded fiber shortening velocities (Knuth *et al.*, 2006; Karatzaferi *et al.*, 2008). For example, maximal rat fiber shortening velocities, determined by the slack test (V_o) and from extrapolation of the force-velocity curve (V_{max}) , were reduced by ~30% and ~16%, respectively, in pH 6.2 saturating Ca^{2+} conditions at 30°C (Knuth *et al.*, 2006) (Fig. 1.3A). The decrements in fiber shortening velocity are thought to be due to slowed myofibrillar ATPase activity (Cooke *et al.*, 1988), secondary to the H^+-mediated reduction in the rate that ADP dissociates from the myosin head (Debold *et al.*, 2012). The effects of acidosis inhibiting both fiber force and velocity resulted in an 18-34% reduction in the peak power of rat fibers at 30º C (Knuth *et al.*, 2006) (Fig. 1.3B). Thus, severe acidosis (pH 6.2) plays an important role in fatigue by acting at multiple steps of the cross-bridge cycle that lead to a reduced myofibrillar Ca^{2+} sensitivity and an impairment in fiber force, velocity and power. Whether the same impairments occur in human skeletal muscle and/or differ between fibers from young and old men and women is not known.

Effects of inorganic phosphate, P_i

Intramuscular concentrations of ATP in quiescent skeletal muscle (~5-6 mmol/kg wet weight) would be depleted rapidly during maximal-intensity contractile activity without the activation of creatine kinase and glycolysis (Sahlin *et al.*, 1998). However,

buffering the fall in intracellular ATP via the creatine kinase reaction results in a rapid decline in phosphocreatine with concomitant increases in inorganic phosphate, P_i, that can reach >30 mM in human skeletal muscle (Wilson *et al.*, 1988; Cady *et al.*, 1989). In saturating Ca^{2+} conditions, 25-30 mM P_i was shown to reduce peak isometric force of rat and rabbit fibers by 5-19% at 30°C (Coupland *et al.*, 2001; Debold *et al.*, 2004) (Fig. 1.3C). Similar to the temperature effects observed in the experiments on acidosis, the reductions in peak isometric force from 30 mM P_i at near *in vivo* temperatures were considerably lower than the ~52% reduction found at 15°C (Debold *et al.*, 2004). Also similar to H^+, elevated P_i caused a rightward shift in the force-calcium relationship, which exacerbated the reductions in peak isometric force at submaximal Ca^{2+} (Debold *et al.*, 2006). However, the observation that the rate of tension development in response to a slack re-extension maneuver of an activated fiber (k_{tr}) is accelerated in the presence of P_i (Wahr *et al.*, 1997; Tesi *et al.*, 2002) but is either not changed or slowed in the presence of H^+ (Metzger & Moss, 1990b) suggests that the mechanisms for the reduction in peak isometric force differs for P_i compared to H^+. Although the mechanisms remain unresolved, it has been suggested that P_i inhibits peak isometric force by reducing the number of high force cross-bridges and/or the force per bridge. The reduction in the number of high force cross-bridges is thought to occur from P_i accelerating the reverse rate constant of the low- to high-force state transition (Palmer & Kentish, 1994). In addition, it has been suggested that P_i induces an unconventional powerstroke (step 4' in Fig. 2.1) where myosin detaches from actin early in the high-force state of the cross-bridge cycle prior to the release of ADP and P_i (Linari *et al.*, 2010; Debold *et al.*, 2013; Caremani *et al.*, 2015). Although all possibilities may be at least partially responsible for

the loss in fiber force, the unconventional powerstrok is the only mechanism currently able to explain the P_i-induced decline in fast fiber contractile economy (i.e., fiber force/myofibrillar ATP turnover) (Linari *et al.*, 2010). The decrements in contractile economy, as a result of decreased fiber force but a maintained myofibrillar ATP hydrolysis rate, would accelerate the accumulation of metabolic by-products and ultimately the development of fatigue.

In contrast to H^+, elevated P_i does not inhibit maximal fiber shortening velocity (V_{max}) at near *in vivo* temperatures (Debold *et al.*, 2004; Karatzaferi *et al.*, 2008) (Fig. 1.3C). However, muscle shortening under a load is more important for athletic prowess and the ability of young and old adults to perform daily activities, and peak fiber power was depressed by 18-26% in 30 mM P_i at 30°C, a somewhat greater decline than observed for peak isometric force alone (Debold *et al.*, 2004) (Fig. 1.3D). This observation is explained by the 30-38% increased curvature in the force-velocity relationship (quantified by the a/P_o ratio), which results in less force generated for any given velocity (Debold *et al.* 2004). Thus, high concentrations of P_i (~25-30 mM) plays an important role in fatigue at the cross-bridge level by inhibiting peak fiber force and power and by decreasing both fiber contractile economy and myofibrillar Ca^{2+} sensitivity.

Combined effects of P_i and H^+

Other than the first few seconds of contractile activity where the intracellular milieu becomes slightly more alkaline from the predominance of ATP generated via the creatine kinase reaction (Adams *et al.*, 1990), intracellular H^+ and P_i accumulate in concert during fatiguing contractions. Thus, in addition to studying the individual effects

of these ions, it's also important to determine their effects in combination to more closely mimic the fatigue environment *in vivo* (Wilson *et al.*, 1988; Burnley *et al.*, 2010). Given that H^+ and P_i appear to influence different sites in the cross-bridge cycle, it's not surprising that the combined effects of these ions act additively to inhibit contractile function at the cross-bridge level. For example, in saturating Ca^{2+}, elevated H^+ (pH 6.2) and P_i (30 mM) depressed peak isometric force in rat slow and fast fibers by 36% and 46%, respectively, at 30°C (Nelson *et al.*, 2014) (Fig. 1.3E). A surprising finding, however, was that the combined condition decreased peak force more than would be predicted from summation of the individual ion effects, which highlights the importance of studying the fatigue-induced effects of multiple metabolites in combination. This observation might be explained, in part, by the increased concentration of dihydrogen phosphate ($H_2PO_4^-$) that occurs in acidic (pH 6.2) compared to neutral conditions (pH 7.0) (Nosek *et al.*, 1987). The dihydrogen phosphate species has been shown to be more closely correlated to the decline in force during *in vivo* fatigue compared with either the monohydrogen phosphate species or pH changes alone (Wilson *et al.*, 1988; Lanza *et al.*, 2007). However, whether dihydrogen phosphate is the dominant fatigue-inducing phosphate species or merely serves as a better marker of the totality of metabolic by-products accumulating within the intracellular milieu remains unknown.

In addition to the combined effects H^+ and P_i have on peak force, these ions also act to synergistically reduce myofibrillar Ca^{2+} sensitivity and peak fiber power. It was recently found in rat fibers that the combined condition of pH 6.2 and 30 mM P_i induced a considerably greater rightward shift in the force-calcium relationship compared to either ion alone (Debold *et al.*, 2006; Nelson & Fitts, 2014). This observation is not

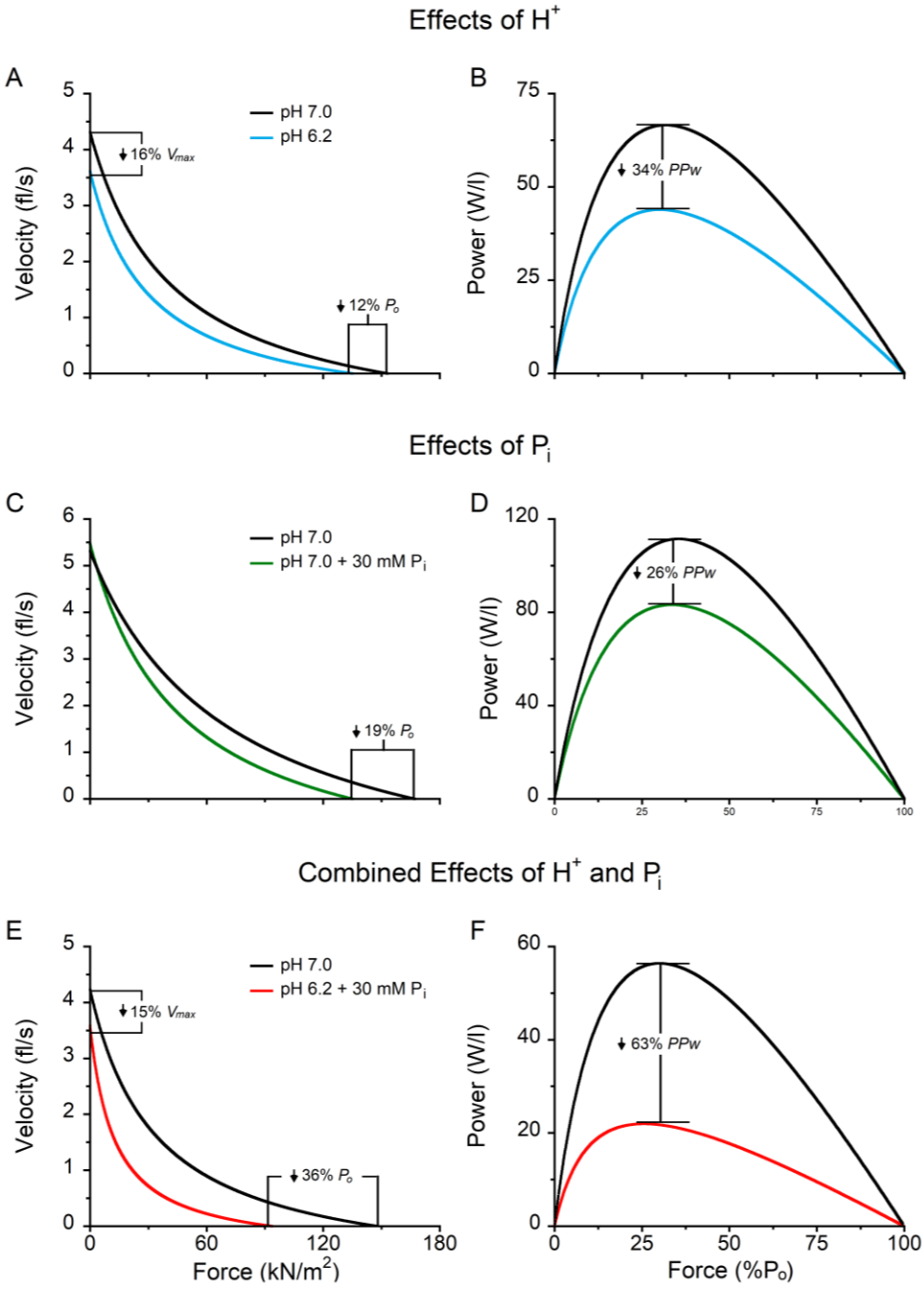

Figure 1.3. The individual and combined effects of H^+ and P_i on force, velocity and power in slow MHC I fibers. Force-velocity and force-power curves obtained from rat MHC I fibers in control pH 7.0 conditions compared to pH 6.2 (A, B), 30 mM P_i (C, D), and combined pH 6.2 + 30 mM P_i (E, F) conditions at 30°C. Shortening velocity (fiber lengths per second) and power (watts per liter) are plotted as a function of the force expressed relative to the fiber cross-sectional area ($kN \cdot m^{-2}$) and as a percentage of the peak isometric force ($\%P_o$), respectively. Error bars around the mean curves have been omitted and displayed only from MHC I fibers for clarity. Findings from fast fibers are qualitatively similar to those presented here. Data were adapted and reprinted from Debold *et al.* (2004), Knuth *et al.* (2006), and Nelson *et al.* (2014), and the figure is published in our recent review (Debold *et al.* 2016).

surprising based on the evidence that the mechanisms for the decreased myofibrillar Ca^{2+} sensitivity differs between P_i and H^+ (Palmer & Kentish, 1994). Importantly, the shift in the force-calcium relationship is more pronounced at 30°C compared to 15°C, suggesting that the decrements in force from these ions may be more important than previously indicated by studies at saturating Ca^{2+}. Furthermore, pH 6.2 and 30 mM P_i conditions reduce peak power in rat and rabbit fibers by 55-63% at 30°C (Karatzaferi *et al.*, 2008; Nelson *et al.*, 2014) (Fig. 1.3F). The large reduction in peak fiber power in this condition is likely explained by the reductions in fiber shortening velocity from H^+ and the inhibition in force from both H^+ and P_i. These reductions in fiber shortening velocity and peak power are further exacerbated when the myosin regulatory light chain (RLC) was phosphorylated (Karatzaferi *et al.*, 2008). The mechanisms for the additional depression with RLC phosphorylation is unknown but is important to identify because high-intensity contractile activity is known to increase RLC phosphorylation (Vandenboom & Houston, 1996; Rassier & Macintosh, 2000).

In summary, H^+ and P_i contribute to fatigue, in large part, both by their direct inhibitory effects on fiber force, velocity, and power and by reducing the sensitivity of the myofilaments to Ca^{2+} – the latter of which is exacerbated at near physiological compared with colder temperatures. Since the accumulation of H^+ and P_i does not differ or is blunted in old compared to young adults during dynamic exercise (Layec *et al.*, 2013; Layec *et al.*, 2014, 2015), it may be that the age-related increase in fatigability is due to an increased sensitivity of the cross-bridge to a given concentration of metabolite accumulation. Thus, the purpose of the studies in chapters 3 and 4 of this dissertation was to test the effects of elevated H^+ and P_i on the contractile mechanics of fibers from young

and old men and women. The primary hypothesis was that the age-related increase in fatigability during dynamic exercise was due, in part, to an increased sensitivity of the cross-bridge to H^+ and P_i. These studies are the first to test the effects of these ions on human skeletal muscle, which differ markedly in their contractile kinetics, fiber type distribution, and metabolic properties compared to rodent muscle (Schiaffino, 2010; Schiaffino & Reggiani, 2011).

Summary of specific aims

Aim 1: Quantify the fatigability of the knee extensor muscles and identify the mechanisms of fatigue in young (≤35 yr), old (60-79 yr) and very old (≥80 yr) men and women elicited by high-velocity concentric contractions. These findings are reported in chapter 2, which is a manuscript recently published in the *Journal of Applied Physiology* (Sundberg *et al.*, 2018).

> *Hypothesis 1*: The reductions in mechanical power during the fatiguing exercise will progressively increase with age (i.e., fatigability in young < old < very old), but there will be no sex differences in fatigability in any of the age cohorts.
>
> *Hypothesis 2*: Mechanisms within both the nervous system and the muscle will contribute to the power loss during the high-velocity fatiguing exercise for all age groups, but the increased fatigability in the old and very old men and women will be due primarily to mechanisms originating within the muscle.

Aim 2: Determine whether cross-bridge mechanisms are contributing to the age-related increase in fatigability.

Aim 2.1: Quantify the effects of a severe fatigue-mimicking condition (pH 6.2 + 30 mM P_i) on the cross-bridge mechanics of fibers from young and old men at 15°C and 30°C. This chapter is also formatted as a manuscript currently in revision in the *Journal of Physiology*.

Hypothesis: The severe fatigue-mimicking condition will elicit greater reductions in maximal shortening velocity and peak power in fibers from old compared with fibers from young men.

Aim 2.2: Quantify the effects of exposing muscle fibers from young and old men and women to a continuum of elevated levels of H^+ and P_i that occur *in vivo*. This chapter is a subset of the data from a study that is still ongoing.

Hypothesis 1: Age-related differences in the H^+- and P_i-induced decrements in fiber shortening velocity and peak power will be more pronounced at low- to moderate-concentrations of these ions compared with the severe fatigue-mimicking condition.

Hypothesis 2: The H^+- and P_i-induced decrements in force, shortening velocity, and peak power will not differ in fibers from men compared with fibers from women.

CHAPTER 2

MECHANISMS FOR THE AGE-RELATED INCREASE IN FATIGABILITY OF THE KNEE EXTENSORS IN OLD AND VERY OLD ADULTS

INTRODUCTION

Human aging is accompanied by a progressive decline in neuromuscular function that can result in functional impairments and a decreased quality of life in older adults. However, the decrements in function that occur with aging can vary depending on the demands of the motor task (Hunter *et al.*, 2016). For example, findings on the age-related changes in fatigability are not uniform across contraction types, such as isometric and dynamic contractions (Christie *et al.*, 2011), or between old (~60-79 yrs) and very old adults (>80 yrs) (McNeil & Rice, 2007; Justice *et al.*, 2014). Paradoxically, many studies have found that old adults (~60-79 yrs) are typically less fatigable than young adults when performing isometric contractions (Christie *et al.*, 2011; Callahan *et al.*, 2016; Hunter, 2017). However, this fatigue resistance appears to reverse with very advanced age (>75-80 yrs) (Justice *et al.*, 2014) and when old adults perform dynamic contractions at moderate- to high-velocities (McNeil & Rice, 2007; Dalton *et al.*, 2010; Callahan & Kent-Braun, 2011; Dalton *et al.*, 2012; Senefeld *et al.*, 2017). The mechanisms for the increased fatigability with aging are not well-understood, particularly among old women or very old adults, but are important to identify in order to develop evidence-based interventions to improve physical function, mobility, and quality of life in old adults.

The aged-related increase in fatigability during high-velocity contractions could be due to any impairment in the neuromuscular system that occurs with aging, including,

cortical atrophy, reduced white matter, and altered brain neurochemistry (Segovia *et al.*, 2001; Marner *et al.*, 2003; Salat *et al.*, 2004; Clark & Taylor, 2011), motor unit remodeling and instability of neuromuscular transmission (Hepple & Rice, 2016; Hunter *et al.*, 2016), or altered bioenergetics, Ca^{2+} handling and cross-bridge kinetics (Miller & Toth, 2013; Layec *et al.*, 2014; Lamboley *et al.*, 2015; Layec *et al.*, 2015; Lamboley *et al.*, 2016). Fortunately, recent advances in non-invasive stimulation procedures allow the identification of the mechanisms of fatigue (Todd *et al.*, 2003, 2016). Thus, the purpose of this chapter was to quantify the fatigability of the knee extensors and identify the mechanisms of fatigue in young (≤35 yr), old (60-79 yr) and very old (≥80 yr) men and women elicited by high-velocity contractions. The first hypothesis was that the reductions in mechanical power during the fatiguing exercise would progressively increase with age (i.e., fatigability in young < old < very old) but that there would be no sex differences in any of the age cohorts. The second hypothesis was that mechanisms within both the nervous system and the muscle would contribute to the power loss during the fatiguing exercise for all age groups, but that the increased fatigability in the old and very old men and women would be due primarily to mechanisms originating within the muscle.

METHODS

Participants and Ethical Approval

One hundred and four individuals participated in this study: 30 young (19-28 yrs, 15 men and 15 women), 62 old (61-79 yrs, 33 men and 29 women), and 12 very old adults (80-93 yrs, 6 men and 6 women). Participants provided written informed consent and underwent a general health screening that included a questionnaire where older participants were excluded if they scored <26 on the mini mental state (Folstein *et al.*,

1975). Participants were healthy, community dwelling adults free of any known neurological, musculoskeletal and cardiovascular diseases. All experimental procedures were approved by the Marquette University Institutional Review Board and conformed to the principles in the Declaration of Helsinki. Anthropometrics and physical activity levels for the participants are reported in Table 2.1.

		Young		Old		Very Old	
Variable	Units	Men (15)	Women (15)	Men (33)	Women (29)	Men (6)	Women (6)
Age*	yr	22.6 ± 2.4	22.6 ± 2.2	70.0 ± 4.6	71.0 ± 5.9	89.0 ± 3.6	83.0 ± 2.6
Height *†	cm	176.8 ± 8.4	164.6 ± 5.5	176.9 ± 8.2	161.2 ± 4.3	176.0 ± 8.3	158.3 ± 6.2
Weight †‡	kg	75.6 ± 10.6	65.1 ± 9.6	84.7 ± 12.1	66.6 ± 12.1	72.3 ± 5.0	72.9 ± 13.3
BMI *	$kg \cdot m^{-2}$	24.1 ± 1.7	24.0 ± 3.2	27.1 ± 3.6	25.6 ± 4.7	25.5 ± 1.7	29.1 ± 4.6
Body Fat *†	%	17.4 ± 3.1	29.6 ± 7.3	30.5 ± 5.5	38.8 ± 7.3	28.7 ± 6.6	41.4 ± 6.3
Physical Activity *	$steps \cdot day^{-1}$	8,623 ± 3,973 (12)	9,825 ± 2,840 (14)	8,510 ± 3,998 (30)	7,825 ± 3,784 (26)	4,590 ± 3,606 (5)	2,654 ± 1,185

Table 2.1. Anthropometrics and physical activity levels of the young, old, and very old men and women. Body fat percentage was measured via dual X-ray absorptiometry (Lunar iDXA, GE, Madison, WI). Physical activity was measured via triaxial accelerometery (GT3X, ActiGraph, Pensacola, FL). The sample sizes (n) for each cohort and certain variables are reported in parentheses. Symbols next to the variable name indicate a significant effect of * age, † sex, or an ‡ age x sex interaction at $P < 0.05$. Values are reported as means ± SD.

Experimental Set Up and Protocol

Participants reported to the laboratory on three occasions, twice for familiarization and once for the experimental session to measure fatigability and the associated mechanisms elicited by high-velocity concentric contractions of the knee extensor muscles.

Experimental Set Up: The experimental setup to measure knee extension torque and velocity was similar to the setup described previously (Hassanlouei *et al.*, 2017). Briefly, testing was performed on the dominant leg of each participant (preferred kicking leg) except when the participant reported a previous surgical procedure, knee or leg pain,

or osteoarthritis of the dominant leg (1 young woman, 2 old women, 3 very old women, 2 old men, and 1 very old man). In all sessions, participants were seated upright in the high Fowler's position with the starting knee position set at 90° flexion in a Biodex System 4 Dynamometer (Biodex Medical, Shirley, NY). The position of the dynamometer was adjusted so that the axis of rotation of the dynamometer's lever arm was aligned with the axis of rotation of the participant's knee. The length of the dynamometer's lever arm was adjusted for each participant and secured with a Velcro strap proximal to the malleoli. Extraneous movements and changes in the hip angle were minimized by securing the participants to the seat with the dynamometer's four-point restraint system. To ensure the measured torques and velocities were generated primarily by the knee extensor muscles, participants were prohibited from grasping any part of the dynamometer with their hands.

Familiarization Sessions: During the familiarization sessions each participant was habituated to electrical stimulation of the femoral nerve and TMS to the motor cortex. Additionally, participants practiced performing brief 2-3 s maximal and submaximal voluntary isometric contractions and maximal voluntary concentric contractions with the knee extensors. The familiarization session also included an assessment of body composition with dual X-ray absorptiometry (Lunar iDXA, GE, Madison, WI).

Experimental Session: The experimental session began with electrical stimulation of the femoral nerve to identify the electrode placement that elicited the maximum peak-to-peak compound muscle action potential (maximum M-wave: M_{max}) of the vastus lateralis (VL), rectus femoris (RF) and vastus medialis (VM). Following the electrical stimulations, participants performed a minimum of 3 brief (2-3 s) knee extension MVCs without stimulation interspersed with 2 knee flexor MVCs. Participants were provided

strong verbal encouragement and visual feedback on their performance with a 56 cm monitor mounted 1-1.5 m directly in front of their line of vision. Each MVC was interspersed with at least 60 s rest, and MVC attempts were continued until the two highest values were within 5% of each other. The highest torque output from the MVCs was used to calculate (1) the target forces for the submaximal isometric contractions needed for optimizing the TMS parameters (i.e., coil placement and stimulator intensity) and, (2) the visual feedback gain in the subsequent MVC trials used to assess voluntary activation.

Once the optimal TMS position and intensity was identified, participants performed five sets of brief isometric contractions (2-3 s per contraction) with the knee extensor muscles to obtain the baseline measures used in identifying the mechanisms of fatigue (Fig 2.1). Each set of contractions included a MVC followed by contractions at 60% and 80% MVC (MVC-60-80%) with TMS delivered at each contraction to estimate the resting twitch amplitude for the calculation of voluntary activation (Todd *et al.*, 2003; Hunter *et al.*, 2006). Single-pulse femoral nerve stimulation was delivered during the MVC and at rest immediately following (<5 s) both the MVC and 80% MVC contractions. Sets of MVC-60-80% contractions were interspersed with at least 2.5 min rest to help ensure repeatable maximal efforts were performed while minimizing residual fatigue from each set. The highest torque output from all MVC attempts was used to calculate the 20% MVC load for the dynamic fatiguing exercise, whereas the median value from the baseline sets of MVC-60-80% contractions was used to identify the mechanisms of fatigue. This approach ensured that each participant's best effort was used to calculate the load for the fatiguing exercise.

Dynamic Fatiguing Exercise: Following the baseline MVC measurements, participants were habituated to performing maximal velocity knee extensions against a 20% MVC load applied by the dynamometer. With this setup, the dynamometer's motor provides a quasi-constant force while allowing velocity to vary. This approach was employed because 1) it more closely mimics common daily activities that require moving an object with constant mass but at different velocities and 2) it allowed participants to generate high mechanical power outputs while still maintaining a full range of motion (ROM) (Dalton *et al.*, 2012). To minimize the effect of the additional braking force applied by the dynamometer at the end of the ROM, the maximum total displacement was set to 95° with the starting position set at 90° knee flexion. A compliant foam pad was placed at ~0° knee flexion, and participants were instructed to kick as fast as possible through the pad to achieve the maximal volitional shortening velocity for every contraction.

For the dynamic fatiguing exercise, participants were verbally cued to kick once every 3 s for a total of 4 min (80 contractions). The low frequency of contractions was selected to maximize muscle perfusion during the exercise by inducing a low muscle duty cycle, i.e., the ratio of the duration of muscle force application to the entire duration between contractions (Broxterman *et al.*, 2014; Sundberg & Bundle, 2015). The average duty cycles were, respectively, 13 ± 1%, 16 ± 1%, and 16 ± 3% for the young, old, and very old adults. The 3% higher duty cycle in the old and very old compared with young adults ($P < 0.001$; $\eta_p^2 = 0.44$) was due to the slower contractile velocities with age ($P < 0.001$; $\eta_p^2 = 0.43$) and not due to differences in the duration between the start of each contraction ($P = 0.116$; $\eta_p^2 = 0.04$). Participants were provided strong verbal

encouragement to generate their maximal effort and to complete the full ROM for every contraction. Upon completion of each contraction, the participant was instructed to relax, and the limb was passively returned to the starting position by the dynamometer. To identify the mechanisms of fatigue induced by the dynamic exercise, two sets of MVC-60-80% isometric contractions were performed in succession as rapidly as possible following the fatiguing exercise with additional sets performed at 2.5, 5 and 10 min following exercise cessation.

Measurements and Data Analysis

Torque and Mechanical Power Output

Torque, position and angular velocity from the dynamometer's transducers were digitized at 500 Hz with a Power 1401 A/D converter and stored online using Spike 2 software [Cambridge Electronics Design (CED), Cambridge, UK]. The torque during each MVC was quantified as the average value over a 0.5 s interval centered on the peak torque of the contraction. The baseline MVC value for each participant was the median torque output recorded from the isometric MVCs during the five sets of MVC-60-80% that were performed prior to the dynamic fatiguing exercise. To compare the changes in MVC between the young, old, and very old men and women following the dynamic exercise, MVC values were expressed as a percentage of the individual-specific baseline MVC value.

For the dynamic fatiguing exercise, contraction-by-contraction mechanical power outputs (W) were calculated as the product of the measured torque (N·m) and angular velocity ($rad \cdot s^{-1}$) and averaged over the entire shortening phase of the knee extension. Because power output increased over the first few contractions in some participants, the

recorded baseline power output for each participant was the highest average obtained from 5 sequential contractions within the first 10 contractions. To quantify the relative reductions in power for each participant, the average power output from the last 5 contractions was expressed as a percentage of the individual-specific baseline power output value.

Electromyography (EMG)

Surface Ag/AgCl EMG electrodes (Grass Products, Natus Neurology, Warwich, RI) were adhered to the skin in a bipolar arrangement overlying the muscle bellies of the vastus lateralis, vastus medialis, rectus femoris, and bicep femoris with an inter-electrode distance of 2.5 cm. The skin was shaved and cleaned with 70% ethanol prior to electrode placement, and the reference electrodes were placed on the patella. Analog EMG signals were amplified (100 X), filtered (13-1,000 Hz band pass, Coulbourn Instruments, Allentown, PA), and digitized at 2,000 Hz with a Power 1401 A/D converter and stored online using Spike 2 software (CED).

Electrical Stimulation

The femoral nerve was stimulated with a constant-current, variable high-voltage stimulator (DS7AH, Digitimer, Welwyn Garden City, Hertforshire, UK) to obtain M_{max} of the vastus lateralis, vastus medialis and rectus femoris. The cathode was placed over the nerve high in the femoral triangle, and the anode was placed over the greater trochanter. Single 200-µs square-wave pulses were delivered with a stimulus intensity beginning at 50 mA and increased incrementally by 50-100 mA until both the unpotentiated resting twitch torque amplitude (Q_{tw}) and M_{max} for all three quadriceps

muscles no longer increased. The intensity was then increased by an additional 20% to ensure the stimuli were supramaximal (range 120-720 mA).

Contractile properties of the knee extensor muscles were quantified with the potentiated resting twitches from the single-pulse femoral nerve stimulations delivered after the MVC and 80% MVC contractions (Fig. 2.1). Stimuli were delivered after both the MVC and 80% MVC contractions to ensure that at least one of the stimuli was delivered while the participant was fully relaxed. The baseline values for each participant were the median obtained from the five sets of MVC-60-80% performed prior to the fatiguing exercise and were reported for the amplitude of the potentiated resting twitch torque (Q_{tw}: N·m), the half relaxation time (ms), and the peak rate of torque development ($Nm \cdot s^{-1}$). The peak rate of torque development was quantified with the derivative of the torque channel as the highest rate of torque increase over a 10 ms interval. To provide an indication of neuromuscular propagation and the ability of the action potential to propagate across the sarcolemma, the peak-to-peak amplitude (M_{max}) and area of the m-wave were reported for all three quadriceps muscles (Fuglevand *et al.*, 1993).

Transcranial Magnetic Stimulation (TMS) & Voluntary Activation

The motor cortex was stimulated by delivering a 1-ms duration magnetic pulse with a concave double-cone coil (110 mm diameter: maximum output 1.4 T) connected to a monophasic magnetic stimulator (Magstim 200^2, Magstim, Whitland, UK). The coil was initially positioned with the center of the coil ~1 cm lateral to the vertex of the motor cortex contralateral to the limb under investigation. The orientation of the coil induced a posterior-to-anterior current flow in the underlying cortical tissue. Identification of the optimal stimulator position was guided by moving along a 1 cm grid drawn on an

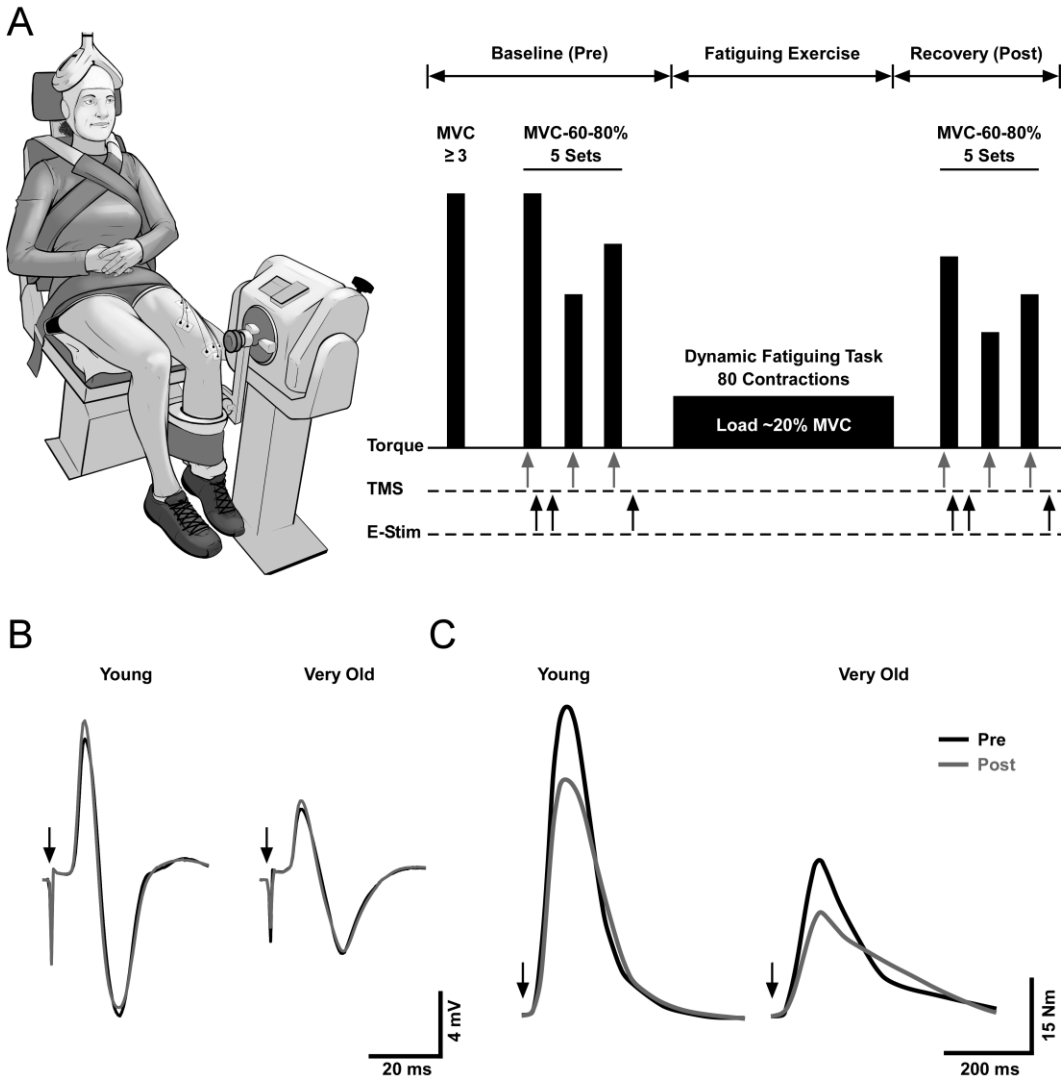

Figure 2.1. Experimental protocol. Schematic of the experimental setup and protocol to measure the fatigability and the mechanisms elicited by high-velocity concentric contractions of the knee extensor muscles (A). Participants performed a minimum of 3 knee extensor MVCs with no stimulations followed by five sets of isometric contractions that included a MVC followed by contractions at both 60 and 80% MVC (MVC-60-80%). TMS to the motor cortex and electrical stimulation to the femoral nerve during the MVC-60-80% contractions are represented by the gray and black arrows, respectively. Following the baseline isometric measurements, participants completed the dynamic fatiguing exercise which consisted of a maximal velocity knee extension performed once every 3 s against a load of ~20% MVC for a total of 4 min (80 total contractions). Two sets of MVC-60-80% isometric contractions were performed in succession as rapidly as possible immediately after the exercise (Post 1 and Post 2), with additional sets completed at 2.5, 5 and 10 min into recovery. The x-axis for the experimental protocol is not to scale, and the timing of the stimuli and contractions are described in detail in the methods. Representative compound muscle action potentials (B) and potentiated resting twitches (C) from before (Pre) and immediately after (Post 1) the fatiguing exercise are displayed for both a young (22 yrs) and very old man (89 yrs).

electroencephalography (EEG) cap and was determined as the location that elicited the greatest motor evoked potential (MEP) in the vastus lateralis while the subject contracted at 20% MVC. This position was marked to ensure repeatable placement of the coil for the remainder of the experiment.

Once the optimal stimulator position was determined, the stimulator intensity for the voluntary activation measurements was identified during brief (2-4 s) isometric contractions at 40% MVC. Single pulse TMS was delivered during each contraction with an intensity starting at 50% stimulator output and increased incrementally by 10% until the peak-to-peak MEP amplitude of the vastus lateralis failed to increase further or began to decrease. If the latter occurred, then the stimulator output was reduced in 5% decrements until the largest peak-to-peak MEP amplitude was achieved in the vastus lateralis. The intensity eliciting the largest MEP was compared to the intensity eliciting the largest twitch torque at the 40% MVC to verify that the stimulator intensities were approximately similar. This additional step ensured that the stimulus intensity did not elicit large activation of the antagonist muscles. This method was used instead of quantifying the biceps femoris MEP amplitude (%M_{max}) because of the difficulty of maximally stimulating the sciatic nerve with surface electrical stimulation. It should also be noted that the knee flexor MVC was on average only 38 ± 8 % of the knee extensor MVC at the 90° knee flexed position. Thus, the effect of any inadvertent activation of the antagonist muscle group on measurements of voluntary activation would be diminished due to the positioning of the participant.

Voluntary activation was quantified from each set of MVC-60-80% contractions based on the technique originally developed for the elbow flexors (Todd *et al.*, 2003) and

later for the knee extensors (Sidhu *et al.*, 2009). Briefly, single pulse TMS was delivered during the MVC, 60% and 80% MVC contractions, and the amplitude of the superimposed twitch torque measured for each contraction. A linear regression was performed between the superimposed twitch torque and the voluntary torque to obtain an estimated resting twitch by extrapolating the regression to the y-intercept (Fig. 2.2).The resting twitch evoked by TMS was estimated rather than measured directly, because the excitability of the corticospinal tract increases markedly from rest to maximal activation (Di Lazzaro *et al.*, 1998). Any 3-point regression with an $R^2 < 0.8$ (Hunter *et al.*, 2006) was excluded from the voluntary activation calculations using *eq. 1* but was still included in the calculations using *eq. 2*. This occurred in 9.7% of the baseline measurement MVC-60-80% sets, 16.0% of the 2 sets performed immediately after the fatiguing exercise, and 10.1% of the 3 sets performed in recovery. In addition, we were unable to obtain estimated resting twitches during either the baseline or following the fatiguing exercise from one old woman. As a result, to ensure all participants were included in the analysis and to provide comparison of the data to all other studies that have used TMS for voluntary activation, we quantified voluntary activation for each set of MVC-60-80% contractions in two ways:

$$\text{Voluntary Activation (\%)} = \left(1 - \frac{\text{SIT}}{\text{eRT}}\right) * 100 \qquad \textit{eq. 1}$$

$$\text{Voluntary Activation (\%)} = \left(\frac{\text{SIT}}{\text{SIT + MVC}}\right) * 100 \qquad \textit{eq. 2}$$

where SIT is the amplitude of the superimposed twitch torque elicited by TMS during the MVC, and eRT is the calculated estimated resting twitch torque. The reported baseline voluntary activation for each participant was the median from the 5 MVC-60-80% sets

performed prior to the dynamic exercise. To compare the changes in voluntary activation between the young, old and very old men and women, voluntary activation immediately following the dynamic exercise were compared to the individual-specific baseline values.

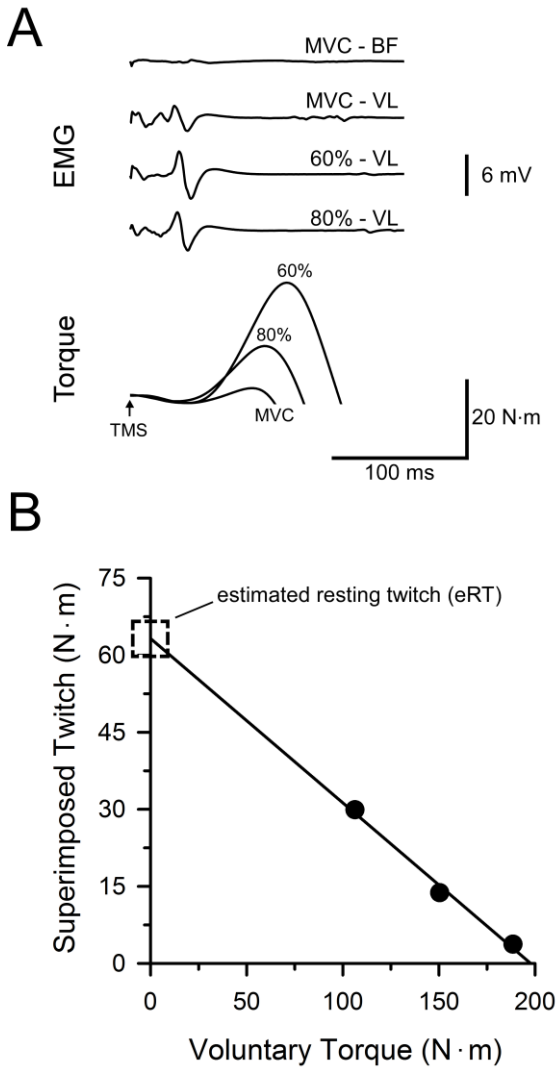

Figure 2.2. Representative data of the method used to assess voluntary activation with TMS. Raw torque and EMG responses evoked by TMS to the motor cortex from a 71 yr old man during the MVC, 60% and 80% MVC contractions (A). The EMG response is depicted for the vastus lateralis (VL) from all three stimuli and for the biceps femoris (BF) from the MVC only. The superimposed twitches are offset and overlaid to depict the amplitude of the twitches from the MVC, 60% and 80% MVC contractions. Linear regressions were performed between the superimposed twitch torque and the voluntary torque to obtain an estimated resting twitch by extrapolating the regression to the y-intercept (B). For comparison of our data set to all other studies that have used TMS to assess voluntary activation, we calculated voluntary activation both with (*eq. 1*) and without the estimated resting twitch (*eq. 2*).

Absolute ($Nm \cdot s^{-1}$) and normalized (s^{-1}) peak rates of torque relaxation were also determined from the TMS delivered during the MVC contractions (Todd *et al.,* 2007). When TMS is delivered to the motor cortex during a MVC, there is a brief transient withdrawal of the descending neural drive following the stimulus that causes the muscle to involuntarily relax. The peak rate of torque relaxation was quantified with the derivative of the torque channel as the greatest rate of torque decrease over a 10 ms interval and was compared before and immediately following the fatiguing dynamic exercise.

Physical Activity (PA) Assessment

Physical activity was quantified for each participant with a triaxial accelerometer (GT3X, ActiGraph, Pensacola, FL) worn around the waist for at least 4 days (2 weekdays and 2 weekend days) as reported previously (Hassanlouei *et al.*, 2017). Participants were provided a PA log and standardized instructions to wear the ActiGraph monitor throughout the course of the day, excluding periods of bathing or sleeping, for a minimum of 4 days. Data were exported at 60 s epochs, analyzed with the Actilife version 6 software (ActiGraph, Pensacola, FL), and recorded as steps per day. Wear time validation was compared to the self-reported activity logs, and data were reported for each participant as long as the accelerometer was worn for a minimum of 3 days (Hart *et al.*, 2011).

Statistical Analyses

Individual univariate analyses of variance (ANOVA) were performed between the subject characteristics and baseline values and age (young, old or very old) and sex (men or women) as the grouping variables. Repeated-measure ANOVAs were performed on

the measures of fatigability (power and MVC torque) and the associated mechanistic measurements (voluntary activation, M-waves, MEPs, and contractile properties) with age (young, old and very old) and sex (men and women) as the between subject factors. The relative changes in mechanical power, MVC, and the mechanistic measurements from the beginning to the end of the fatiguing exercise were also compared with an individual univariate ANOVA with age and sex as the grouping variables. When a significant main effect for age or an interaction was found, pair-wise post hoc comparisons were performed using Tukey's test. Simple linear regression analyses were performed between the reductions in mechanical power and the mechanistic measurements to identify the primary mechanisms of fatigue.

Normal distributions and homogeneity of variance of the data were performed prior to any statistical comparisons and were assessed using the Kolmogorov–Smirnov test and Levene's statistic, respectively. If the assumptions of a normal distribution and/or homogeneity of variance were violated, then the non-parametric Kruskal-Wallis test was performed instead of the univariate ANOVA, with age and/or sex as the grouping variables (e.g., voluntary activation). If the assumptions were violated for the repeated-measure ANOVAs, then the non-parametric Friedman's test was performed (e.g., voluntary activation). All significance levels were set at $P < 0.05$ and all statistics were performed using SPSS (version 24, IBM, Chicago, IL). Because of the large differences in sample sizes between age groups, we report the effect size (η_p^2) along with the p-values. Data are presented as the mean ± standard deviation (SD) in the text and tables and the mean ± standard error of the mean (SE) in the figures.

RESULTS

Mechanical Power Output

The power output at the beginning of the dynamic exercise showed a main effect of age ($P < 0.001$; $\eta_p^2 = 0.51$) and was 97% and 217% higher in the young (245.3 ± 75.7 W) compared to old (124.8 ± 51.7 W; $P < 0.001$) and very old adults (77.3 ± 17.2 W; $P < 0.001$), respectively, and 61% higher in the old compared to the very old ($P = 0.001$) (Fig. 2.3). In addition, the initial power outputs were 64% higher in all men (189.4 ± 86.2 W) compared with all women (115.8 ± 59.2 W; $P < 0.001$; $\eta_p^2 = 0.22$) irrespective of age.

Fatigability (*Reductions in power*): The relative reductions in power from the beginning to the end of the dynamic exercise showed a main effect of age ($P < 0.001$; $\eta_p^2 = 0.19$) and was greater in the very old (44 ± 15%; $P < 0.05$) and old (31 ± 20%; $P < 0.05$) compared to the young (17 ± 12%), and greater in the very old compared to the old ($P < 0.05$) (Fig. 3). However, there were no sex differences in the relative reductions in power ($P = 0.801$; $\eta_p^2 = 0.00$) for the young (men = 17 ± 12%, women = 17 ± 12%), old (men = 30 ± 20%, women = 32 ± 21%) or very old adults (men = 44 ± 16%, women = 44 ± 16%) (Fig. 2.3).

Range of Motion

The total range of motion (ROM) at the beginning of the fatiguing exercise showed a main effect of age ($P < 0.001$; $\eta_p^2 = 0.12$) and was greater in both the young (91.3 ± 2.5°; $P < 0.001$) and the old (89.5 ± 5.3°; $P = 0.007$) compared to the very old adults (86.9 ± 3.4°) but did not differ between the young and old adults ($P = 0.211$).

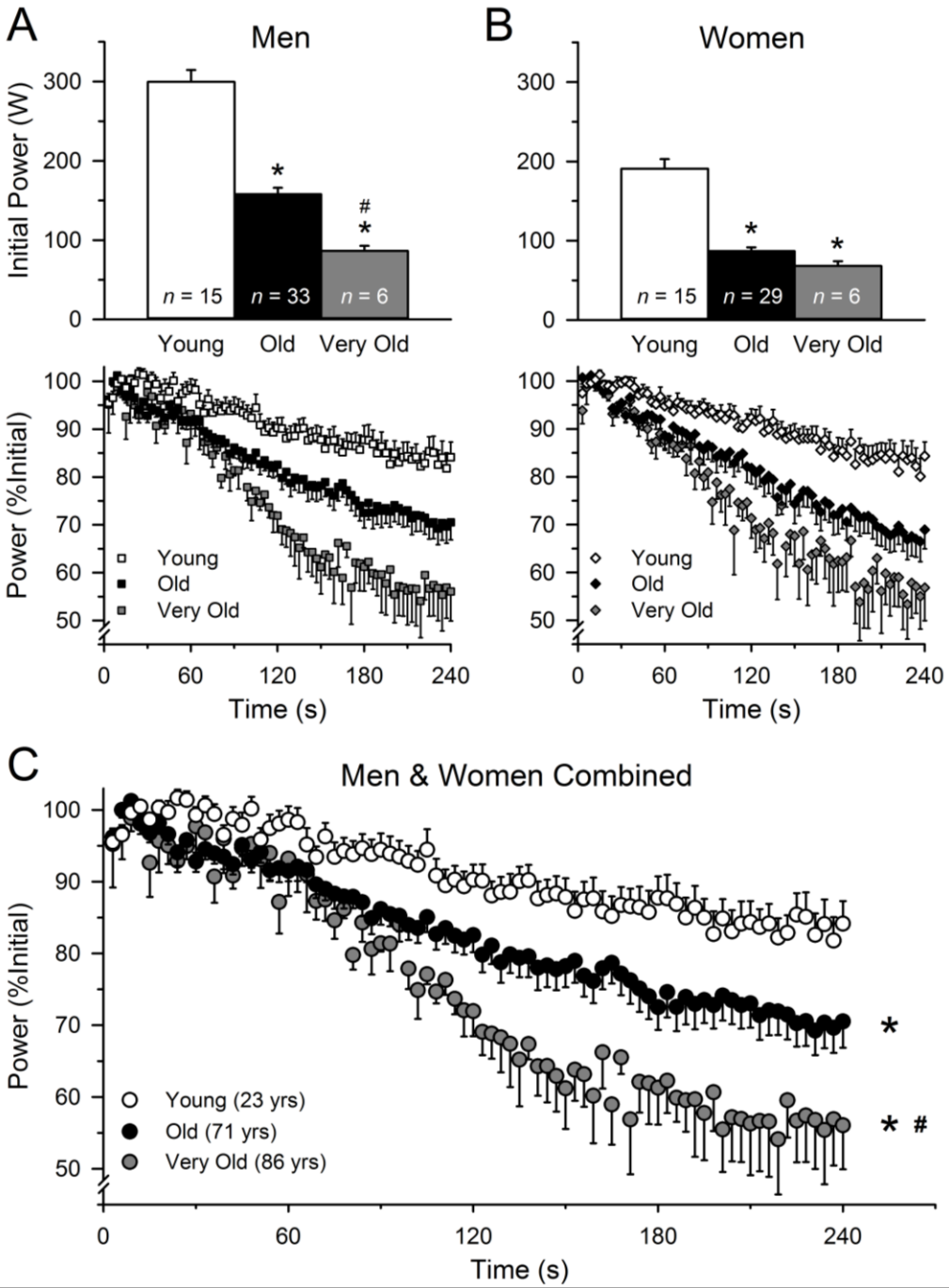

Figure 2.3. Power output during the high-velocity fatiguing exercise. Mean absolute mechanical power outputs and contraction-by-contraction relative power outputs (%Initial) measured from the dynamic fatiguing exercise for the young, old, and very old men (A) and women (B). Because the relative reductions in power did not differ between men and women in any of the three age cohorts ($P > 0.05$), the men and women were combined for the young, old, and very old (C). Fatigability progressively increased with age, so that the least amount of relative power loss occurred in the young adults and the most occurred in the very old adults. *significantly different from young and $^{\#}$significantly different from old ($P < 0.05$). Values are means ± SE.

There were also no sex differences in the ROM at the beginning of the dynamic exercise between the men (89.9 ± 4.2°) and women (89.6 ± 5.0°; $P = 0.755$; $\eta_p^2 = 0.00$).

However, the ROM at the end of the dynamic exercise was lower than at the start of the exercise by 1.8 ± 2.1° in the young ($P < 0.001$; $\eta_p^2 = 0.60$), 7.7 ± 8.6° in the old ($P < 0.001$; $\eta_p^2 = 0.51$), and 17.7 ± 8.6° in the very old adults ($P = 0.001$; $\eta_p^2 = 1.00$). The reductions in the ROM over the course of the fatiguing exercise showed a main effect of age ($P < 0.001$; $\eta_p^2 = 0.25$) and were greater in the old and very old compared to the young adults ($P < 0.001$) and in the old compared to the very old ($P < 0.001$) but did not differ between the men (7.1 ± 9.8°) and women (7.3 ± 8.3°; $P = 0.675$; $\eta_p^2 = 0.00$).

MVC Torque Output

Baseline isometric MVC torque outputs obtained from the five sets of MVC-60-80% contractions showed a main effect of age ($P < 0.001$; $\eta_p^2 = 0.41$) and were 67% and 145% higher in the young (223.8 ± 74.8 N·m) compared to the old (134.2 ± 48.1 N·m; $P < 0.001$) and very old adults (91.2 ± 28.8 N·m; $P < 0.001$), respectively, and 47% higher in the old compared to the very old ($P = 0.003$) (Fig. 2.4). Additionally, the MVC torque outputs were 61% higher in all men (189.9 ± 73.3 N·m) compared with all women (117.6 ± 47.4 N·m; $P < 0.001$; $\eta_p^2 = 0.32$) irrespective of age.

Fatigability (*Reductions in MVC torque*): All cohorts (young, old and very old men and women) had a significant reduction in their MVC torque following the dynamic fatiguing exercise ($P < 0.001$; $\eta_p^2 = 0.86$) (Fig. 2.4). However, the relative reductions in MVC immediately following the exercise (Post 1) were not different between the age groups (young = 22 ± 6%, old = 24 ± 10%, very old = 24 ± 12%; $P = 0.665$; $\eta_p^2 = 0.01$) or between men (24 ± 9%) and women (23 ± 10%; $P = 0.680$; $\eta_p^2 = 0.00$). There were also

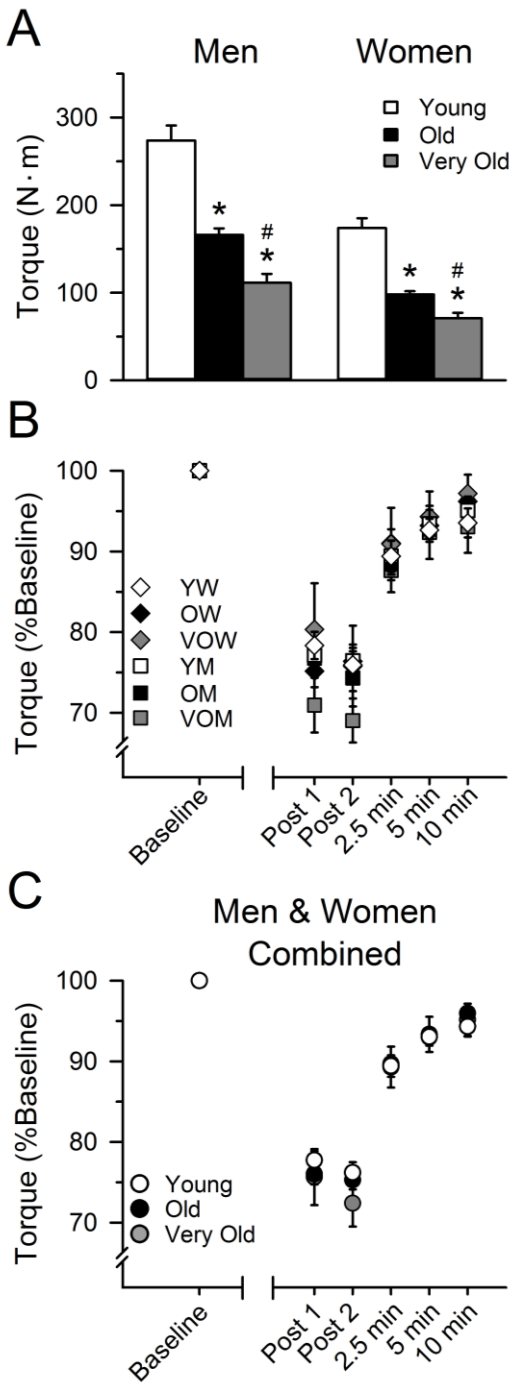

Figure 2.4. MVC isometric torque output before and after the high-velocity fatiguing exercise. Absolute isometric torque outputs prior to the dynamic fatiguing exercise progressively decreased with age and were greater in men compared to women (A). The relative loss in isometric torque immediately following the fatiguing exercise (Post 1 & Post 2) and into recovery (2.5, 5 & 10 min) did not differ between the sexes for the young men (YM) and women (YW), old men (OM) and women (OW), nor the very old men (VOM) and women (VOW) (B). Similarly, when the men and women were combined in the three age cohorts, the relative loss in isometric torque did not differ between the age groups at any time point (C). *significantly different from young and #significantly different from old ($P < 0.05$). Values are means ± SE.

no differences in MVC torque (%Baseline) during the recovery measurements based on age (P = 0.192; η_p^2 = 0.03) or sex (P = 0.339; η_p^2 = 0.01) (Fig. 2.4). Because no age or sex differences were observed in recovery, we restricted our analyses of the mechanistic measurements to those performed immediately following the fatiguing exercise (Post1).

Voluntary Activation

Baseline voluntary activation from the five sets of MVC-60-80% contractions and calculated with the estimated resting twitch (*eq. 1*) were not different between the age groups (young = 98 ± 2%, old = 97 ± 3%, very old = 95 ± 7%; P = 0.317; η_p^2 = 0.02) or between men (97 ± 3%) and women (97 ± 4%; P = 0.835; η_p^2 = 0.00). Of the initial 103 participants with baseline voluntary activation measurements, 7 participants (1 young woman, 3 old women, 3 old men) were excluded from the post-fatiguing exercise comparisons due to an inability to obtain a reliable estimated resting twitch (i.e., 3-point regression $R^2 < 0.80$). As a result, the calculations from *eq. 2* were used to test whether voluntary activation changed immediately following the fatiguing dynamic exercise.

Similar to the data from *eq. 1*, baseline voluntary activation calculated with the superimposed twitch (*eq. 2*) did not differ between age groups (P = 0.052; η_p^2 = 0.06) or between men (0.7 ± 1.0%) and women (0.9 ± 1.6%; P = 0.761; η_p^2 = 0.00) (Table 2.2). The ability to voluntarily activate the muscle following the fatiguing exercise (Post 1) did not change compared to baseline in the young men (P = 0.564; η_p^2 = 0.02) or women (P = 0.109; η_p^2 = 0.18), very old men (P = 0.414; η_p^2 = 0.13) or women (P = 0.655; η_p^2 = 0.04), or the old men (P = 1.000; η_p^2 = 0.00). However, the superimposed twitch (%) increased compared to baseline in the old women (P = 0.023; η_p^2 = 0.18) indicating a reduction in the ability to volitionally activate the muscle (Fig. 2.5). Regression analyses with all

participants included, revealed no association between the relative reductions in power and changes in voluntary activation (r = 0.191, *P* = 0.053).

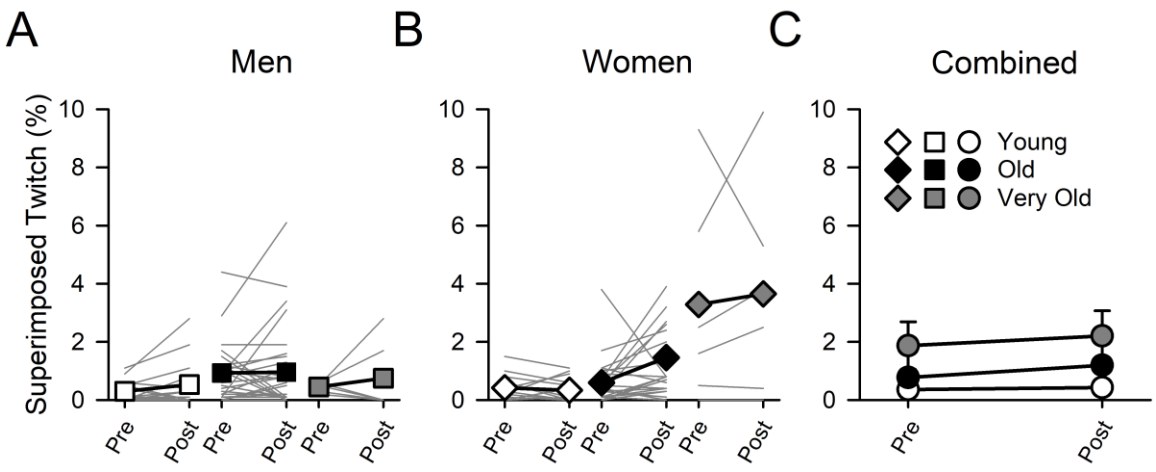

Figure 2.5. Voluntary activation from the motor cortex before and immediately after the high-velocity fatiguing exercise. Voluntary activation (*eq. 2*) measured with TMS delivered to the motor cortex before (Pre) and immediately following the fatiguing exercise (Post 1) for men (A) and women (B). Group means for each age cohort are depicted by the black outlined symbols, while the individual data are depicted by the gray lines. Because voluntary activation did not differ between men and women (*P* > 0.05), the men and women were combined for the young, old, and very old (C). Baseline voluntary activation did not differ between the age groups (*P* > 0.05) and did not change compared to baseline immediately following the fatiguing exercise (Post 1). Values for each group are means ± SE. Error bars are omitted in panels A and B and are obscured by the symbols for the young and old in panel C.

M-waves & MEPs

Baseline M-wave peak-to-peak amplitudes (M_{max}) and areas for the VL, VM and RF are presented in Table 2.2. Because the changes in the VL, VM and RF M-wave areas and M_{max} following the fatiguing exercise were similar, we only report the data for the VL. The VL M-wave area immediately following the fatiguing exercise (Post 1) increased compared to baseline for the young (pre = 84.2 ± 17.8 mV·ms, post = 86.1 ± 17.9 mV·ms; *P* = 0.003; η_p^2 = 0.27), old (pre = 58.5 ± 19.4 mV·ms, post = 62.9 ± 19.5

mV·ms; $P < 0.001$; $\eta_p^2 = 0.40$), and very old (pre = 42.3 ± 17.5 mV·ms, post = 45.1 ± 18.2 mV·ms; $P = 0.021$; $\eta_p^2 = 0.40$) (Fig. 2.6), but the relative changes did not differ between the age groups ($P = 0.103$; $\eta_p^2 = 0.05$) or between the sexes ($P = 0.785$; $\eta_p^2 = 0.00$). The VL M_{max} immediately following the fatiguing exercise increased compared to

		Young (≤35 yrs)		Old (60-79 yrs)		Very Old (≥80 yrs)	
Variable	Units	Men (15)	Women (15)	Men (33)	Women (29)	Men (6)	Women (6)
Electrical Stimulation							
Twitch Torque - Q_{tw} *†	N·m	58.8 ± 17.0	37.2 ± 9.6	46.7 ± 12.1	29.6 ± 6.4	35.6 ± 6.8	22.8 ± 4.6
Rate of Torque Dev. *†	$Nm \cdot s^{-1}$	1,270 ± 373	800 ± 216	945 ± 260	584 ± 132	675 ± 73	440 ± 107
Norm. Rate of Torque Dev.*	s^{-1}	21.6 ± 2.1	21.7 ± 3.4	20.2 ± 1.9	19.8 ± 1.6	19.3 ± 2.6	19.2 ± 1.9
1/2 Relaxation Time *†‡	ms	69 ± 14	77 ± 14	70 ± 12	100 ± 31 (27)	78 ± 22	76 ± 20
VL M_{max} Amplitude *†	mV	18.1 ± 2.1	11.9 ± 2.5	10.5 ± 3.6	7.1 ± 3.1	7.8 ± 2.3	3.8 ± 1.8
VL M-wave Area *†	mV·ms	98.1 ± 10.9	70.3 ± 11.3	67.8 ± 17.6	47.8 ± 15.6	53.5 ± 12.3	31.1 ± 14.8
VM M_{max} Amplitude*†	mV	18.9 ± 4.3	15.8 ± 3.2	14.2 ± 3.5	9.6 ± 3.1	10.0 ± 2.8	7.3 ± 1.2
VM M-wave Area*†	mV·ms	119.1 ± 33.6	100.7 ± 22.7	92.1 ± 20.6	64.6 ± 22.8	76.1 ± 20.2	59.3 ± 7.2
RF M_{max} Amplitude*†	mV	9.9 ± 2.3	7.0 ± 1.6	6.4 ± 1.9	4.1 ± 1.7	4.5 ± 2.3	2.1 ± 1.4
RF M-wave Area*†	mV·ms	54.6 ± 10.1	38.1 ± 8.2	37.5 ± 9.8	24.1 ± 8.0	28.5 ± 13.9	13.6 ± 9.3
Transcranial Magnetic Stimulation							
Voluntary Activation (*eq. 1*)	%	97.9 ± 1.9	97.4 ± 2.4	96.3 ± 3.7	97.2 ± 2.9	97.7 ± 0.5	90.8 ± 8.7 (5)
Voluntary Activation (eq. *2*)	%	0.3 ± 0.4	0.4 ± 0.4	0.9 ± 1.2	0.6 ± 0.7	0.5 ± 0.2	3.3 ± 3.6
Estimated Resting Twitch*†	N·m	37.6 ± 13.9	25.9 ± 10.6	32.3 ± 12.8	18.9 ± 7.0	20.5 ± 4.0	17.7 ± 9.8 (5)
Peak Relaxation Rate*†	$N \cdot m \cdot s^{-1}$	–2,840 ± 784	–1,534 ± 388	–1,330 ± 471	–628 ± 181	–1,029 ± 309	–546 ± 179
Norm. Peak Relaxation Rate*†	s^{-1}	–10.5 ± 1.3	–9.0 ± 1.4	–8.1 ± 1.7	–6.5 ± 1.6	–9.1 ± 1.5	–7.7 ± 2.5
VL MEP_{max} *	$\%M_{max}$	37.0 ± 9.6	38.0 ± 9.8	27.7 ± 8.3	26.8 ± 8.9	29.0 ± 8.0	39.9 ± 18.7
VM MEP_{max} *	$\%M_{max}$	44.8 ± 13.6	39.1 ± 11.8	32.0 ± 11.7	30.3 ± 11.1	35.1 ± 12.6	43.6 ± 18.5
RF MEP_{max} *	$\%M_{max}$	51.7 ± 10.7	51.9 ± 7.7	40.9 ± 10.7	37.2 ± 10.5	39.9 ± 10.4	51.2 ± 16.8
VL Silent Period	ms	222 ± 47	237 ± 56	266 ± 55 (31)	237 ± 59 (28)	219 ± 31	248 ± 74 (3)

Table 2.2. Baseline neuromuscular performance measures from the young, old, and very old men and women. Variables from electrical stimulation to the femoral nerve were the median values from the stimuli delivered at rest following the MVC and 80% MVC contractions (see Fig. 2.1). M_{max} for the vastus lateralis (VL), vastus medialis (VM), and rectus femoris (RF) was the peak-to-peak maximal compound muscle action potential amplitude. Variables from TMS the motor cortex were the median values from the five sets of MVC-60-80% performed prior to the dynamic exercise. The peak-to-peak MEP amplitudes (MEP_{max}) from the TMS during the MVC were expressed relative to the M_{max} ($\%M_{max}$) obtained from the electrical stimulation delivered during the MVC. The sample sizes (*n*) for each cohort and certain variables are reported in parentheses. Symbols next to the variable name indicate a significant effect of * age, † sex, or an ‡ age x sex interaction at $P < 0.05$. Values are reported as means ± SD.

baseline in the old (pre = 8.9 ± 3.8 mV, post = 9.5 ± 3.7 mV; $P < 0.001$; $\eta_p^2 = 0.30$) but did not change in the young (pre = 15.0 ± 3.9 mV, post = 15.0 ± 3.8 mV; $P = 0.738$; $\eta_p^2 =$

0.00) or very old adults (pre = 5.8 ± 2.9 mV, post = 5.9 ± 2.7 mV; P = 0.490; η_p^2 = 0.04). Accordingly, the relative change in the VL M_{max} showed a main effect of age (P = 0.024; η_p^2 = 0.07) and was greater in the old (8.3 ± 14.5 %) compared to the young (0.4 ± 4.5 %; P = 0.016) but did not differ between the young and very old (4.0 ± 15.2 %; P = 0.691), the old and very old (P = 0.515), nor between the men (4.1 ± 2.1 %) and women (4.2 ± 2.2 %; P = 0.965; η_p^2 = 0.00). Regression analyses revealed no association between the relative reductions in power and the changes in the VL M-wave area (r = 0.168, P = 0.089) or M_{max} (r = 0.122, P = 0.216).

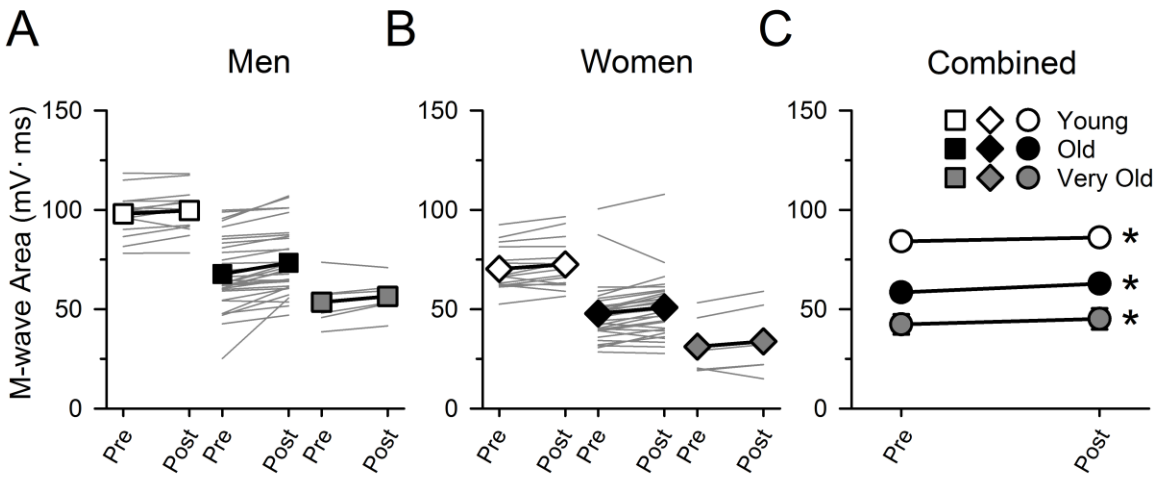

Figure 2.6. Compound muscle action potentials before and immediately after the high-velocity fatiguing exercise. The compound muscle action potential areas (M-wave Area) of the vastus lateralis (VL) measured before (Pre) and immediately following the fatiguing exercise (Post 1) for men (A) and women (B). Group means for each age cohort are depicted by the black outlined symbols, while the individual data are depicted by the gray lines. Because the changes in the m-wave area elicited by the fatiguing exercise did not differ between the men and women in any of the three age cohorts (P > 0.05), the men and women were combined for the young, old, and very old (C). The baseline m-wave areas were greater in the young (84.2 ± 17.8 mV·ms) compared to the old (58.5 ± 19.4 mV·ms; P < 0.001) and greater in the old compared to the very old (42.3 ± 17.5 mV·ms; P = 0.003), but the relative increase in the m-wave area following the fatiguing exercise (*, P < 0.05) did not differ between the young, old and very old (P > 0.05). Values for each group are means ± SE. Error bars are omitted in panels A and B and are obscured by the symbols in panel C.

Baseline MEP data for the vastus lateralis (VL), vastus medialis (VM) and rectus femoris (RF) are in Table 2.2. The peak-to-peak MEP amplitudes ($\%M_{max}$) following the fatiguing exercise (Post 1) did not change compared to baseline for the VL (pre = 31 ± 11%, post = 34 ± 12%; $P = 0.054$; $\eta_p^2 = 0.04$), VM (pre = 35 ± 13%, post = 36 ± 14%; $P = 0.915$; $\eta_p^2 = 0.00$) or RF (pre = 44 ± 12%, post = 45 ± 14%; $P = 0.668$; $\eta_p^2 = 0.00$).

Involuntary Contractile Properties

Baseline contractile properties from the electrical stimulation are presented in Table 2.2. The relative decrease in the amplitude of the potentiated twitch (Q_{tw}) following the fatiguing exercise (Post 1) showed a main effect of age ($P = 0.001$; $\eta_p^2 = 0.14$) and was less in the young (-16 ± 17 %) compared to old (-30 ± 19 %; $P = 0.002$) and very old (-35 ± 12 %; $P = 0.005$) but did not differ between the old and very old ($P = 0.562$) or between men (-28 ± 17 %) and women (-24 ± 20 %; $P = 0.139$; $\eta_p^2 = 0.02$) (Fig. 2.7). Similarly, the relative decrease in the rate of torque development showed a main effect of age ($P < 0.001$; $\eta_p^2 = 0.15$) and was less in the young (-16 ± 18 %) compared to old (-33 ± 22 %; $P = 0.001$) and very old (-39 ± 16 %; $P = 0.003$) but did not differ between the old and very old ($P = 0.550$) or between men (-31 ± 20 %) and women (-27 ± 23 %; $P = 0.185$; $\eta_p^2 = 0.02$). Of the 104 participants, 9 participants (6 old women, 2 old men, 1 very old woman) were unable to fully relax for the electrical stimulation after the fatiguing exercise. For the remaining 95 participants (30 young, 54 old, 11 very old), the relative increase in the half relaxation time showed a main effect of age ($P = 0.001$; $\eta_p^2 = 0.14$) and was less in the young (29 ± 28 %) compared to old (67 ± 54 %; $P = 0.002$) and very old (72 ± 59 %; $P = 0.034$) but did not differ between the old and very old ($P = 0.945$) or between men (53 ± 41 %) and women (59 ± 60 %; $P = 0.998$; $\eta_p^2 = 0.00$).

Baseline absolute ($Nm \cdot s^{-1}$) and normalized (s^{-1}) rates of torque relaxation from TMS to the motor cortex are also presented in Table 2.2. The relative decrease in the absolute peak rate of torque relaxation immediately following the fatiguing exercise (Post 1) showed a main effect of age ($P < 0.001$; $\eta_p^2 = 0.19$) and was less in the young (-26 ± 11 %) compared to the old (-40 ± 20 %; $P = 0.002$) and very old (-53 ± 14 %; $P < 0.001$) but did not differ between the old and very old ($P = 0.051$) nor between men (-36 ± 17 %) and women (-29 ± 21 %; $P = 0.754$; $\eta_p^2 = 0.00$). To account for the changes in the MVC torque outputs following the fatiguing exercise, the peak rates of torque relaxation were normalized to each individual's MVC. Similar to the results from the absolute peak rate of torque relaxation, the relative decrease in the normalized peak rate of torque relaxation following the fatiguing exercise showed a main effect of age ($P < 0.001$; $\eta_p^2 = 0.25$) and was less in the young (-6 ± 9 %) compared to the old (-24 ± 20 %; $P < 0.001$) and very old (-35 ± 15 %; $P < 0.001$) but did not differ between the old and very old ($P = 0.122$) nor between men (-19 ± 19 %) and women (-22 ± 20 %; $P = 0.760$; $\eta_p^2 = 0.00$).

Simple linear regression analyses revealed that the relative changes for all the contractile property measurements were significantly associated with the relative changes in mechanical power output during the fatiguing exercise: Q_{tw} ($r = 0.75$; $P < 0.001$), rate of torque development of the Q_{tw} ($r = 0.74$; $P < 0.001$), half relaxation time ($r = -0.47$; $P < 0.001$), absolute peak rate of torque relaxation ($r = 0.64$; $P < 0.001$), and normalized peak rate of torque relaxation ($r = 0.54$; $P < 0.001$). However, the most closely associated variable with the reduction in mechanical power during the fatiguing exercise was the reduction in the potentiated twitch torque amplitude (Q_{tw}) (Fig. 2.7).

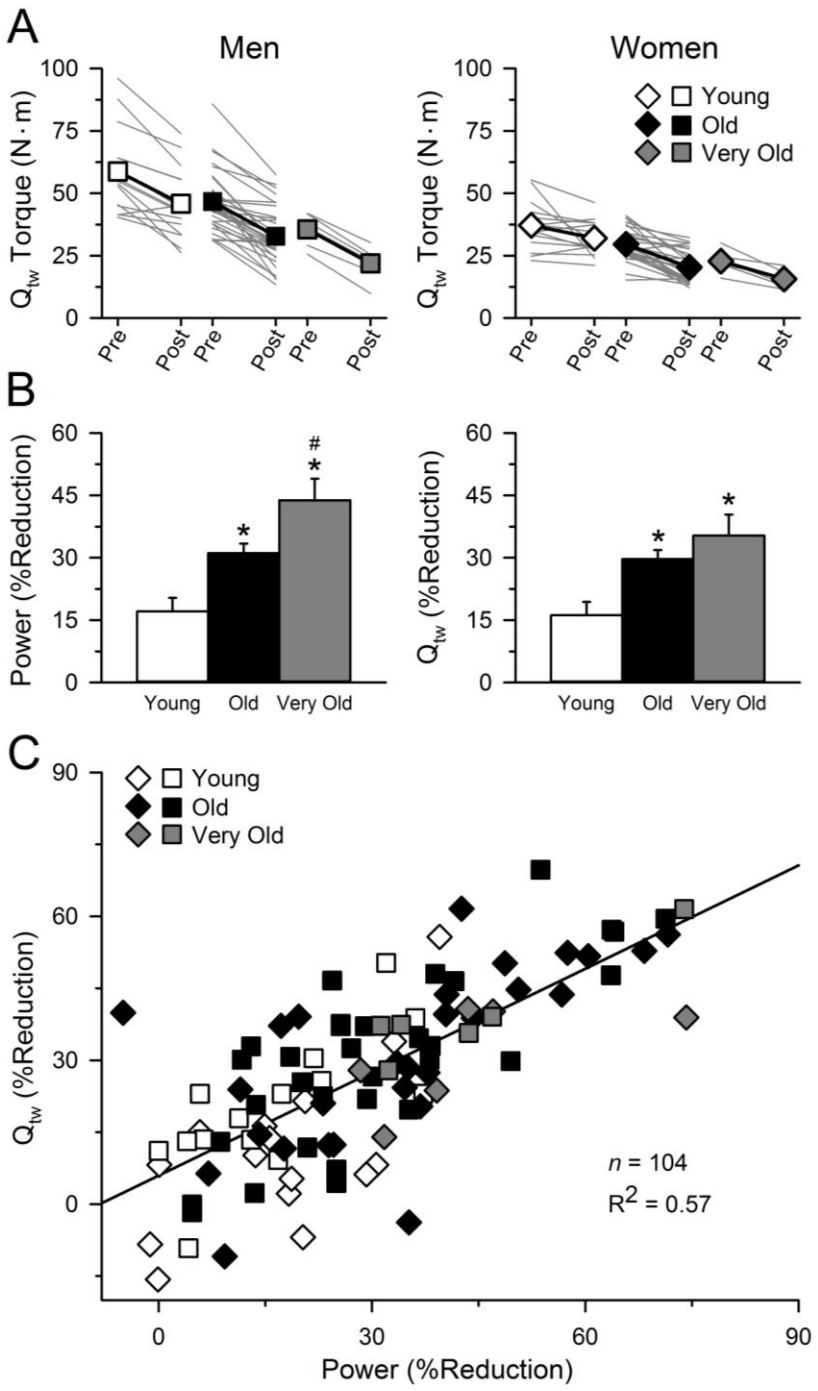

Figure 2.7. Electrically-evoked potentiated twitch amplitudes before and immediately after the high-velocity fatigue exercise. The potentiated twitch torque amplitude (Q_{tw}) measured before (Pre) and immediately after the fatiguing exercise (Post 1) for the young, old, and very old men and women (A). Group means for each age cohort are depicted by the black outlined symbols, while the individual data are depicted by the gray lines. In general, the relative reductions in the Q_{tw} elicited by the fatiguing exercise showed a qualitatively similar trend with aging to the relative reductions in mechanical power (B). Regression analyses revealed that the percent reductions in mechanical power were best predicted by the percent reductions in the Q_{tw} (C). *significantly different from young and #significantly different from old ($P < 0.05$). Values are means ± SE.

DISCUSSION

This chapter determines the fatigability of knee extensor muscles and identifies the primary mechanisms of fatigue in young, old, and very old men and women elicited by high-velocity concentric contractions. We show that aging of the neuromuscular system results in a progressive increase in the fatigability of the knee extensors during high-velocity contractions that is more pronounced in the very old adults (≥80 yrs) and occurs similarly in both men and women (Fig. 2.3). We provide novel evidence that the neural drive from the motor cortex remains near optimal for the young, old, and very old adults but may play a minor role for the increased power loss of the knee extensors in old women (Fig. 2.5). Importantly, the age-related increase in power loss was strongly associated with the changes in the electrically-evoked contractile properties (Fig. 2.7), suggesting that the age-related increase in fatigability during high-velocity contractions was determined primarily by cellular mechanisms that disrupt excitation contraction coupling and/or cross-bridge function.

The progressive age-related increase in fatigability of the lower limb is determined primarily by mechanisms within the muscle

In support of our hypotheses, we found that the power loss of the knee extensors performing a high-velocity fatiguing exercise progressively increased with age from a 17% loss in the young (23 yrs) to a 31% loss in the old (71 yrs) and a 44% loss in the very old adults (86 yrs). Importantly, we also show that the age-related increase in fatigability was similar for both men and women (Fig. 2.3). A portion of the progressive increase in fatigability with aging may be the result of the decreased physical activity levels and increased sedentary behavior that is commonly observed in old compared to

young adults (Martin *et al.*, 2014). Indeed, the physical activity of the very old adults in our study was significantly lower than both the young and old (Table 2.1). However, because the old adults still experienced ~2-fold greater losses in relative mechanical power compared to the young (Fig. 2.3), despite having similar physical activity, it is unlikely that the age differences in fatigability observed here were due to differences in physical activity alone. Furthermore, our results likely underestimate the extent of the increased fatigability with aging, because in addition to the greater reductions in power, there were also greater decrements in the range of motion during the dynamic exercise for both the very old (~18°) and the old (~8°) compared to the young (~2°). The reduced range of motion would ultimately lead to a progressive decrease in the amount of mechanical work (J) performed per contraction throughout the exercise. Thus, incorporating our findings with others (Petrella *et al.*, 2005; McNeil & Rice, 2007; Dalton *et al.*, 2010; Callahan & Kent-Braun, 2011; Dalton *et al.*, 2012; Senefeld *et al.*, 2017) reveals that age-related changes within the neuromuscular system result in an increased fatigability during high-velocity contractions that continually progresses into the latest stages of life and occurs similarly for both men and women (Fig. 2.3).

In testing the mechanisms for the increased fatigability with age, we found that the ability of the motor cortex to volitionally activate the muscle was reduced following the dynamic exercise in only the old women (Fig. 2.5). The exercise-induced reduction in the ability to volitionally activate the muscle, when assessed by delivering TMS to the motor cortex, suggests that suboptimal neural drive from the cortical motor neurons may be contributing to the increased fatigability with age in women. However, this mechanism likely plays only a minor role, because 1) the changes in voluntary activation

were not associated with the relative reductions in power, and 2) the change in voluntary activation following the exercise was highly variable between individuals (Fig. 2.5). There were also no changes in the MEP amplitudes (%M_{max}) when measured during the MVC immediately following the fatiguing exercise, suggesting that the excitability of the corticospinal tract projecting to the quadriceps muscles was unaltered in all three age cohorts. Additionally, our findings are supported by studies on the dorsiflexors (McNeil & Rice, 2007), plantarflexors (Dalton *et al.*, 2010), and knee extensors (Dalton *et al.*, 2012) that found no differences in the ability to voluntarily activate the muscle following high-velocity fatiguing exercises between groups of young and old men. However, it is important to note that methodological limitations make it difficult to evaluate the mechanisms of fatigue during a dynamic contraction. Thus, we must infer that the changes observed in the maximal isometric contractions following the dynamic exercise are an accurate reflection of the voluntary activation during the exercise. Clearly, the fatigue-induced reductions in the isometric MVC rarely coincide directly with the changes in mechanical power (Dalton *et al.*, 2010; Senefeld *et al.*, 2017). Accordingly, the reduction in MVC torque in our study was similar across all three age groups (Fig. 2.4) despite large differences between the groups in the loss of power (Fig. 2.3). Future studies that develop a reliable measurement to test the ability of the nervous system to voluntarily activate the muscle during a dynamic contraction will clarify whether the nervous system is contributing to the increased fatigability with age.

There is growing evidence that the aging process is accompanied by motor unit remodeling and instability of the neuromuscular junction that is exacerbated after the age of ~75-80 yrs (Hepple & Rice, 2016). Thus, it is plausible that the progressive age-related

increase in fatigability during high-velocity exercise is due to impairments in neuromuscular transmission and the excitability of the sarcolemma. To test this possibility, we quantified the changes in the compound muscle action potential (m-wave) area and amplitude of the quadriceps muscles elicited by the high-velocity exercise. Our data however, showed an increase in the m-wave area of the vastus lateralis immediately following the exercise for all three age cohorts that occurred similarly for both the men and women (Fig. 2.6). The mechanisms for the potentiation of the m-wave following a fatiguing exercise are unclear (Rodriguez-Falces & Place, 2017), but we observed no association between the changes in the m-wave and the reductions in power, suggesting that the mechanism for the increased fatigability with age does not involve the neuromuscular junction or the ability of the action potential to propagate across the sarcolemma. These findings are in agreement with the increased m-wave area of the vastus medialis observed in young (~25 yrs) and old men (~74 yrs) following a high-velocity knee extension exercise (Dalton *et al.*, 2012), but in contrast to the decreased m-wave amplitude observed in the soleus of older men (~78 yrs) following a high-velocity plantarflexor exercise (Dalton *et al.*, 2010). The explanation for the disparities between the studies is unclear but may involve the differential effect of aging on these two muscle groups (Candow & Chilibeck, 2005).

In contrast to the limited involvement of the nervous system (Fig. 2.5) or neuromuscular propagation (Fig. 2.6) in explaining the increased fatigability with aging, we found strong support that the progressive age-related increase in power loss during high-velocity exercise was closely associated with mechanisms that disrupt contractile function within the muscle (Fig. 2.7). Specifically, the greater age-related reductions in

mechanical power were closely associated with changes in the involuntary twitch properties elicited by electrical stimulation to the femoral nerve, as well as the peak rates of relaxation elicited by TMS to the motor cortex. The reduction in the electrically-evoked twitch amplitude for example, explained 57% of the variance for the reduction in power during the fatiguing exercise (Fig 2.7). Although the specific cellular and molecular mechanisms cannot be identified by the changes in the involuntary contractile properties, these properties do provide valuable insight to the cellular processes that likely contribute to fatigue (Fitts, 1994; Kent-Braun *et al.*, 2012). For example, the greater slowing of the relaxation rates in the old compared to young adults following the exercise indicate that the mechanism likely involves factors that slows cross-bridge detachment and/or the uptake of Ca^{2+} back into the sarcoplasmic reticulum (Fitts, 1994). Additionally, the greater reductions in the amplitude (Fig. 2.7) and the rates of torque development of the potentiated twitch in the old and very old adults compared to the young suggest that the mechanism also likely involves factors that either 1) decrease the amplitude of the Ca^{2+} transient, 2) reduces the number of cross-bridges formed and/or the amount of force generated per cross-bridge, and/or 3) slows the transition step from the low- to high-force state of the cross-bridge cycle (Fitts, 1994; Allen *et al.*, 2008; Debold *et al.*, 2016).

The leading cellular mechanisms purported to be responsible for the exercise-induced reductions in mechanical power within the muscle are an accumulation of metabolic by-products (i.e., H^+, P_i, $H_2PO_4^-$) that act to both directly inhibit cross-bridge function (Fitts, 2008; Debold *et al.*, 2016) and to impair excitation-contraction coupling (Fitts, 1994; Allen *et al.*, 2008). Thus, it is plausible that age-related changes within the

muscle result in an increased production of metabolic by-products and/or an increased sensitivity of the muscle to a given concentration of metabolite accumulation during high-velocity exercise. However, the decrease in pH and increase in intracellular [P_i] during a dynamic plantarflexor exercise did not differ or was blunted in old compared to young adults (Layec *et al.*, 2013; Layec *et al.*, 2014, 2015), suggesting that the age-related increase in fatigability is not likely due to an increased production of metabolic by-products. In chapters 3 and 4, I test the hypothesis that the increased fatigability with age is explained, at least in part, by an increased sensitivity of the cross-bridge to elevated levels of H^+ and P_i in fibers from old compared to young adults.

Concluding remarks

Our data provide evidence that aging of the neuromuscular system results in an increased fatigability during high-velocity contractions of the knee extensors that continually progresses into the latest stages of life (≥80 yrs) and occurs similarly for both men and women. By coupling non-invasive stimulation procedures to both the motor cortex and the peripheral nervous system with measures of surface EMG and torque output, we were able to localize the primary mechanism for the increased fatigability with aging to factors within the muscle. We conclude that the age-related increased power loss during high-velocity fatiguing exercise of the lower limb is determined primarily by cellular mechanisms that disrupt excitation contraction coupling and/or cross-bridge function and that the mechanisms are similar for both men and women.

CHAPTER 3

EFFECTS OF ELEVATED H^+ AND P_i ON THE CONTRACTILE MECHANICS OF SKELETAL MUSCLE FIBERS FROM YOUNG AND OLD MEN: IMPLICATIONS FOR HUMAN MUSCLE FATIGUE

INTRODUCTION

Human aging is accompanied by a progressive decline in neuromuscular function acting to reduce mobility, increase the risk of falling, and limit the performance of daily activities in older adults. Pivotal for the age-related decline in function is the loss in muscle mass that can approach 30% in individuals ≥ 60 years of age (Doherty, 2003). However, the age-related losses in maximal strength and the ability to generate power occur earlier in life and at a more rapid rate than the losses in total muscle mass, suggesting that other factors such as changes in the nervous system and 'muscle quality' also contribute to the losses in function with age (Reid & Fielding, 2012; Russ *et al.*, 2012; Hepple & Rice, 2016; Hunter *et al.*, 2016). Additionally, the age-related decline in the ability to generate power is exacerbated by the increase in fatigability that occurs when older adults perform moderate- to high-velocity contractions (McNeil & Rice, 2007; Dalton *et al.*, 2010; Callahan & Kent-Braun, 2011; Dalton *et al.*, 2012). Despite the growing recognition that muscle power output is an important predictor of functional impairments in older adults (Reid & Fielding, 2012), the primary mechanisms for the accelerated loss in power and the increase in fatigability with aging remain unresolved. In chapter 2, it was observed that the age-related increase in power loss during a dynamic knee extension exercise was strongly associated with the reductions in both the amplitude and rate of torque development of the electrically-evoked twitch. The latter is thought to

be limited by the forward rate constant of the low- to high-force state of the cross-bridge cycle suggesting that the mechanism responsible for the age-related increase in fatigability is likely due to cellular mechanisms that disrupt cross-bridge function (Fitts, 1994, 2008).

In isolated permeabilized muscle fibers, the kinetics of the low- to high-force state of the cross-bridge cycle can be measured by employing a rapid slack re-extension maneuver of a maximally Ca^{2+}-activated fiber (Metzger & Moss, 1990a, b). The rapid re-extension of the fiber dissociates myosin from actin, and the rate of force redevelopment (k_{tr}) following the re-extension represents the sum of the forward and reverse rate constants of the low- to high-force state of the cross-bridge cycle (Brenner & Eisenberg, 1986; Metzger *et al.*, 1989). Two metabolic by-products implicated in fatigue, inorganic phosphate (P_i) and hydrogen (H^+), have been shown to directly affect the cross-bridge cycle at this transition step but by different mechanisms (Debold *et al.*, 2016). Specifically, P_i is thought to induce an unconventional powerstroke where myosin dissociates from actin early in the low- to high-force transition (Linari *et al.*, 2010; Caremani *et al.*, 2013; Debold *et al.*, 2016), resulting in the acceleration of the rate of force development (Dantzig *et al.*, 1992) and k_{tr} (Wahr *et al.*, 1997; Tesi *et al.*, 2002). In contrast, H^+ is thought to inhibit the forward rate constant of the low- to high-force state (Metzger & Moss, 1990b), which may explain the lack of difference in k_{tr} in rat fibers exposed to a control (pH 7.0 + 0 mM P_i) compared to a combined P_i (30 mM) and H^+ (pH 6.2) condition (Nelson *et al.*, 2014). However, because the resting concentration of P_i in quiescent human skeletal muscle is ~3-5 mM (Kemp *et al.*, 2007), these previous studies may have underestimated the effect of H^+ on k_{tr}. In addition, no studies have tested the

effects of P_i and H^+ on human skeletal muscle and only a single study has measured k_{tr} of 'slow type' fibers from old compared to young adults (Power *et al.*, 2016). Thus, the first aim of this chapter was to compare the k_{tr} of fibers expressing slow myosin heavy chain I (MHC I) and fast MHC II from young (<30 yrs) and old adults (>70 yrs) in conditions mimicking quiescent human muscle (pH 7.0 + 4 mM P_i) and severe fatigue (pH 6.2 + 30 mM P_i). We hypothesized that the k_{tr} of both fiber types would be lower in the fibers from old compared to young adults, and that the fatigue-mimicking condition would slow k_{tr} but would do so to a greater extent in the fibers from old adults.

In addition to the experiments on the low- to high-force transition of the cross-bridge cycle, experiments on peak isometric force (P_o), shortening velocity (V_o and V_{max}), and peak fiber power are necessary to assess whether cross-bridge mechanisms are responsible for the age-related loss in power and increase in fatigability. When studied in isolation at cold temperatures (<20°C), both P_i and H^+ cause large reductions in P_o and peak fiber power, while H^+ alone also slows shortening velocity (Metzger & Moss, 1987; Chase & Kushmerick, 1988; Cooke *et al.*, 1988; Godt & Nosek, 1989; Debold *et al.*, 2004; Knuth *et al.*, 2006). Subsequent studies performed at near physiological temperatures (30°C) have generally found a reduced effect of P_i and H^+ on P_o and peak power, but that the effect of H^+ on shortening velocity was unaltered by temperature (Debold *et al.*, 2004; Knuth *et al.*, 2006; Karatzaferi *et al.*, 2008). The mitigated effect of these ions at near *in vivo* temperatures has caused considerable debate over their role in the fatigue process (Fitts, 2016; Westerblad, 2016). However, when the effects of elevated H^+ (pH 6.2) and P_i (30 mM) were studied in combination at 30°C, which is more relevant to the fatigue process *in vivo*, they had a synergistic effect that caused marked

reductions in P_o (~35-50%), peak power (~55-65%), and V_{max} (~20%) of rat and rabbit fibers (Karatzaferi *et al.*, 2008; Nelson *et al.*, 2014).

Therefore, the second aim of this chapter was to test the effects of the fatigue-mimicking condition (pH 6.2 + 30 mM P_i) on isometric force (P_o), shortening velocity (V_o and V_{max}), and peak power in fibers from young and old adults at 15°C and 30°C. We hypothesized that the age-related increase in fatigability during dynamic exercise is due, in part, to an increased sensitivity of the cross-bridge of old adult fibers to H^+ and P_i. Importantly, because we integrated measures of whole-muscle function with single cell contractile mechanics, the third aim of this chapter was to explore the mechanisms for the age-related loss in 'muscle quality' (i.e., decreased strength or power after normalizing for differences in muscle mass, volume or cross-sectional area).

METHODS

Participants and Ethical Approval

Six young men (20-29 yrs) and six old men (73-89 yrs) volunteered and provided their written informed consent to participate in this study. Participants underwent a general health screening and were excluded from the study if they were taking medications that affect the central nervous system, muscle mass or neuromuscular function (e.g., hormone-replacement therapies, anti-depressants, glucocorticoids). All participants were apparently healthy, community dwelling adults free of any known neurological, musculoskeletal or cardiovascular diseases. All experimental procedures were approved by the Marquette University Institutional Review Board and conformed to the principles in the Declaration of Helsinki.

Whole-muscle Knee Extensor Function & Fatigability

Participants reported to the laboratory on four occasions, twice for familiarization, once for an experimental session to measure whole-muscle function of the knee extensors, and once for a muscle biopsy of the vastus lateralis. The familiarization sessions were used to habituate the participants to electrical stimulation of the femoral nerve and transcranial magnetic stimulation (TMS) to the motor cortex. Participants also practiced performing maximal voluntary isometric and concentric contractions with the knee extensors during the familiarization sessions. The experimental session assessed whether the old adults demonstrated conventional age-related changes of the knee extensor muscles compared to the young adults, including, (1) lower thigh lean muscle mass, (2) lower absolute and mass specific isometric strength and mechanical power outputs, and (3) an increased fatigability (reductions in mechanical power) when performing a high-velocity dynamic exercise (Dalton *et al.*, 2012; Reid & Fielding, 2012). The results for the fatigability measurements are a subset from the data reported in chapter 2, and only the methods that were not included in chapter 2 are described below.

Thigh lean mass: Body composition and thigh lean mass was assessed with dual X-ray absorptiometry (Lunar iDXA, GE, Madison, WI, USA). Thigh lean mass was quantified for the region of interest from the manufacturer's software (enCORE 14.10.022, GE), with the distal demarcation set at the tibiofemoral joint and the proximal demarcation set as a diagonal bifurcation through the femoral neck. DXA measures of thigh lean mass with these landmarks are strongly correlated with measures from magnetic resonance imaging (MRI) but underestimate the age-related loss in thigh muscle mass (Maden-Wilkinson *et al.*, 2013).

Muscle Biopsy

A muscle biopsy from the vastus lateralis of the leg tested in the whole-muscle experiments was obtained from each participant (Bergstrom, 1962). Participants were instructed to refrain from strenuous exercise of the lower limb for 48 hrs prior to the biopsy and arrived at the laboratory fasted and without consumption of caffeine. The biopsy location was cleaned with 70% ethanol, sterilized with 10% providone-iodine, and anaesthetized with 1% lidocaine HCl. A small ~1 cm incision was made overlying the distal 1/3 of the muscle belly, and the biopsy needle inserted under local suction to obtain the tissue sample. Two longitudinal bundles from the biopsy sample were immediately submerged in cold glycerol skinning solution (see below) and stored at -20°C. The remaining biopsy sample was immediately frozen in liquid nitrogen and stored at -80°C. All single fiber contractile experiments were completed within 4 weeks of the biopsy.

Single Fiber Morphology and Contractile Mechanics

Solutions: The composition of the relaxing (pCa 9.0, where pCa = -log[Ca^{2+}]) and activating (pCa 4.5) solutions were derived from an iterative computer program using the stability constants adjusted for temperature, pH and ionic strength (Fabiato & Fabiato, 1979; Fabiato, 1988). All solutions contained (in mM) 20 imidazole, 7 ethylene glycol-bis(β-aminoethyl ether)-*N,N,N',N'*-tetraacetic acid (EGTA), 4 MgATP, and 14.5 creatine phosphate. Inorganic phosphate (P_i) was added as K_2HPO_4 to yield a concentration of 4 or 30 mM. Although no P_i was added to the 0 mM P_i solution, there is evidence that the actual concentration of P_i is between 0.4 and 0.7 mM due to the hydrolysis and resynthesis of ATP and to impurities in stock reagents (Pate & Cooke, 1989). Mg^{2+} was added as $MgCl_2$ with a specified free concentration of 1 mM, and Ca^{2+} was added as

$CaCl_2$. The ionic strength was adjusted to 180 mM with KCl, and the pH was adjusted to 7.0 or 6.2 with KOH and HCl. The skinning solution was composed of 50% relaxing solution and 50% glycerol (vol:vol).

Experimental setup: Single fiber experiments were performed on a microsystem as described previously (Nelson *et al.*, 2014). On the day of experimentation, a fiber segment (~2-3 mm) was isolated from the biopsy, and the ends secured with 4.0 monofilament posts tied with 10.0 nylon sutures to a force transducer (400A, Aurora Scientific, Aurora, Ontario, CA) and high-speed servomotor (controller 312C, Aurora Scientific) in a plastic chamber containing cold relaxing solution (Moss, 1979). Once the fiber was attached, the position of the force transducer and servomotor were adjusted so the fiber could be suspended in 100-120 μL of relaxing solution cooled to 12°C by a temperature-controlled Peltier unit. The fiber remained in the 12°C relaxing solution, except when transferred either into air for imaging or to a second Peltier unit for activation at 15°C or 30°C. To view the fiber at 800X magnification, the microsystem was transferred to the stage of an inverted microscope. The sarcomere length was adjusted to 2.5 μm using a calibrated eyepiece micrometer, and the fiber length measured as the distance between the two points of attachment via a mechanical micrometer (Starrett, Athol, MA, USA). Fiber width was determined from a digital image (CoolSNAP ES, Roper Scientific Photometrics, Tucson, AZ, USA) taken while the fiber was briefly suspended in air (<5 s). The fiber width was measured at 3 locations along the segment length, and the average fiber diameter and cross-sectional area (CSA) were calculated assuming that the fiber forms a cylinder while in air.

Experimental design: All single fiber contractile experiments began with a sequence of 4-5 contractions (activating solution – pH 7.0 + 0 mM P_i) to determine the maximal Ca^{2+}-activated isometric force (P_o) and unloaded shortening velocity (V_o) at 15°C. Each fiber was then selected for one of two sets of experiments: 1) unloaded shortening velocity (V_o) and rates of force redevelopment (k_{tr}) or 2) force-velocity tests. For the first set of experiments, k_{tr} was measured in a low (15°C) and high (30°C) temperature in two control conditions (pH 7.0 + 0 mM P_i and pH 7.0 + 4 mM P_i) and an experimental condition mimicking fatigue (pH 6.2 + 30 mM P_i). Fiber V_o was also measured in all three activating conditions at 15°C, but with one control condition (pH 7.0 + 4 mM P_i) and the experimental fatigue condition (pH 6.2 + 30 mM P_i) at 30°C. For the fibers selected for the second set of experiments, force-velocity measurements were performed in 15°C and 30°C but with only one control condition (pH 7.0 + 4 mM P_i) and the experimental fatigue condition (pH 6.2 + 30 mM P_i). The pH 7.0 + 0 mM P_i control condition was used for comparison with other single fiber experiments in animals (Metzger & Moss, 1990b; Knuth *et al.*, 2006; Nelson *et al.*, 2014) and humans (D'Antona *et al.*, 2003; Trappe *et al.*, 2003; Frontera *et al.*, 2008; Lamboley *et al.*, 2015), whereas, the pH 7.0 + 4 mM P_i control condition was used to more closely mimic the [P_i] in the quiescent human quadriceps muscle (Kemp *et al.*, 2007). Because of the tendency for higher temperatures (>25°C) to damage isolated fibers, all experiments were conducted first at 15°C followed by 30°C. However, within each temperature the control and experimental fatigue conditions were randomized to alleviate the potential of an order effect. Fibers with visible tears or that had a decrease in the maximal Ca^{2+}-activated isometric tension to <90% of the initial P_o within a condition were excluded from further

analysis. Unlike in animal experiments (Debold *et al.*, 2004; Karatzaferi *et al.*, 2008), the fast MHC II fibers from the humans in this study, particularly from the old adults, deteriorated too rapidly to obtain full data sets in 30°C. As a result, data are reported for the fast MHC II fibers at 15°C and the slow MHC I fibers at 15°C and 30°C.

Unloaded shortening velocity (V_o) and rate of force redevelopment (k_{tr}) experiments: Unloaded shortening velocity (Vo) was determined using the slack test (Edman, 1979). Fibers were maximally activated in saturating Ca^{2+} (pCa 4.5), allowed to generate peak isometric force (P_o), and then rapidly shortened with the servomotor to a predetermined distance so that force was momentarily reduced to zero. The fiber remained activated until the redevelopment of force, after which, the fiber was returned to relaxing solution and reextended to its original position. Fibers were activated 4-5 times in each condition and slacked at varying distances (100-450 μm in 15°C and 200-450 μm in 30°C) that never exceeded a distance >20% fiber length. The V_o for each condition was the slope of the least squares regression line between the slack distance and the time required to begin the redevelopment of force. The reported P_o was the average from all the contractions within each condition.

To test the effects of age and metabolites (H^+ and P_i) on the low- to high-force transition of the cross-bridge cycle, the rate constant of force redevelopment (k_{tr}) was measured following a rapid slack re-extension maneuver of a maximally Ca^{2+}-activated fiber (Metzger & Moss, 1990a, b). This maneuver is similar to the slack test with the addition of the rapid re-extension of the activated fiber, which dissociates myosin from actin. The slack distance for each fiber was 400-450 μm with the duration prior to re-extension set to 10 ms in 30°C, 20 ms for fibers with a $V_o > 2.0$ fl·s^{-1} in 15°C, and 40-60

ms for fibers with a $V_o < 2.0$ fl·s^{-1} in 15°C. Force redevelopment following the re-extension was fit with a first-order exponential function, where k_{tr} is the exponential time constant (s^{-1}) of the rate of force redevelopment (Metzger & Moss, 1990b).

Force-velocity experiments: In the second set of experiments, force-velocity and force-power curves were obtained as described previously (Debold *et al.*, 2004; Nelson *et al.*, 2014). Fibers were maximally activated in saturating Ca^{2+}, allowed to generate peak isometric force, and then subjected to three predetermined submaximal isotonic loads (300-FC1 Force Controller, Positron Development, Inglewood, CA, USA). To ensure the fiber did not shorten >20% fiber length, the duration of each isotonic load was 20-30 ms for experiments at 30°C and 20-50 ms at 15°C. Fibers were activated 4-6 times under each condition to obtain 12-18 different isotonic loads, and each force-velocity plot was fit with a residual minimizing, iterative procedure using the hyperbolic Hill equation:

$$(\mathrm{P} + a) * (V + b) = (\mathrm{P_o} + a) * b \qquad \textit{eq. 3}$$

where P is force, V is velocity, P_o is peak isometric force, and a and b are constants with units of force and velocity, respectively (Hill, 1938). Absolute (μN·fl·s^{-1}) and size specific power (W·l^{-1}) were calculated as the product of shortening velocity (fl·s^{-1}) and absolute (μN) and size specific force (kN·m^{-2}), respectively, and the peak fiber power determined using the parameters from the force-velocity curve (Widrick *et al.*, 1996).

Myosin heavy chain (MHC) composition: MHC composition of the isolated fibers were determined by sodium dodecyl sulfate-polyacrylamide gel electrophoresis (SDS-PAGE) and silver staining as described previously (Giulian *et al.*, 1983). Briefly, following the contractile experiments, each fiber was solubilized in 80 μL of SDS sample

buffer [6.7 $mg \cdot mL^{-1}$ ethylenediaminetetraacetic acid (EDTA), 1% SDS, 0.06 M tris(hydroxymethyl)aminomethane (pH 6.8), 0.001% bromophenol blue, 15% glycerol, 5% β-mercaptoethanol] and loaded on a gel made up of a 3% acrylamide/bis (19:1) stacking layer and 5% separating layer. Gels were run 20-24 hours at 4°C (SE600, Hoefer, Holliston, MA), stained, imaged and visually inspected to classify the MHC isoform composition (I, I/IIa, I/IIa/IIx, IIa, IIa/IIx and IIx) of each fiber.

The MHC distribution of the vastus lateralis for each participant was determined by homogenizing a portion of the biopsy sample (>10 mg) in 30X (vol:weight) RIPA buffer with a protease and phosphatase inhibitor cocktail (Thermo Fisher Scientific, Waltham, MA, USA). The homogenized samples were run in quadruplicate for each participant with SDS-PAGE, and the relative abundance of each MHC isoform (I, IIa, and IIx) was quantified using densitometry and averaged over the four runs. Because of the low abundance of MHC IIx in most participants, we combined the IIa and IIx for each participant and report the values as MHC II. The amount of the thigh lean mass composed of slow MHC I and fast MHC II muscle for each participant (TLM_{MHC}) was estimated based on the measured terms in the following equation:

$$\mathrm{TLM_{MHC}} = \mathrm{MHC\ (\%)} * \mathrm{TLM_{Total}} \qquad \textit{eq. 4}$$

where MHC (%) is the relative abundance of the MHC isoform (I or II) from the muscle homogenate and TLM_{Total} is the total thigh lean mass from the DXA scan (Fig. 3.1).

Statistical Analyses

Anthropometrics, whole-muscle knee extensor function, and MHC distribution were compared between age groups (young and old) using an unpaired t-test. For the

whole-limb experiments, repeated-measure analysis of variance (ANOVA) was performed on the measure of fatigability (reductions in power) and the mechanistic measurements (voluntary activation, m-wave & electrically-evoked contractile properties) for both young and old adults. The relative reductions in mechanical power from the beginning to the end of the fatiguing exercise were compared between age groups with an unpaired t-test. Simple linear regression analyses were performed between the reductions in mechanical power and the mechanistic measurements to identify the mechanisms of fatigue in the intact neuromuscular system. Statistical analyses for the whole-muscle knee extensor function, fatigability and the MHC distribution were performed using SPSS (version 24.0, IBM Corp., Armonk, NY, USA).

To test for differences in single fiber morphology and contractile mechanics between young and old adults, a nested ANOVA was used with age group (young and old) and fiber type (I, IIa, and IIa/IIx) as the fixed factors. No pure MHC IIx, hybrid I/IIa, or hybrid I/IIa/IIx fibers were observed in this study. When a significant main effect of fiber type was observed, pair-wise post hoc comparisons were performed using Tukey's method. A repeated-measures nested ANOVA was employed to test the effect of temperature (15°C and 30°C) and activating condition (pH 7.0 + 0 mM P_i, pH 7.0 + 4 mM P_i, and pH 6.2 + 30 mM P_i) on the contractile mechanics of the different fiber types isolated from young and old adults. Because of the small number of hybrid MHC IIa/IIx fibers tested, we grouped the pure MHC IIa with the hybrid MHC IIa/IIx fibers and refer to the grouped data as MHC II. We elected to group the fast MHC fiber types rather than exclude all hybrid MHC IIa/IIx fibers, because none of the outcomes differed when the MHC II fibers were grouped versus when hybrid MHC IIa/IIx were excluded. Statistical

analyses for the single fiber morphology and contractile mechanics were performed using Minitab (version 18.0, Minitab Inc., State College, PA, USA). All significance levels were set at $P < 0.05$. Data are presented as the mean ± standard deviation (SD) in the text and tables and the mean ± standard error of the mean (SE) in the figures.

RESULTS

Whole-Muscle Knee Extensor Function, Fatigability, and MHC Distribution

Anthropometrics, physical activity levels, and whole-muscle knee extensor function measurements are presented in Table 3.1. The physical activity levels assessed by triaxial accelerometry did not differ between the young and old adults. As expected, thigh lean mass and absolute isometric torque and mechanical power outputs of the knee extensors were lower in old compared to young adults. Even after correcting for the differences in thigh lean mass, the isometric torque and power outputs remained lower in old adults by 38% and 53%, respectively. Calculations from the MHC distribution analysis revealed that the lower total thigh lean mass in old adults was primarily determined by a lower amount of fast MHC II muscle (Fig. 3.1) (young = 4.2 ± 1.4 kg, old = 2.2 ± 0.6 kg; $P = 0.011$), which was strongly correlated with the absolute power output ($r = 0.861$, $P < 0.001$) and isometric strength ($r = 0.785$, $P = 0.002$) of the knee extensors. In contrast, there was no difference in the slow MHC I thigh lean mass in the old (3.4 ± 0.9 kg) compared to young adults (3.0 ± 0.9 kg; $P = 0.504$), nor was there a correlation between MHC I lean mass and knee extensor power output ($r = -0.198$, $P = 0.537$) or isometric strength ($r = 0.024$, $P = 0.940$). The fatigability of the knee extensor muscles was ~2.5 fold greater in the old compared to young adults, with an average relative reduction in power of 32 ± 12% in old compared to 12 ± 13% in young adults.

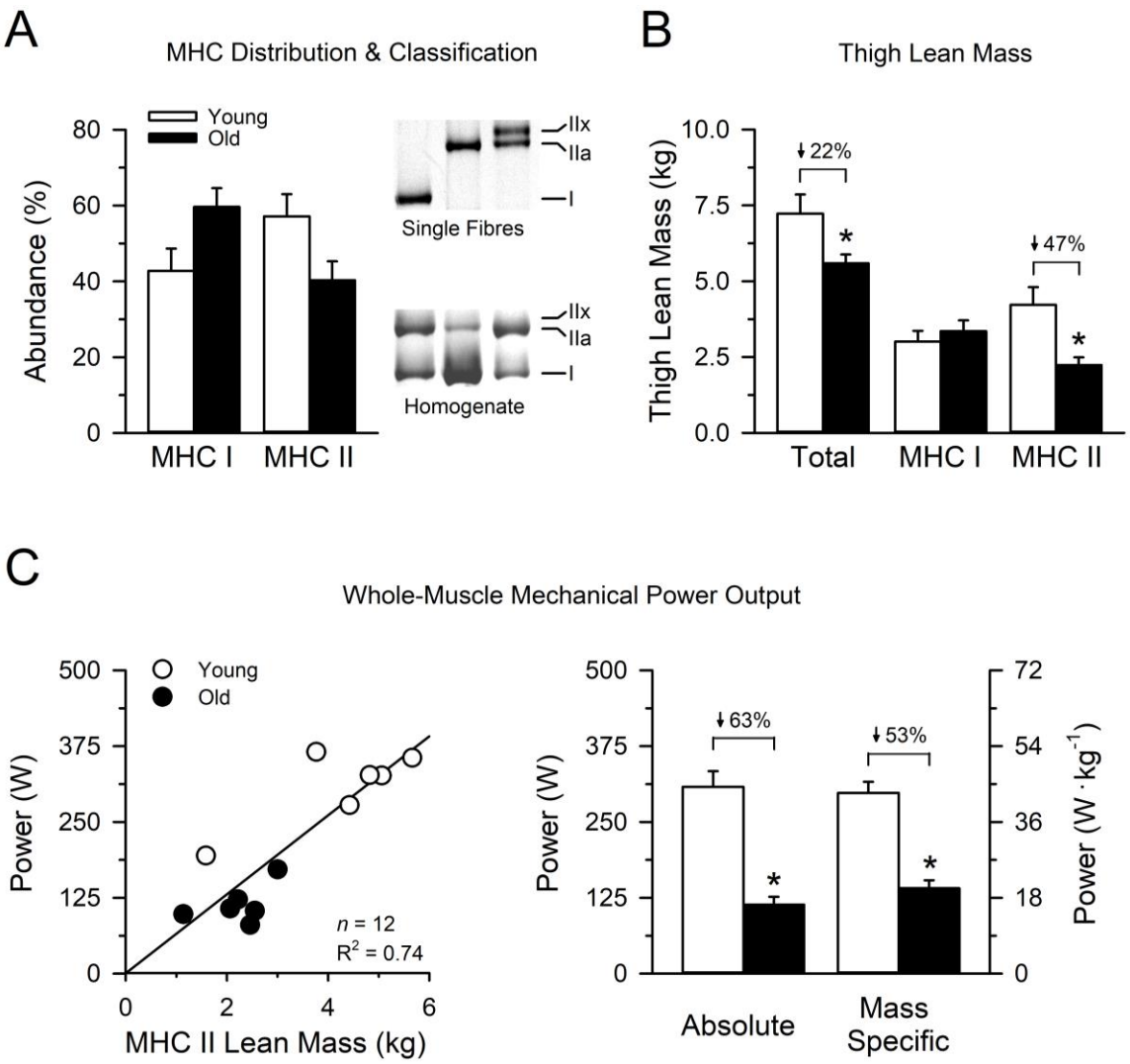

Figure 3.1. Whole-muscle power output and myosin heavy chain (MHC) distribution in the young and old men. There was a trend (P = 0.053) towards a higher relative abundance of MHC I and lower abundance of MHC II in the vastus lateralis muscle of old compared to young adults (A). Total thigh lean mass was 22% lower in old compared to young adults, with a selective loss in the fast MHC II lean mass with aging and no age differences in the slow MHC I lean mass (B). Mean absolute mechanical power outputs from the high-velocity exercise were 63% lower in old compared to young adults and remained 53% lower in old adults after correcting for differences in the total thigh lean mass (C). Linear regression analyses revealed that the differences in the absolute power outputs with aging were strongly associated with the differences in the fast MHC II lean mass (C). Muscle homogenates in the gel image (5% SDS-PAGE) in panel A are from two young adults (outside lanes) and an old adult (middle lane). Gels (5% SDS-PAGE) were also used to classify single fibers based on the MHC isoforms (I, IIa, IIx) following the contractile experiments. Single fibers in the gel image in panel A were classified from left-to-right as type I, IIa, and hybrid IIa/IIx, respectively. *significantly different from the young (P < 0.05). Values are means ± SE.

		Young Men (6)	Old Men (6)	*P* -value
Age	yr	23.3 ± 3.1	81.5 ± 7.2	**<0.001**
Height	cm	178.9 ± 8.9	170.0 ± 7.4	0.089
Weight	kg	74.8 ± 11.3	75.8 ± 10.2	0.877
BMI	$kg \cdot m^{-2}$	23.3 ± 1.9	26.2 ± 2.9	0.064
Whole-Body Fat	%	17.6 ± 4.6	30.1 ± 7.7	**0.009**
Whole-Body Lean Mass	kg	59.5 ± 9.9	50.5 ± 4.0	0.066
Thigh Lean Mass	kg	7.2 ± 1.5	5.6 ± 1.5	**0.039**
Physical Activity	$steps \cdot day^{-1}$	9,175 ± 4,947	7,977 ± 3,232	0.630
Isometric				
MVC Torque	$N \cdot m$	283 ± 59	137 ± 54	**<0.001**
Mass Specific Torque	$N \cdot m \cdot kg^{-1}$	17.9 ± 2.4	11.1 ± 2.2	**<0.001**
Voluntary Activation (*eq. 1*)	%	97.9 ± 2.0	96.6 ± 2.3	0.321
Voluntary Activation (*eq. 2*)	%	0.4 ± 0.4	0.6 ± 0.4	0.356
Dynamic				
Mechanical Power	W	308 ± 63	114 ± 31	**<0.001**
Mass Specific Power	$W \cdot kg^{-1}$	42.9 ± 6.5	20.2 ± 4.7	**<0.001**
Angular Velocity	$rad \cdot s^{-1}$	4.5 ± 0.2	3.5 ± 0.3	**<0.001**
Fatigability - Power	% Δ	–12 ± 13	–32 ± 12	**0.019**
Femoral Nerve Stimulation				
Twitch Torque (Q_{tw})	$N \cdot m$	59.4 ± 11.5	38.2 ± 6.2	**0.003**
Rate of Torque Dev. (dT/dt)	$N \cdot m \cdot s^{-1}$	1,267 ± 324	722 ± 129	**0.007**
1/2 Relaxation Time	ms	71 ± 16	76 ± 23	0.675
VL M_{max} Amplitude	mV	18.0 ± 1.7	7.5 ± 2.7	**<0.001**
VL M-wave Area	$mV \cdot ms$	101.0 ± 9.5	51.5 ± 17.9	**<0.001**

Table 3.1. Anthropometrics, knee extensor function, and physical activity levels for the young and old men. Body fat percentage and lean mass were measured via dual X-ray absorptiometry, and physical activity was measured via triaxial accelerometry. Maximal voluntary contraction (MVC) torque was the highest torque output recorded from the MVC attempts in the experimental session. Voluntary activation was assessed with TMS to the motor cortex and was the median from the five sets of MVC-60-80% contractions performed prior to the dynamic exercise. Mechanical power was the highest average obtained from 5 sequential contractions of the first 10 contractions performed during the dynamic fatiguing exercise. Mass specific torque and power were calculated with the thigh lean mass. Variables from electrical stimulation to the femoral nerve were the median values from the stimuli delivered at rest following the MVC and 80% MVC contractions. M_{max} for the vastus lateralis (VL) was the peak-to-peak maximal compound muscle action potential amplitude. The sample size (*n*) for each cohort is reported in parentheses. Bold font highlights a significant age difference at $P < 0.05$. Values are means ± SD.

Voluntary activation: Baseline voluntary activation calculated using the estimated resting twitch (*eq. 1*) and the superimposed twitch (*eq. 2*) did not differ between young and old adults (Table 3.1). Furthermore, the ability to volitionally activate the knee extensor muscles immediately following the fatiguing exercise did not change compared to baseline for young (*eq 1*: $P = 0.709$; *eq 2*: $P = 0.644$) or old adults (*eq 1*: $P = 0.293$; *eq 2*: $P = 0.548$).

Neuromuscular propagation (m-wave): Baseline m-wave peak-to-peak amplitudes (M_{max}) and areas for the vastus lateralis (VL) are presented in Table 3.1. Despite larger baseline VL M_{max} and m-wave areas in young compared with old men, neither variable changed following the fatiguing exercise for either age group ($P > 0.05$).

Electrically-evoked contractile properties: Baseline contractile properties elicited by electrical stimulation to the femoral nerve are also presented in Table 3.1. The amplitude of the potentiated resting twitch torque (Q_{tw}) decreased following the fatiguing exercise by 23 ± 15% in young ($P = 0.008$) and 30 ± 9% in old adults ($P < 0.001$). Similarly, the rates of torque development (dT/dt) decreased by 21 ± 18% in young ($P = 0.023$) and 37 ± 13% in old adults ($P = 0.002$), whereas, the half relaxation time increased following the fatiguing exercise by 22 ± 18% in young ($P = 0.036$) and 94 ± 59% in old adults ($P = 0.004$). Regression analyses revealed that the relative changes in all contractile properties were strongly associated with the relative reductions in power output during the fatiguing exercise: Q_{tw} ($r = 0.82$; $P = 0.001$), dT/dt ($r = 0.89$; $P < 0.001$), and half relaxation time ($r = -0.68$; $P = 0.014$). However, the most closely associated variable was the reduction in the rate of torque development (dT/dt), which

explained 79% of the variance in the loss in power during the fatiguing exercise (Fig. 3.2).

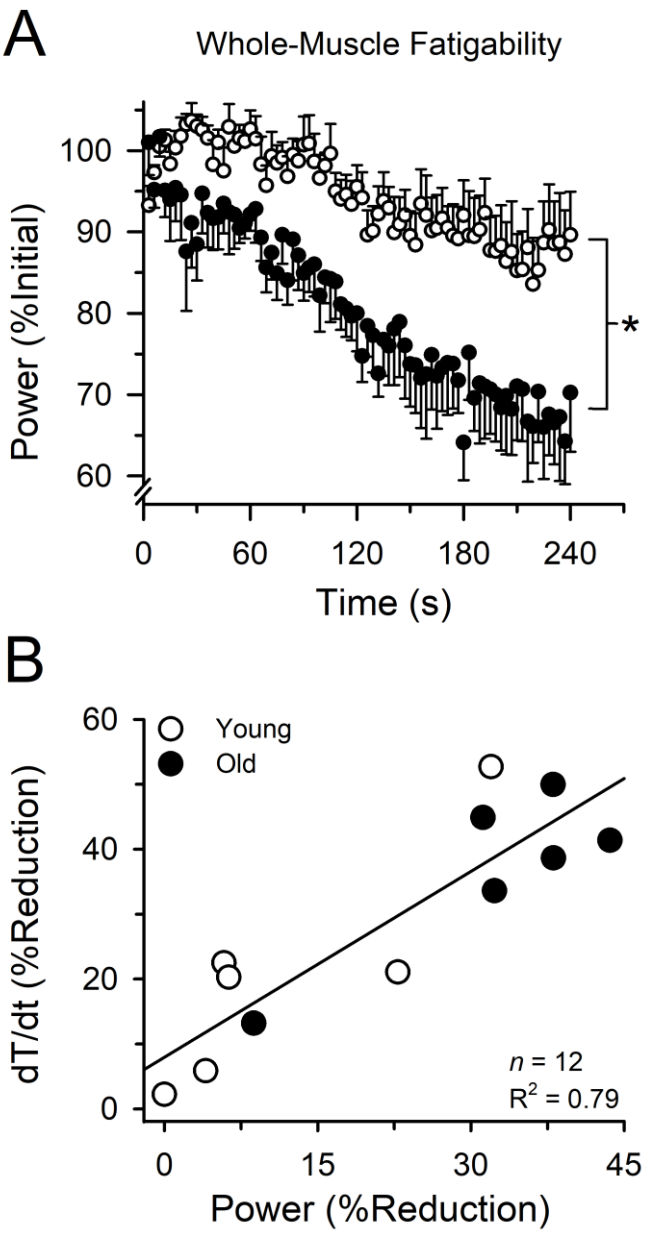

Figure 3.2. Fatigability (reductions in power) of the knee extensors during a high-velocity fatiguing exercise in young and old men. The fatigability of the knee extensor muscles was ~2.5 fold greater in the old compared to young adults, with an average relative reduction in power of 32% in the old compared to 12% in the young (A). Regression analyses revealed that the percent reductions in mechanical power were best predicted by the percent reductions in the rates of torque development (dT/dt) from the electrically-evoked twitches (B). *significantly different from the young ($P < 0.05$). Values are means ± SE.

Single Fiber Morphology and Contractile Mechanics

Presented in Table 3.2 are the fiber diameter, cross-sectional area (CSA), peak isometric force (P_o), and unloaded shortening velocity (V_o) at 15°C (pH 7.0 + 0 mM P_i) for all 254 fibers studied (Young = 122 & Old = 132). The CSA of MHC I fibers did not differ between young and old adults ($P = 0.415$). Similarly, absolute P_o ($P = 0.455$) and size specific P_o ($P = 0.717$) did not differ for MHC I fibers with age. However, the CSA of both MHC IIa and IIa/IIx fibers were 59% and 54% smaller in fibers from old compared to young adults ($P < 0.001$). Accordingly, the absolute P_o was 52% and 50% lower for MHC IIa and IIa/IIX fibers from old compared to young adults ($P < 0.001$). The differences in absolute P_o were explained entirely by the differences in fiber CSA as indicated by the greater size specific P_o in old compared to young adults for the MHC IIa ($P = 0.002$) and no age differences for the MHC IIa/IIx fibers ($P = 0.146$). Independent of age, the size specific P_o of MHC I fibers (183 ± 27 kN·m^{-2}) was 17% lower than MHC IIa fibers (220 ± 39 kN·m^{-2}) and 24% lower than MHC IIa/IIx fibers (243 ± 41 kN·m^{-2}) ($P < 0.001$), with no differences between IIa and IIa/IIx fibers ($P = 0.676$).

The unloaded shortening velocity (V_o) did not differ between fibers from young and old adults for MHC I ($P = 0.215$), IIa ($P = 0.537$) or IIa/IIx fibers ($P = 0.440$). Independent of age, V_o was 67% slower in MHC I (1.31 ± 0.34 fl·s^{-1}) compared with IIa fibers (3.96 ± 0.98 fl·s^{-1}; $P < 0.001$), and 32% slower in MHC IIa compared with IIa/IIx fibers (5.85 ± 1.72 fl·s^{-1}; $P < 0.001$).

		MHC I			MHC IIa			MHC IIa/IIx		
		Young (56)	Old (59)	Diff.	Young (60)	Old (53)	Diff.	Young (6)	Old (20)	Diff.
Diameter	μm	85.4 ± 14.4	77.7 ± 17.2	↔	99.7 ± 10.9	62.8 ± 13.8	↓ 37%	81.0 ± 8.6	54.7 ± 8.2	↓ 32%
CSA	μm^2	5,890 ± 1,890	4,965 ± 2,139	↔	7,895 ± 1,597	3,249 ± 1,464	↓ 59%	5,200 ± 1,150	2,402 ± 700	↓ 54%
Absolute P_o	mN	1.05 ± 0.32	0.90 ± 0.37	↔	1.57 ± 0.27	0.76 ± 0.30	↓ 52%	1.17 ± 0.20	0.58 ± 0.16	↓ 50%
Size Specific P_o	$kN \cdot m^{-2}$	180.5 ± 25.7	185.9 ± 28.3	↔	202.4 ± 26.2	240.9 ± 40.4	↑ 19%	227.4 ± 24.0	247.3 ± 44.6	↔
V_o	$fl \cdot s^{-1}$	1.38 ± 0.41	1.24 ± 0.24	↔	4.03 ± 1.05	3.89 ± 0.91	↔	5.31 ± 0.84	6.01 ± 1.89	↔

Table 3.2. Peak fiber force (P_o) and unloaded shortening velocity (V_o) in pH 7.0 + 0 mM P_i activating solution at 15°C. Fiber diameter and CSA were calculated from a digital image taken while the fiber was briefly suspended in air (<5 s). Peak isometric force (P_o) and unloaded shortening velocity (V_o) were measured from the slack test. The number of fibers (*n*) for each cohort is reported in parentheses. The percent difference between young and old for each myosin heavy chain (MHC) isoform were reported when $P < 0.05$. Values are means ± SD.

Effects of P_i and H^+ on Single Fiber Contractile Mechanics

Peak isometric force (*P_o*): The absolute P_o of fibers from young and old adults for all testing conditions are shown in Figure 3.3. For fast MHC II fibers from young adults, P_o at 15°C was reduced by 23 ± 3% and 54 ± 3% in the 4 mM P_i (1.19 ± 0.23 mN) and the fatigue condition (0.71 ± 0.14 mN) compared to 0 mM P_i (1.54 ± 0.28 mN) ($P < 0.001$). Similarly, the P_o of MHC II fibers from old adults was reduced by 25 ± 5% and 57 ± 4% in the 4 mM P_i (0.54 ± 0.22 mN) and the fatigue condition (0.31 ± 0.14 mN) compared to 0 mM P_i (0.72 ± 0.29 mN) ($P < 0.001$). Although the P_i- and H^+-induced reductions in P_o did not differ with age, the absolute P_o of old adult MHC II fibers in all conditions was 53-56% lower than the P_o of young MHC II fibers ($P < 0.001$). The lower P_o in MHC II fibers with age was due to a smaller CSA in fibers from old compared to young adults.

Independent of age, the relative reductions in P_o elicited by the 4 mM P_i and fatigue conditions in slow MHC I fibers at 15°C were greater than the reductions

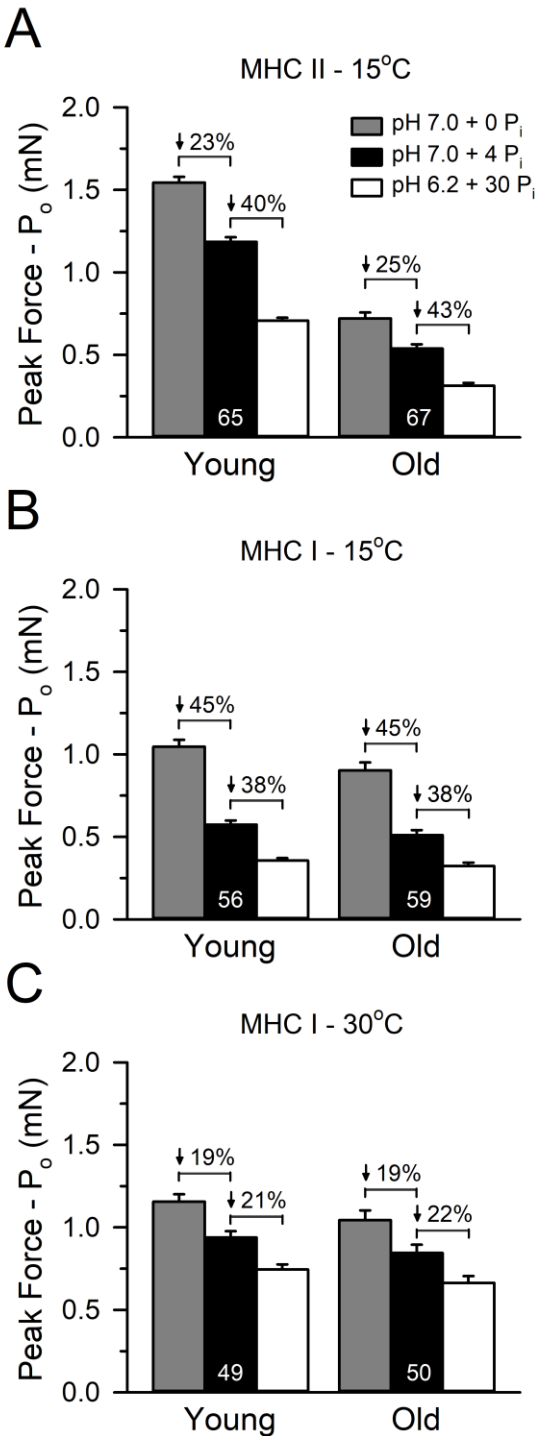

Figure 3.3. Peak isometric force (P_o) of single fibers from young and old men. The peak isometric force (P_o) was lower in the 4 mM P_i control condition compared to the 0 mM P_i control condition, and was lower in the fatigue condition (pH 6.2 + 30 mM P_i) compared to both control conditions for the MHC II at 15°C (A) and MHC I at 15°C (B) and 30°C (C). However, the relative decrease in peak isometric force elicited by P_i and H^+ were similar in fibers isolated from young and old men for both fiber types and all conditions. Values are means ± SE, with the number of fibers (*n*) displayed within the bars.

observed in MHC II fibers (Fig. 3.3). For the young adult MHC I fibers, P_o was reduced by 45 ± 4% and 66 ± 4% in the 4 mM P_i (0.57 ± 0.19 mN) and the fatigue condition (0.36 ± 0.11 mN) compared to 0 mM P_i (1.05 ± 0.32 mN) ($P < 0.001$). Similar to the findings from fast MHC II fibers, there was no age difference for the P_i- and H^+-induced decrements in P_o for slow MHC I fibers from young and old adults. Specifically, compared to 0 mM P_i (0.90 ± 0.36 mN), the P_o of MHC I fibers from old adults was reduced by 45 ± 6% and 66 ± 4% in the 4 mM P_i (0.51 ± 0.24 mN) and fatigue condition, respectively (0.32 ± 0.16 mN) ($P < 0.001$).

Increasing temperature from 15°C to 30°C resulted in an increase in MHC I fiber P_o of 15 ± 8%, 72 ± 20%, and 119 ± 35% in the 0 mM P_i, 4 mM P_i, and fatigue condition, respectively. The greater increases in P_o in the 4 mM P_i and fatigue condition resulted in a reduced P_i- and H^+-induced effect on P_o at 30°C compared to 15°C. However, the findings at 30°C remained qualitatively similar to the findings from 15°C, with no age differences observed in the P_i- and H^+-induced decrements in P_o at 30°C (Fig. 3.3). Independent of age, P_o was reduced by 19 ± 4% and 37 ± 3% in the 4 mM P_i (0.89 ± 0.32 mN) and the fatigue condition (0.70 ± 0.26 mN) compared to 0 mM P_i (1.10 ± 0.37 mN) ($P < 0.001$)

Rate of force redevelopment (k_{tr}): The k_{tr} of the fibers from young and old adults for all conditions are shown in Figure 3.4. For MHC II fibers at 15°C, there was no age difference in k_{tr} in the 0 mM P_i (Young = 9.5 ± 1.4 s^{-1}, Old = 10.4 ± 2.7 s^{-1}; $P = 0.597$), 4 mM P_i (Young = 11.4 ± 1.7 s^{-1}, Old = 11.6 ± 3.0 s^{-1}; $P = 0.950$) or the fatigue condition (Young = 7.8 ± 1.2 s^{-1}, Old = 8.0 ± 2.0 s^{-1}; $P = 0.838$). Independent of age, k_{tr} was 15 ± 8% higher in 4 mM P_i compared to 0 mM P_i ($P < 0.001$) and was reduced by 20 ± 9%

and 31 ± 7% in the fatigue condition compared to the 0 and 4 mM P_i conditions, respectively ($P < 0.001$).

The k_{tr} of MHC I fibers was ~3-fold slower than the k_{tr} of MHC II fibers for all 3 conditions at 15°C. Similar to the findings from MHC II fibers at 15°C, there was no age difference in k_{tr} of MHC I fibers in the 0 mM P_i (Young = 3.2 ± 0.5 s^{-1}, Old = 3.5 ± 0.4 s^{-1}; $P = 0.279$), 4 mM P_i (Young = 3.6 ± 0.6 s^{-1}, Old = 4.0 ± 0.5 s^{-1}; $P = 0.161$) or the fatigue condition (Young = 2.9 ± 0.4 s^{-1}, Old = 3.1 ± 0.4 s^{-1}; $P = 0.108$). Also similar to the findings from MHC II fibers, the k_{tr} for MHC I fibers increased by 14 ± 10% in 4 mM P_i compared to 0 mM P_i ($P < 0.001$) and was reduced by 8 ± 11% and 20 ± 6% in the fatigue condition compared to the 0 and 4 mM P_i conditions, respectively ($P < 0.001$). The reductions in k_{tr} elicited by the fatigue condition were greater in MHC II compared to MHC I fibers ($P < 0.001$).

The k_{tr} of MHC I fibers increased 14- to 18-fold with the increase in temperature from 15°C to 30°C for all 3 conditions. There was no age difference in k_{tr} of MHC I fibers at 30°C in the 0 mM P_i (Young = 53.6 ± 7.5 s^{-1}, Old = 51.4 ± 7.8 s^{-1}; $P = 0.782$) or 4 mM P_i conditions (Young = 68.7 ± 7.7 s^{-1}, Old = 64.4 ± 8.6 s^{-1}; $P = 0.261$), but the absolute k_{tr} in the fatigue condition was lower in fibers from old (39.1 ± 5.8 s^{-1}) compared to young adults (43.6 ± 5.3 s^{-1} $P = 0.049$). The relative reduction in k_{tr} elicited by the fatigue condition however, did not differ with age ($P = 0.140$). Independent of age, k_{tr} was 28 ± 14% higher in 4 mM P_i compared to 0 mM P_i ($P < 0.001$) and was reduced by 20 ± 13% and 38 ± 6% in the fatigue condition compared to the 0 and 4 mM P_i conditions, respectively ($P < 0.001$). Unlike the reduced effects of P_i and H^+ on P_o in

30°C compared to 15°C, the P_i- and H^+-induced effects on the absolute and relative changes in k_{tr} were exacerbated with the increase in temperature (Fig. 3.4).

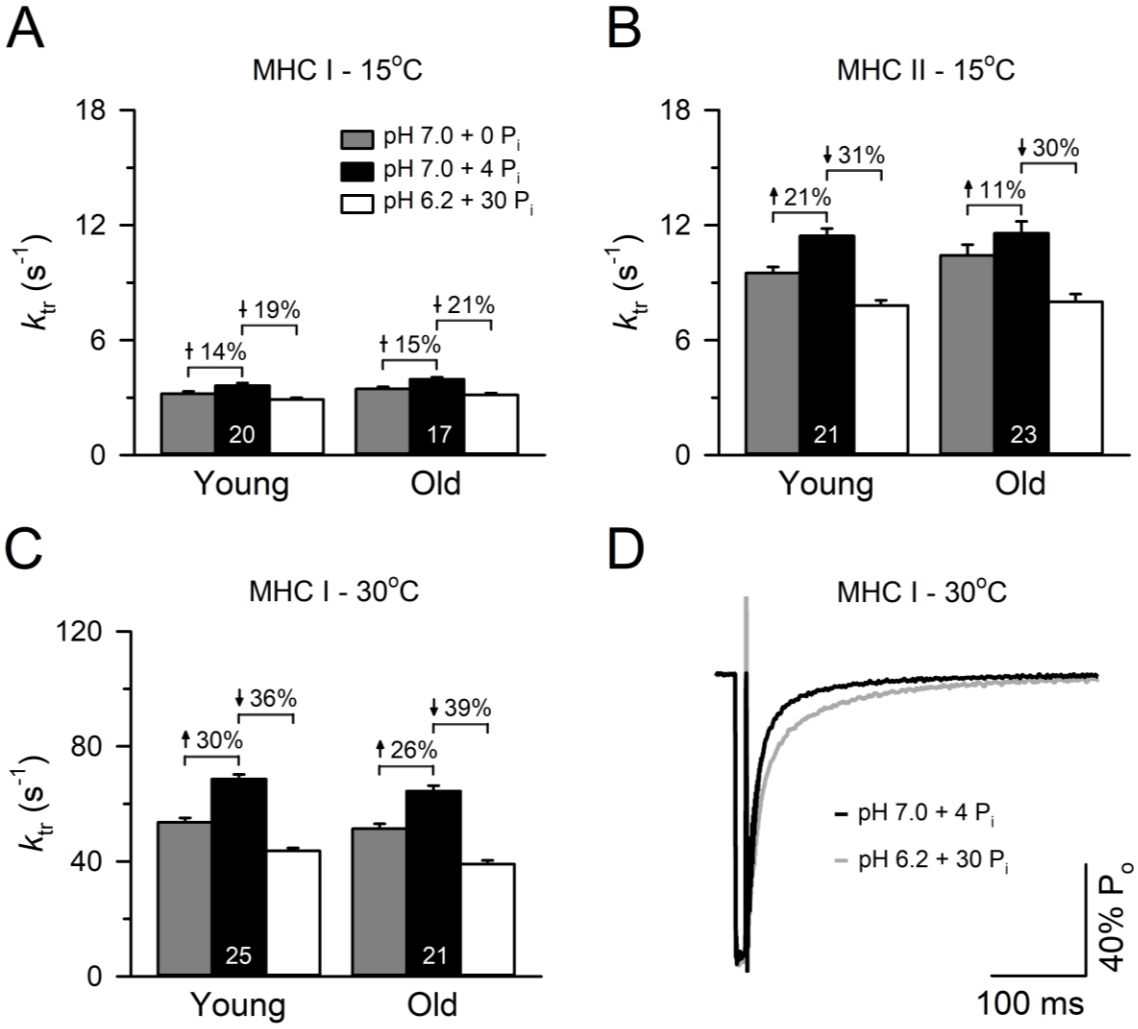

Figure 3.4. Rate of force redevelopment (k_{tr}) of single fibers from young and old men. The rate of force redevelopment (k_{tr}) was accelerated in the 4 mM P_i control condition compared to the 0 mM P_i control condition for the MHC I at 15°C (A) and 30°C (C) and MHC II at 15°C (B). In contrast, the fatigue condition (pH 6.2 + 30 mM P_i) decreased k_{tr} compared to both control conditions for both fiber types, and did so similarly in fibers isolated from young and old adults. The k_{tr} of MHC I fibers increased 18-fold with an increase in temperature from 15°C to 30°C in the 4 mM P_i control condition (C), and the effect of the fatigue condition was exacerbated by the increase in temperature. Shown in panel D is representative force redevelopment (k_{tr}) traces normalized to the peak isometric force (%P_o) for a MHC I fiber isolated from an 84 year old in both a control (pH 7.0 + 4 mM P_i) and fatigue condition (pH 6.2 + 30 mM P_i) at 30°C. Traces are superimposed to compare the differences between the two conditions. Values are means ± SE, with the number of fibers (*n*) displayed within the bars.

Unloaded shortening velocity (V_o): The V_o of the fibers from young and old adults for all conditions are shown in Figure 3.5. For MHC II fibers at 15°C, there was no age difference in V_o in the 0 mM P_i (young = 3.79 ± 1.07 fl·s^{-1}, old = 3.83 ± 1.09 fl·s^{-1}; P = 0.972), 4 mM P_i (young = 3.78 ± 1.09 fl·s^{-1}, old = 3.84 ± 1.08 fl·s^{-1}; P = 0.908) or the fatigue condition (young = 2.04 ± 0.41 fl·s^{-1}, old = 2.06 ± 0.46 fl·s^{-1}; P = 0.937). Independent of age, the fatigue condition elicited a 45 ± 9% reduction in V_o compared to both the 0 and 4 mM P_i conditions (P < 0.001). For MHC I fibers at 15°C, there was also no age difference in V_o in the 0 mM P_i (young = 1.18 ± 0.36 fl·s^{-1}, old = 1.10 ± 0.23 fl·s^{-1}; P = 0.972), 4 mM P_i (young = 1.19 ± 0.34 fl·s^{-1}, old = 1.11 ± 0.23 fl·s^{-1}; P = 0.908) or the fatigue condition (young = 0.82 ± 0.18 fl·s^{-1}, old = 0.81 ± 0.15 fl·s^{-1}; P = 0.937). Also similar to the findings from MHC II fibers, the V_o of MHC I fibers was reduced by 26 ± 12% and 28 ± 11% in the fatigue condition compared to the 0 and 4 mM P_i conditions, respectively (P < 0.001). However, the absolute and relative reductions in V_o in fast MHC II fibers were greater than occurred in slow MHC I fibers (P < 0.001).

The V_o of the MHC I fibers increased ~11-fold with the increase in temperature from 15°C to 30°C for both the 4 mM P_i and fatigue condition. The V_o of MHC I fibers at 30°C was significantly lower in fibers from old (11.74 ± 1.13 fl·s^{-1}) compared to young adults in the 4 mM P_i condition (12.27 ± 1.32 fl·s^{-1}; P = 0.021), but did not differ with age in the fatigue condition (young = 9.38 ± 1.35 fl·s^{-1}, old = 8.78 ± 1.28 fl·s^{-1}; P = 0.144). In addition, the relative reductions in V_o elicited by the fatigue condition did not differ with age (P = 0.567). Unlike the reduced effect observed in the fatigue condition on P_o in 30°C compared to 15°C, the relative reductions in V_o were unaffected by the increase in temperature.

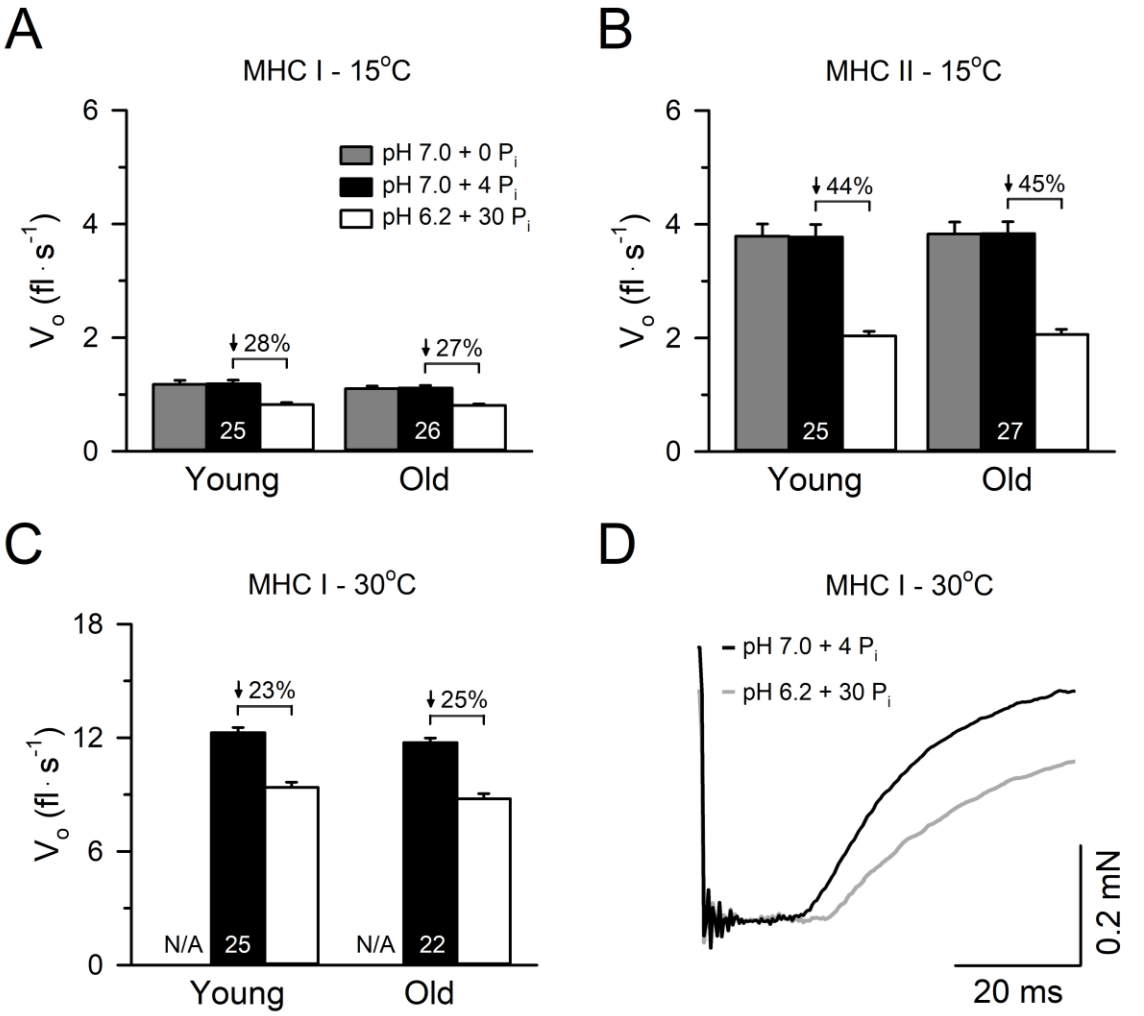

Figure 3.5. Unloaded shortening velocity (V_o) of single fibers from young and old men. The unloaded shortening velocity (V_o) did not differ between the two control conditions (pH 7.0 + 0 mM P_i and pH 7.0 + 4 mM P_i) for the MHC I (A) or MHC II fibers at 15°C (B). In contrast, the fatigue condition (pH 6.2 + 30 mM P_i) decreased V_o compared to both control conditions for both fiber types, and did so similarly in fibers isolated from young and old adults. The V_o of MHC I fibers increased 11-fold with an increase in temperature from 15°C to 30°C in the control condition (C), but the effect of the fatigue condition was unaltered by temperature. Shown in panel D are representative slack traces with a slack distance of 450 μm for a MHC I fiber isolated from an 84 year old in both the control (pH 7.0 + 4 mM P_i) and fatigue condition (pH 6.2 + 30 mM P_i) at 30°C. Traces are superimposed to compare the differences between the two conditions. Values are means ± SE, with the number of fibers (*n*) displayed within the bars.

Force-velocity curves and peak power: Force-velocity and force-power curves for MHC II fibers from young and old adults at 15°C are shown in Figure 3.6, with key

parameters reported in Table 3.3. In the 4 mM P_i condition, the maximal shortening velocity calculated from the Hill equation (V_{max}; $P = 0.684$) and the curvature of the force-velocity relationship (a/P_o; $P = 0.233$) did not differ in MHC II fibers with age. In contrast, the absolute P_o (Young = 1.23 ± 0.20 mN, Old = 0.56 ± 0.19 mN; $P < 0.001$) and peak power ($P = 0.001$) were 50-55% lower in fibers from old compared to young adults. The age differences in absolute P_o and peak power however, were explained entirely by the differences in fiber CSA as indicated by the, respective, 18% and 35% greater size specific P_o (young = 158 ± 20 $kN \cdot m^{-2}$, old = 186 ± 36 $kN \cdot m^{-2}$; $P = 0.012$) and peak power ($P = 0.043$) observed in old compared to young adults. The fatigue condition decreased all parameters of the force-velocity relationship compared to the 4 mM P_i condition for MHC II fibers from young and old men ($P < 0.001$), including, P_o (-41 ± 5%), V_{max} (-16 ± 9%), peak power (-57 ± 5%), and a/P_o (-14 ± 16%), with no age differences in the relative reductions for any of the measurements (Table 3.3).

		PPw ($\mu N \cdot fl \cdot s^{-1}$)		PPw ($W \cdot l^{-1}$)		V_{max} ($fl \cdot s^{-1}$)		a/P_o	
Solution	Temp.	Young (40)	Old (40)	Young (40)	Old (40)	Young (40)	Old (40)	Young (40)	Old (40)
pH 7.0 + 4 mM P_i	15°C	127.3 ± 27.6	63.9 ± 21.2*	16.5 ± 3.8	22.2 ± 7.9*	3.24 ± 0.81	3.27 ± 0.78	0.05 ± 0.01	0.06 ± 0.02
pH 6.2 + 30 mM P_i	15°C	56.1 ± 14.1	27.7 ± 10.2*	7.3 ± 1.9	9.5 ± 3.6	2.76 ± 0.69	2.66 ± 0.55	0.04 ± 0.01	0.05 ± 0.02
% Change		– 56 ± 4	– 57 ± 4	– 56 ± 5	– 57 ± 5	– 15 ± 8	– 18 ± 10	– 17 ± 12	– 12 ± 18

Table 3.3. Force-velocity parameters and peak power (PPw) of fast MHC II fibers at 15°C. Absolute ($\mu N \cdot fl \cdot s^{-1}$) and size specific ($W \cdot l^{-1}$) peak fiber power (PPw) were calculated with the fitted-parameters from the force-velocity curves. The maximal shortening velocity (V_{max}) was calculated using the hyperbolic Hill equation, and the a/P_o ratio is a unitless parameter describing the curvature of the force-velocity relationship. The number of fibers (*n*) for each cohort is reported in parentheses. The percent difference between the control (pH 7.0 + 4 mM P_i) and fatigue condition (pH 6.2 + 30 mM P_i) were reported when $P < 0.05$. *significantly different from the young ($P < 0.05$). Values are means ± SD.

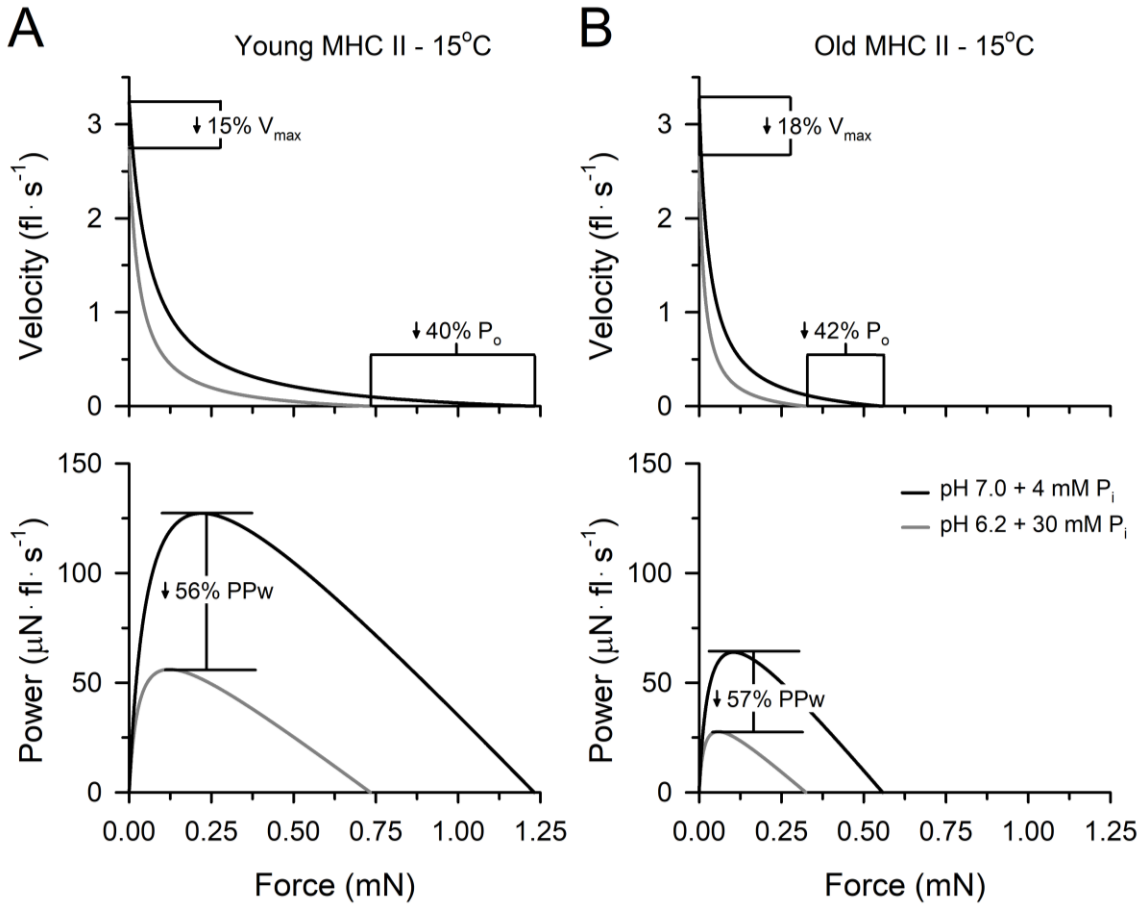

Figure 3.6. Force-velocity and force-power curves of fast MHC II fibers from young and old men at 15°C. Absolute peak fiber power (PPw) and peak isometric force (P_o) of the fast MHC II fibers from young adults (A) were ~2-fold greater than in fibers from old adults (B). The fatigue condition (pH 6.2 + 30 mM P_i) caused significant decreases in the maximum shortening velocity (V_{max}), peak isometric force (P_o), and peak power (PPw) compared to the control condition (pH 7.0 + 4 mM P_i) in fibers from young and old men; however, the relative reductions did not differ with age. The variances around the mean curves were omitted for clarity and are presented in Table 3.3.

Figures 3.7 and 3.8 show the mean force-velocity and force-power curves for MHC I fibers from young and old adults at 15°C and 30°C, respectively, with key parameters reported in Table 3.4. In the 4 mM P_i condition at 15°C, there were no age differences in any of the force-velocity parameters (Fig. 3.7 and Table 3.4). The fatigue condition significantly decreased P_o (-37 ± 6%), V_{max} (-14 ± 8%), and peak power (-48 ± 6%) ($P < 0.001$), but did not alter a/P_o ($P = 0.283$), and no age differences were observed

in the relative reductions for any of the measurements (Fig. 3.7). Independent of age, the relative reductions in P_o and peak power elicited by the fatigue condition were greater in MHC II compared to MHC I fibers ($P < 0.001$), but the reductions in V_{max} did not differ between fiber types ($P = 0.356$).

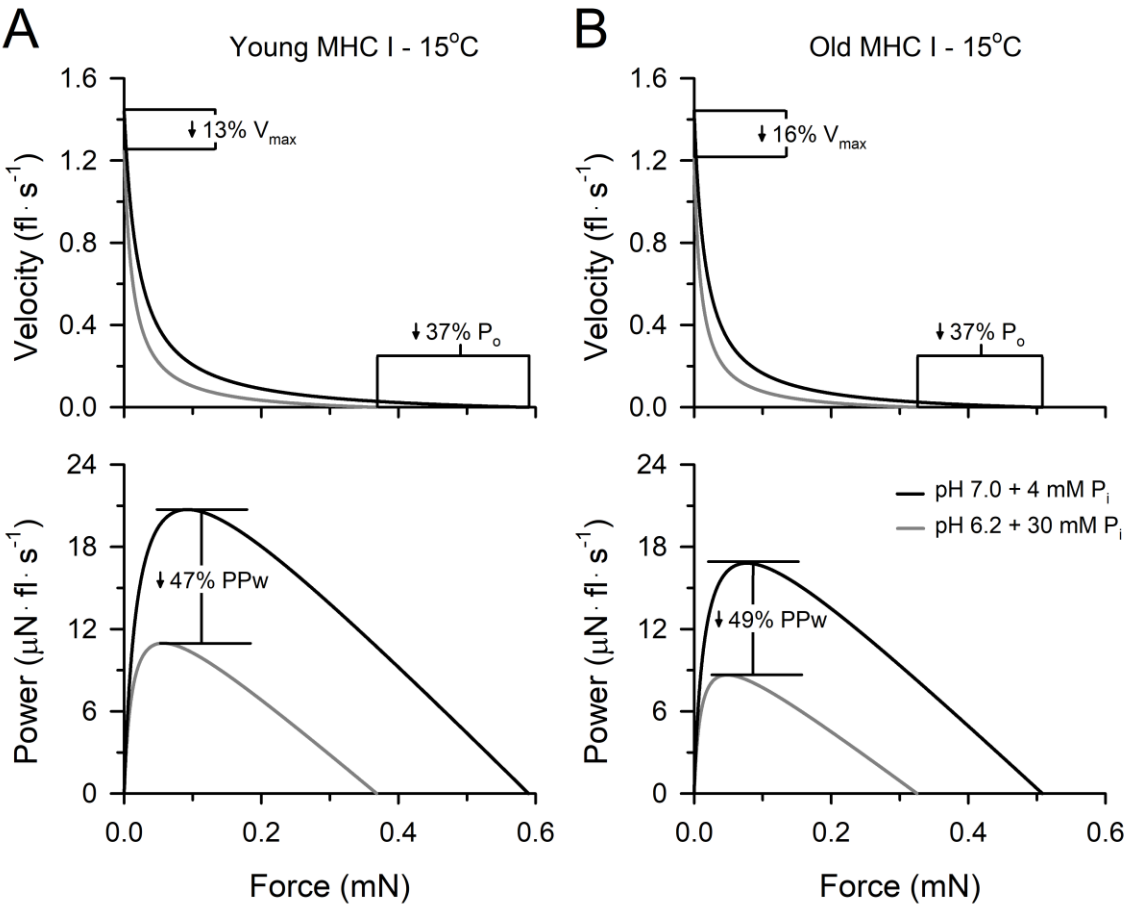

Figure 3.7. Force-velocity and force-power curves of slow MHC I fibers from young and old men at 15°C. The fatigue condition (pH 6.2 + 30 mM P_i) caused significant decreases in the maximum shortening velocity (V_{max}), peak isometric force (P_o), and peak power (PPw) compared to the control condition (pH 7.0 + 4 mM P_i) in MHC I fibers from young (A) and old adults (B); however, the relative reductions did not differ with age. The variances around the mean curves were omitted for clarity and are presented in Table 3.4.

Increasing temperature from 15°C to 30°C increased all parameters of the force-velocity relationship in the 4 mM P_i condition ($P < 0.001$), including, P_o (62 ± 14%), V_{max} (455 ± 80%), peak power (3,285 ± 568%), and a/P_o (563 ± 135%). Similar to the results from MHC I fibers at 15°C, there were no age differences for any force-velocity

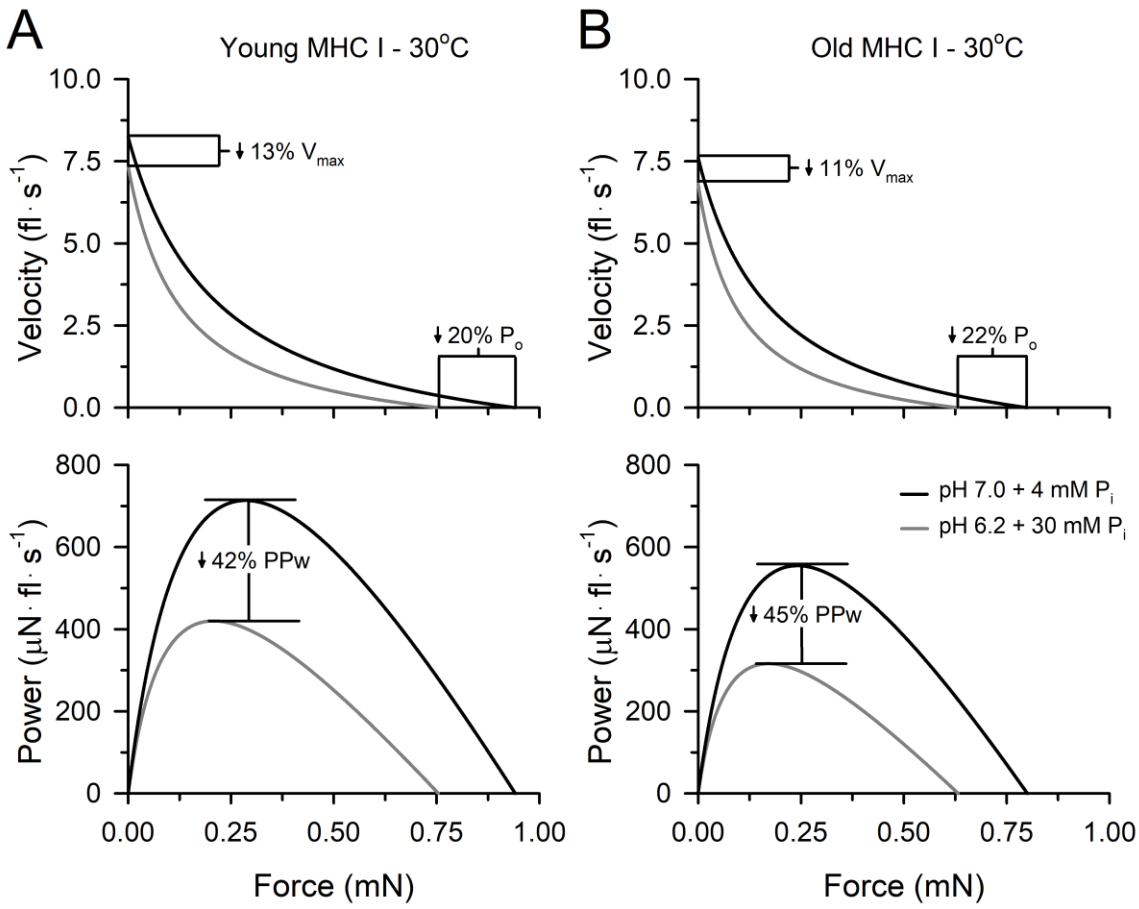

Figure 3.8. Force-velocity and force-power curves of slow MHC I fibers from young and old men at 30°C. The fatigue condition (pH 6.2 + 30 mM P_i) caused significant decreases in the maximum shortening velocity (V_{max}), peak isometric force (P_o), and peak power (PPw) compared to the control condition (pH 7.0 + 4 mM P_i) in MHC I fibers from young (A) and old adults (B); however, the relative reductions did not differ with age. The variances around the mean curves were omitted for clarity and are presented in Table 3.4.

parameters in 4 mM P_i at 30°C (Fig. 3.8 and Table 3.4). However, the fatigue condition significantly decreased all parameters of the force-velocity relationship compared to the 4

mM P_i condition ($P < 0.001$), including, P_o (-21 ± 3%), V_{max} (-11 ± 10%), peak power (-43 ± 7%), and a/P_o (-29 ± 12%), with no age differences in the relative reductions for any of the measurements (Table 3.4). Independent of age, the relative reductions in P_o ($P < 0.001$), peak power ($P = 0.001$), and V_{max} ($P = 0.041$) elicited by the fatigue condition were less in 30°C compared 15°C.

		PPw ($\mu N \cdot fl \cdot s^{-1}$)		PPw ($W \cdot l^{-1}$)		V_{max} ($fl \cdot s^{-1}$)		a/P_o	
Solution	Temp.	Young (30)	Old (32)	Young (30)	Old (32)	Young (30)	Old (32)	Young (30)	Old (32)
pH 7.0 + 4 mM P_i	15°C	20.7 ± 8.3	16.8 ± 6.6	3.7 ± 0.6	3.7 ± 0.8	1.44 ± 0.16	1.44 ± 0.22	0.03 ± 0.00	0.03 ± 0.01
pH 6.2 + 30 mM P_i	15°C	11.0 ± 4.2	8.6 ± 3.6	2.0 ± 0.3	1.9 ± 0.3	1.25 ± 0.16	1.21 ± 0.16	0.03 ± 0.01	0.03 ± 0.01
% Change		– 46 ± 5	– 49 ± 7	– 46 ± 5	– 49 ± 7	– 13 ± 7	– 16 ± 8	↔	↔
pH 7.0 + 4 mM P_i	30°C	713.3 ± 278.0	555.6 ± 268.2	127.8 ± 21.1	120.3 ± 27.0	8.23 ± 0.64	7.61 ± 1.00	0.23 ± 0.03	0.22 ± 0.05
pH 6.2 + 30 mM P_i	30°C	419.9 ± 177.7	315.8 ± 174.0	73.9 ± 14.2	66.9 ± 19.3	7.34 ± 0.85	6.82 ± 1.32	0.16 ± 0.03	0.15 ± 0.03
% Change		– 42 ± 7	– 45 ± 7	– 42 ± 7	– 45 ± 7	– 11 ± 8	– 11 ± 11	– 27 ± 14	– 31 ± 9

Table 3.4. Force-velocity parameters and peak power (PPw) of slow MHC I fibers at 15°C and 30°C. Absolute ($\mu N \cdot fl \cdot s^{-1}$) and size specific ($W \cdot l^{-1}$) peak fiber power (PPw) were calculated with the fitted-parameters from the force-velocity curves. The maximal shortening velocity (V_{max}) was calculated using the hyperbolic Hill equation, and the a/P_o ratio is a unitless parameter describing the curvature of the force-velocity relationship. A lower a/P_o ratio indicates greater curvature of the force-velocity relationship. The number of fibers (*n*) for each cohort is reported in parentheses. The percent difference between the control (pH 7.0 + 4 mM P_i) and fatigue condition (pH 6.2 + 30 mM P_i) were reported when $P < 0.05$. Values are means ± SD.

DISCUSSION

The purpose of this study was to determine the mechanisms for the accelerated loss in muscle power and increased fatigability with aging by integrating measures of whole-muscle function and single fiber contractile mechanics. We observed marked atrophy of fast MHC II fibers in the old compared to young men that corresponded closely with our estimates of the total thigh lean mass composed of MHC II compared to

MHC I muscle. The lower MHC II lean mass was strongly associated with the age differences in isometric strength and power output suggesting that the accelerated age-related loss in whole-muscle function is due, in large, part to the selective atrophy and/or loss of fast MHC II fibers. Despite a lower amount of the fatigable MHC II muscle with age, we observed a 2.5-fold increase in fatigability during the high-velocity knee extension exercise in the old compared to young men. We confirmed previous findings from non-human studies (Cooke *et al.,* 1988; Karatzaferi *et al.*, 2008; Nelson *et al.*, 2014) that elevated levels of H^+ (pH 6.2) and P_i (30 mM) act synergistically to depress cross-bridge function by inhibiting isometric force, shortening velocity, peak power and the low-to high-force transition of the cross-bridge cycle. However, the depressive effects of these ions under saturating Ca^{2+} conditions were similar in fibers from old compared to young men, suggesting that the age-related increase in fatigability cannot be attributed to an increased sensitivity of the cross-bridge to H^+ and P_i.

Increased fatigability and decreased strength and power with aging are determined primarily by changes within the muscle

The older men in this study demonstrated hallmark signs of aging of the knee extensor muscles, that included, a 22% lower thigh lean mass, 54% lower maximal isometric strength, 63% lower mechanical power output (Fig. 3.1), and a 2.5-fold increase in fatigability during a high-velocity exercise compared to the younger men (Fig. 3.2). The accelerated age-related loss in strength and power relative to the loss in muscle mass is often observed in aging studies and commonly referred to as a decrease in 'muscle quality' (Doherty, 2003; Reid & Fielding, 2012; Russ *et al.*, 2012). Despite its widespread recognition, the primary mechanisms responsible for the age-related loss in

'muscle quality' remain elusive. Our data, which integrated measures of whole-muscle function and single cell contractile properties, shed light on this unanswered question and revealed that the accelerated loss in muscle strength and power with age was primarily determined by the selective atrophy of fast MHC II fibers.

Multiple mechanisms have been proposed to explain the decrease in 'muscle quality' with aging, including, decreased voluntary neural drive (Russ *et al.*, 2012; Venturelli *et al.*, 2015), infiltration of adipose and connective tissue into the muscle (Lexell, 1995; Kent-Braun *et al.*, 2000), motor unit remodeling and instability of the neuromuscular junction (Hepple & Rice, 2016; Hunter *et al.*, 2016), and/or impaired cross-bridge mechanics and Ca^{2+} handling (Frontera *et al.*, 2000b; Miller & Toth, 2013; Lamboley *et al.*, 2015; Lamboley *et al.*, 2016; Power *et al.*, 2016). In our study, the ability of the older men to activate the knee extensors during a maximal voluntary isometric contraction was not different compared to the young men. These findings are in agreement with a majority of other studies on both dynamic and isometric contractions that have found no age differences in voluntary activation when older participants are provided practice and familiarization to the procedures (Klass *et al.*, 2007; Hunter *et al.*, 2016; Rozand *et al.*, 2017). Similarly, we found no age differences in any contractile properties of the isolated fibers, other than a lower absolute peak isometric force and power output in MHC II fibers from old compared to young adults (Fig. 3.3 and Fig. 3.6). However, when the differences in absolute isometric force and peak power were normalized to the differences in fiber size, the old adult MHC II fibers generated higher size specific force and power compared to the young adult fibers (Tables 3.2 & 3.3). The preservation or even increase in size specific fiber force and power with aging is in

agreement with a large number of studies (Trappe *et al.*, 2003; Korhonen *et al.*, 2006; Frontera *et al.*, 2008; Slivka *et al.*, 2008; Miller *et al.*, 2013; Venturelli *et al.*, 2015; Grosicki *et al.*, 2016) but in contrast to others (Larsson *et al.*, 1997; Frontera *et al.*, 2000b; Lamboley *et al.*, 2015; Power *et al.*, 2016). The explanation for the disparities between studies is unknown, but clearly, when corrected for changes due to MHC II fiber atrophy, single fiber contractile function was not impaired in our old participants who had similar physical activity levels to the young participants.

An alternative hypothesis to describe the accelerated age-related loss in strength and power is not due to a decrease in 'muscle quality' per se, but rather, is attributed to the selective atrophy of muscle expressing the fast MHC II isoform. Because MHC II fibers generate higher size specific force and power compared to MHC I fibers (Tables 3.2-3.4) (Trappe *et al.*, 2003; Miller *et al.*, 2015; Grosicki *et al.*, 2016), a selective loss and atrophy in MHC II fibers would be consistent with a more rapid loss in both isometric strength and power production with age. Accordingly, we observed a trend (P = 0.053) towards a 17% lower relative abundance of MHC II in the vastus lateralis of the old compared to young men. However, what is more important for the absolute isometric force and mechanical power production of whole-muscle is not the relative distribution of the MHC isoforms, but rather, the respective anatomical cross-sectional area and total muscle mass that is composed of fast MHC II muscle. Our estimate of the total thigh lean mass composed of MHC II compared to MHC I revealed a 47% lower MHC II lean mass in the old compared to young men with no differences in MHC I lean mass (Fig. 3.1). Most importantly, the lower MHC II lean mass in old adults described 74% of the variance in knee extensor power and 62% of the variance in isometric strength with age.

Notably, the estimated 47% lower MHC II lean mass was in close agreement with the ~55% smaller cross-sectional area observed in the isolated MHC IIa and IIa/IIx fibers from old compared to young adults. These findings suggest that the primary mechanism for the accelerated loss in muscle strength and power with age is a selective atrophy of fast MHC II fibers. Whether the same mechanism is responsible for the age-related decrements in muscle strength and power in mobility impaired older adults or in old women is unknown.

Paradoxically, despite a lower amount of muscle mass composed of fast fatigable MHC II fibers in the old compared to young men, we observed a 2.5-fold increase in fatigability during the high-velocity exercise with age (Fig. 3.2). Because the voluntary activation and VL m-wave immediately following the fatiguing exercise did not change compared to baseline for either the old or young men, the increased age-related fatigability could not be attributed to either impaired neural drive or altered neuromuscular propagation. In contrast, 79% of the variance in the reductions in power during the fatiguing exercise was explained by the reduction in the rate of torque development of the involuntary, electrically-evoked twitch (Fig. 3.2). This finding suggests that the age-related increase in fatigability is primarily determined by cellular mechanisms that disrupt contractile function within the muscle and is in agreement with numerous other aging studies (McNeil & Rice, 2007; Dalton *et al.*, 2010, 2012).

P_i and H^+ inhibit cross-bridge function and are important mediators in human muscle fatigue

To test whether cross-bridge mechanisms could explain the age-related increase in fatigability, we exposed muscle fibers from the vastus lateralis of young and old men

to conditions mimicking quiescent human muscle (pH 7.0 + 4 mM P_i) and severe fatigue (pH 6.2 + 30 mM P_i) at 15°C and 30°C. We selected the severe fatigue condition, because 1) human skeletal muscle can reach this level of metabolite accumulation during high-intensity volitional contractions (Wilson *et al.*, 1988; Cady *et al.*, 1989), 2) we could more directly compare our data from human fibers to studies on rat and rabbit fibers (Karatzaferi *et al.*, 2008; Nelson *et al.*, 2014), and 3) we anticipated that the age-differences in the sensitivity of the contractile proteins to these ions, if present, would be most obvious under a severe fatigue condition. At 15°C, we found that the fatigue-mimicking condition caused marked reductions in isometric force (P_o), shortening velocity (V_o and V_{max}), k_{tr}, and peak power of fibers from young and old men, and that the effect was greater in MHC II compared to MHC I fibers for V_o, k_{tr} and peak power, but not for P_o or V_{max}. As expected, increasing the temperature to 30°C increased all of the contractile parameters for the MHC I fibers. However, while the increase in temperature reduced the effect of the fatigue-mimicking condition on P_o by ~50% (Fig. 3.3), it had little-to-no effect on V_o, V_{max} and peak power and exacerbated the effect on k_{tr} (Fig. 3.4). Contrary to our hypothesis, we found no evidence in any of the contractile parameters that fibers from old adults were more sensitive to the depressive effects of H^+ and P_i compared to fibers from young adults.

Our observation of a 37% lower P_o in the fatigue-mimicking condition compared to the ~0 mM P_i control condition in MHC I fibers at 30°C was similar to the 36% decrease observed in slow fibers from rats studied under the same conditions (Nelson *et al.*, 2014). These findings suggest that, at least for MHC I fibers, the combined effects of H^+ and P_i on isometric force are similar across mammalian species. However, when we

compared the P_o of the fatigue-mimicking condition to the 4 mM P_i control condition, which is more representative of quiescent human skeletal muscle (Kemp *et al.*, 2007), the decrement in P_o was reduced to ~21% (Fig. 3.3). This finding suggests that other factors such as the P_i- and H^+-induced decreases in Ca^{2+} sensitivity (Palmer & Kentish, 1994; Parsons *et al.*, 1997; Debold *et al.*, 2006; Nelson & Fitts, 2014) and/or decreases in myoplasmic free Ca^{2+} (Allen *et al.*, 2011) likely play an important role in the fatigue-induced reductions in isometric force *in vivo.* In addition, the relatively large decrease in P_o when the [P_i] was increased from ~0 to 4 mM is consistent with other studies that have shown a hyperbolic relationship between the concentration of P_i and isometric force (Fryer *et al.*, 1995; Wang & Kawai, 1997; Coupland *et al.*, 2001; Tesi *et al.*, 2002; Pathare *et al.*, 2005). Importantly, because slow MHC I fibers are more sensitive to P_i at low concentrations compared to fast MHC II fibers (Fig. 3.3) (Fryer *et al.*, 1995; Wang & Kawai, 1997), the fiber type differences in the size specific P_o ($kN \cdot m^{-2}$) were much greater at the more physiological [P_i] of 4 compared to ~0 mM.

As expected increasing the [P_i] from ~0 to 4 mM increased k_{tr} of both MHC I and MHC II fibers from young and old adults (Fig. 3.4). This observation is consistent with the hypothesis that P_i decreases P_o by dissociating myosin from actin early in the low- to high-force transition step of the cross-bridge cycle, resulting in a decreased number of high-force cross-bridges and an increased k_{tr} (Debold *et al.*, 2016). However, when H^+ (pH 6.2) was added with P_i (30 mM) in the condition mimicking fatigue, k_{tr} was reduced in both fiber types at 15°C, and the effect was exacerbated in MHC I fibers when temperature was increased to 30°C (Fig. 3.4). This novel finding supports the hypothesis that H^+ inhibits the forward rate constant of the low- to high-force transition of the cross-

bridge cycle, and that previous studies underestimated this effect by using the ~0 mM P_i control condition (Metzger & Moss, 1990b; Nelson *et al.*, 2014). The explanation for the increased effect at higher temperatures is unclear, but may be due in part to a greater inhibition of the forward rate constant by H^+ at 30°C.

Interestingly, we observed no age differences in k_{tr} for the MHC I or II fibers from old compared to young adults (Fig. 3.4). This is contrary to our hypothesis that was based on the lower k_{tr} reported in 'slow type' fibers in a group of old compared to young men (Power *et al.*, 2016). To our knowledge, this is the only other study to test the effect of age on the low- to high-force transition of the cross-bridge by measuring k_{tr}. The explanation for the discrepancies between our study and the Power *et al.* (2016) study is unclear but may be the result of several factors that include: 1) Power *et al.* (2016) binned the 'slow type' fibers based on V_o, whereas we identified the MHC composition of the fibers with SDS-PAGE; 2) the temperature of the experiments differed between the studies, with ours performed at 15°C and 30°C, and theirs performed at 10°C; and 3) we set the resting sarcomere spacing to 2.5 μm with direct measurements from an eyepiece micrometer, and Power *et al.* (2016) set the sarcomere spacing to ~2.8 μm using a fast Fourier transform analysis. It is also notable that the 'slow type' fibers from the old men studied by Power *et al.* (2016) had lower V_o and size specific P_o compared to the young men, whereas, we observed no age differences in any of the contractile parameters.

Although increasing the [P_i] from ~0 to 4 mM had marked effects on P_o and k_{tr}, it had no effect on the unloaded shortening velocity (V_o) of MHC I or II fibers from young and old adults (Fig. 3.5). This finding is consistent with the results from rat fibers that P_i has no effect on shortening velocity (Debold *et al.*, 2004; Karatzaferi *et al.*, 2008).

However, when H^+ (pH 6.2) was added with P_i (30 mM) in the condition mimicking fatigue, the shortening velocity (V_o and V_{max}) was inhibited in both fiber types at 15°C, and remained inhibited in MHC I fibers when temperature was increased to 30°C (Fig. 3.5-3.8). The inhibition in shortening velocity on human fibers was generally in close agreement to studies on rat fibers using either the combined pH 6.2 + 30 mM P_i condition (Nelson *et al.*, 2014) or a pH 6.2 only condition (Knuth *et al.*, 2006), which suggests that H^+ is the primary ion that depresses velocity (Metzger & Moss, 1987; Karatzaferi *et al.*, 2008). Although the mechanism by which H^+ slows shortening velocity is not fully elucidated, the primary hypothesis is that acidosis slows the ADP-bound isomerization step and/or the release of ADP from myosin (Debold *et al.*, 2016). Importantly, increasing the temperature to 30°C had little-to-no effect on the fatigue-mimicking condition's reduction in shortening velocity for the MHC I fibers (Fig. 3.5 and Table 3.4).

Since the ability of muscle to generate power is essential for older adults to maintain daily function (Reid & Fielding, 2012), the effect of H^+ and P_i on peak fiber power is more important than their effect on peak isometric force or the maximum shortening velocity alone. We observed that the fatigue-mimicking condition induced a 57% decrease in peak fiber power in fast MHC II fibers (Fig. 3.6) and a 48% decrease in power for slow MHC I fibers (Fig. 3.7). Although the fatigue-induced decrements in fiber power did not differ with age, the absolute power generated in the old MHC II fibers may have reached a critically low value in the fatigue condition where maintaining balance and the necessary power for movement may be compromised. Independent of age, the fiber type dependence for the loss in power was due to the increased curvature (i.e., decreased a/P_o) of the force-velocity relationship in the fatigue-mimicking condition for

the fast fibers that was not observed in slow fibers at 15°C (Tables 3.3 and 3.4). Notably, the fiber-type differences we observed in the H^+- and P_i-induced decrements in power were not observed under a similar fatigue-mimicking condition in rat fibers (Nelson *et al.*, 2014). The discrepancies between studies may be due to differences in the contractile kinetics between mammalian species, or perhaps that we used the more physiological [P_i] of 4 mM compared to the ~0 mM P_i condition used by Nelson *et al.* (2014).

Increasing the temperature from 15°C to 30°C resulted in over a 30-fold increase in peak fiber power and over a 7-fold increase in the curvature constant, a/P_o, of the force-velocity relationship for MHC I fibers. The increase in the curvature constant to 0.22 in 30°C (Table 3.4) is the same as the force-velocity curvature constant reported for the human adductor pollicis muscle *in vivo* (De Ruiter *et al.*, 2000; Jones *et al.*, 2006; Jones, 2010) – a muscle that is composed of ~80% slow MHC I fibers (Round *et al.*, 1984). Additionally, the fatigue-mimicking condition caused a 43% decrease in peak fiber power, which was greater than could be attributed to the combined 21% and 11% decreases in P_o and V_{max}, respectively (Fig. 3.8). The larger decrements in peak fiber power could be explained by the 29% decrease in a/P_o (i.e., an increase in the curvature of the force-velocity relationship). These findings are strikingly similar to the changes observed in the force-velocity relationship of the fatigued human adductor pollicis muscle *in vivo* (De Ruiter *et al.*, 2000; Jones *et al.*, 2006; Jones, 2010), and provide direct evidence that H^+ and P_i are important mediators of human muscle fatigue by directly inhibiting cross-bridge function.

Concluding remarks

Both neural drive and single fiber contractile function were well-preserved in the old compared to young men providing little evidence for an age-related decrease in 'muscle quality'. Instead, we found that the accelerated age-related loss in whole-muscle strength and power was strongly associated with the selective atrophy of fast MHC II fibers. Thus, we propose that scientists and clinicians should be cautious when interpreting lower size specific strength and power as evidence for a decrease in 'muscle quality'. We also provide the first evidence to confirm the findings from non-human studies that elevated levels of H^+ and P_i act synergistically to depress cross-bridge function, and conclude that these ions are important mediators of human muscle fatigue.

CHAPTER 4

CUMULATIVE EFFECTS OF H^+ AND P_i ON THE FORCE-VELOCITY RELATIONSHIP OF YOUNG AND OLD ADULT SKELETAL MUSCLE FIBERS

INTRODUCTION

In chapter 2, the age-related increase in power loss during a high-velocity knee extension exercise was strongly associated with changes in the involuntary, electrically-evoked contractile properties for both men and women. These findings provided strong evidence that the age-related increase in fatigability was determined primarily by cellular mechanisms that disrupt excitation contraction coupling and/or cross-bridge function. The leading cellular mechanisms purported to be responsible for the fatigue-induced reductions in power are an accumulation of metabolic by-products (i.e., H^+, P_i, $H_2PO_4^-$) that act to both directly inhibit cross-bridge function (Fitts, 2008; Debold *et al.*, 2016) and to impair excitation-contraction coupling (Fitts, 1994; Allen *et al.*, 2008). However, because the decrease in pH and increase in intracellular [P_i] during a dynamic plantarflexor exercise did not differ or was blunted in old compared to young adults (Layec *et al.*, 2013; Layec *et al.*, 2014, 2015), the age-related increase in fatigability is not likely due to an increased production of metabolic by-products.

In chapter 3, we tested an alternative hypothesis that the increased fatigability with age could be explained by an increased sensitivity of the cross-bridge to elevated levels of H^+ and P_i. A severe fatigue-mimicking condition (pH 6.2 + 30 mM P_i) was used in these studies, because it was anticipated that the age-differences in the sensitivity of the contractile proteins to these ions, if present, would be most obvious under this

condition. However, the effects of elevated H^+ and P_i on cross-bridge function may have been saturated in the severe fatigue-mimicking condition, potentially masking any age-related differences in the sensitivity of the cross-bridge to these ions. For example, numerous studies have observed a hyperbolic relationship between the concentration of P_i and peak isometric force, where any increase in [P_i] above ~25-30 mM had little-to-no effect on peak force (Fryer *et al.*, 1995; Wang & Kawai, 1997; Coupland *et al.*, 2001; Tesi *et al.*, 2002; Pathare *et al.*, 2005). Whether a similar hyperbolic relationship is observed in peak power and force when H^+ and P_i are simultaneously elevated in conditions that more closely mimic the fatigue environment *in vivo* is not known.

Therefore, the purpose of chapter 4 was to expose muscle fibers from young and old men and women to a continuum of elevated levels of H^+ and P_i that regularly occur *in vivo*. The first hypothesis was that the decrements in fiber force and power would have a hyperbolic relationship with the increase in the concentrations of H^+ and P_i. The second hypothesis was that the decrements in power would be more pronounced in fibers from old compared to young men and women at low levels of H^+ and P_i, and that these age differences would no longer be present in the severe fatigue-mimicking condition (pH 6.2 + 30 mM P_i).

METHODS

Participants and Ethical Approval

Three young men (25, 26, and 32 yrs), three young women (21, 22, and 23 yrs), four old men (70, 73, 74, and 90 yrs), and 2 old women (75 and 79 yrs) volunteered and provided their written informed consent to participate in this study. Participants

underwent a general health screening and were excluded from the study if they were taking medications that can affect the central nervous system, muscle mass or neuromuscular function (e.g., hormone-replacement therapies, anti-depressants, glucocorticoids). All participants were apparently healthy, community dwelling adults free of neurological, musculoskeletal and cardiovascular diseases. All experimental procedures were approved by the Marquette University Institutional Review Board and conformed to the principles in the Declaration of Helsinki.

Experimental Design

The methods used for the single fiber contractile experiments were similar to the force-velocity experiments described in chapter 3. Briefly, single fiber contractile experiments began with a sequence of 4-5 contractions (activating solution – pH 7.0 + 0 mM P_i) to determine the maximal Ca^{2+}-activated isometric tension (P_o) and unloaded shortening velocity (V_o) at 15°C. Each fiber then underwent a series of force-velocity experiments at 15°C in a condition that mimics quiescent human skeletal muscle (pH 7.0 + 4 mM P_i), and in conditions that mimic mild (pH 6.8 + 12 mM P_i), moderate (pH 6.6 + 20 mM P_i), and severe fatigue (pH 6.2 + 30 mM P_i). The order of the control and experimental fatigue conditions were randomized to alleviate the potential of an order effect. Fibers with visible tears or that had a decrease in the maximal Ca^{2+}-activated isometric tension to <90% of the initial P_o within a condition were excluded from further analysis. Following the contractile experiments, each fiber was solubilized in SDS sample buffer, and the MHC composition determined with SDS-PAGE as described in chapter 3. The data presented in this chapter are a preliminary report of a study that is still

ongoing. As a result, many of the findings are underpowered, particularly regarding the comparisons between the sexes within each age group.

Statistical Analyses

To test for differences in single fiber morphology and contractile mechanics between young and old men and women, a nested ANOVA was used with age (young & old), sex (men & women), and fiber type (I & IIa) as the fixed factors. Of the 192 fibers studied, no pure MHC IIx, hybrid I/IIa, or hybrid I/IIa/IIx fibers were tested and only 7 hybrid IIa/IIx fibers were studied. As a result, the statistical analyses was restricted to include only the pure MHC I and IIa fibers. A repeated-measures nested ANOVA was employed to test the effect of the activating conditions on the force-velocity parameters of the MHC I and IIa fibers from young and old men and women. Statistical analyses for the single fiber morphology and contractile mechanics were performed using Minitab (version 18.0, Minitab Inc., State College, PA, USA). All significance levels were set at $P < 0.05$. Data are presented as the mean ± standard deviation (SD) in the text and tables and the mean ± standard error of the mean (SE) in the figures.

RESULTS

Single Fiber Morphology and Contractile Mechanics

Presented in Table 4.1 are the fiber diameter, cross sectional area (CSA), peak isometric force (P_o), and unloaded shortening velocity (V_o) from the 83 MHC I fibers studied in the pH 7.0 + 0 mM P_i condition. No age or sex differences were observed in any of the morphological or contractile parameters measured for the slow MHC I fibers in the pH 7.0 + 0 mM P_i condition.

		Men			Women			*P* -value		
		Young (18)	Old (27)	Diff.	Young (20)	Old (18)	Diff.	Age	Sex	Age x Sex
Diameter	μm	93.5 ± 16.7	82.2 ± 20.7	↔	83.0 ± 7.2	77.4 ± 10.1	↔	0.208	0.320	0.657
CSA	μm^2	7,070 ± 2,493	5,633 ± 3,003	↔	5,453 ± 935	4,776 ± 1,217	↔	0.273	0.273	0.675
Absolute P_o	mN	1.07 ± 0.28	0.96 ± 0.40	↔	0.93 ± 0.15	0.97 ± 0.26	↔	0.744	0.650	0.490
Size Specific P_o	$kN \cdot m^{-2}$	156.3 ± 20.9	181.5 ± 33.9	↔	172.6 ± 28.2	206.2 ± 38.1	↔	0.057	0.189	0.779
V_o	$fl \cdot s^{-1}$	1.40 ± 0.37	1.43 ± 0.28	↔	1.39 ± 0.33	1.19 ± 0.16	↔	0.404	0.322	0.228

Table 4.1. Peak isometric force (P_o) and unloaded shortening velocity (V_o) of slow MHC I fibers in pH 7.0 + 0 mM P_i activating solution at 15°C. Fiber diameter and CSA were calculated from a digital image taken while the fiber was briefly suspended in air (<5 s). Peak isometric force (P_o) and unloaded shortening velocity (V_o) were measured from the slack test. The number of fibers (*n*) for each cohort is reported in parentheses. The percent difference between young and old men and women were reported when $P < 0.05$. Values are means ± SD.

Presented in Table 4.2 are the fiber diameter, CSA, absolute and size specific P_o, and V_o from the 102 MHC IIa fibers studied in the pH 7.0 + 0 mM P_i condition. The CSA of MHC IIa fibers was 44% smaller in fibers from old (3,356 ± 1,538 μm^2) compared to young adults (6,004 ± 2,787 μm^2) and 36% smaller in fibers from women (3,499 ± 1,250 μm^2) compared to men (5,499 ± 3,047 μm^2). Accordingly, the absolute P_o was 40% lower in fibers from old (0.75 ± 0.29 mN) compared to young adults (1.25 ± 0.57 mN) and 34% lower in fibers from women (0.77 ± 0.25 mN) compared to men (1.16 ± 0.60 mN). The differences in absolute P_o were explained entirely by the differences in fiber CSA as indicated by the 10% greater size specific P_o in old (232 ± 40 $kN \cdot m^{-2}$) compared to young adults (211 ± 26 $kN \cdot m^{-2}$) and no sex differences in the size specific P_o in men (221 ± 38 $kN \cdot m^{-2}$) compared to women (225 ± 34 $kN \cdot m^{-2}$). Independent of age and sex, the size specific P_o was 20% lower in MHC I (179 ± 35 $kN \cdot m^{-2}$) compared with IIa fibers (223 ± 36 $kN \cdot m^{-2}$) ($P < 0.001$).

The unloaded shortening velocity (V_o) of MHC IIa fibers did not differ between fibers from young (3.80 ± 0.81 $fl \cdot s^{-1}$) and old adults (3.60 ± 0.90 $fl \cdot s^{-1}$). Independent of

age however, the V_o of MHC IIa fibers was 15% lower in fibers from women (3.38 ± 0.82 $fl \cdot s^{-1}$) compared to men (3.99 ± 0.81 $fl \cdot s^{-1}$).

		Men			Women			*P* -value		
		Young (19)	Old (32)	Diff.	Young (25)	Old (26)	Diff.	Age	Sex	Age x Sex
Diameter	μm	103.3 ± 25.4	66.9 ± 15.8	↓ 35%	71.6 ± 9.1	59.7 ± 13.0	↓ 17%	**0.007**	**0.015**	0.142
CSA	μm^2	8,520 ± 2,311	3,705 ± 1,718	↓ 57%	4,093 ± 1,044	2,927 ± 1,176	↓ 29%	**0.009**	**0.013**	0.091
Absolute P_o	mN	1.77 ± 0.45	0.80 ± 0.30	↓ 55%	0.86 ± 0.21	0.68 ± 0.25	↓ 21%	**0.024**	**0.028**	0.118
Size Specific P_o	$kN \cdot m^{-2}$	209.4 ± 26.3	228.1 ± 42.2	↑ 9%	212.1 ± 26.9	236.4 ± 36.4	↑ 11%	**0.045**	0.462	0.887
V_o	$fl \cdot s^{-1}$	3.94 ± 0.89	4.02 ± 0.79	↔	3.67 ± 0.75	3.09 ± 0.78	↔	0.207	**0.018**	0.178

Table 4.2. Peak isometric force (P_o) and unloaded shortening velocity (V_o) of fast MHC IIa fibers in pH 7.0 + 0 mM P_i activating solution at 15°C. The number of fibers (*n*) for each cohort is reported in parentheses. The percent difference between young and old men and women were reported when $P < 0.05$. Boldfaced *P*-values highlight statistical significance at $P < 0.05$. Values are means ± SD.

Cumulative Effects of P_i and H^+ on the Force-Velocity Relationship and Peak Power

Figure 4.1 depicts force-velocity and force-power curves from a representative fast MHC IIa fiber exposed to a condition mimicking quiescent human skeletal muscle (pH 7.0 + 4 mM P_i) and conditions that mimic mild (pH 6.8 + 12 mM P_i), moderate (pH 6.6 + 20 mM P_i), and severe fatigue (pH 6.2 + 30 mM P_i). The cumulative effects of progressively elevating the levels of H^+ and P_i caused the force-velocity relationship to shift down and to the left (Fig. 4.1A). The P_i- and H^+-induced decrements in fiber force and velocity caused peak fiber power to progressively decrease with increasing concentrations of H^+ and P_i (Fig. 4.1B).

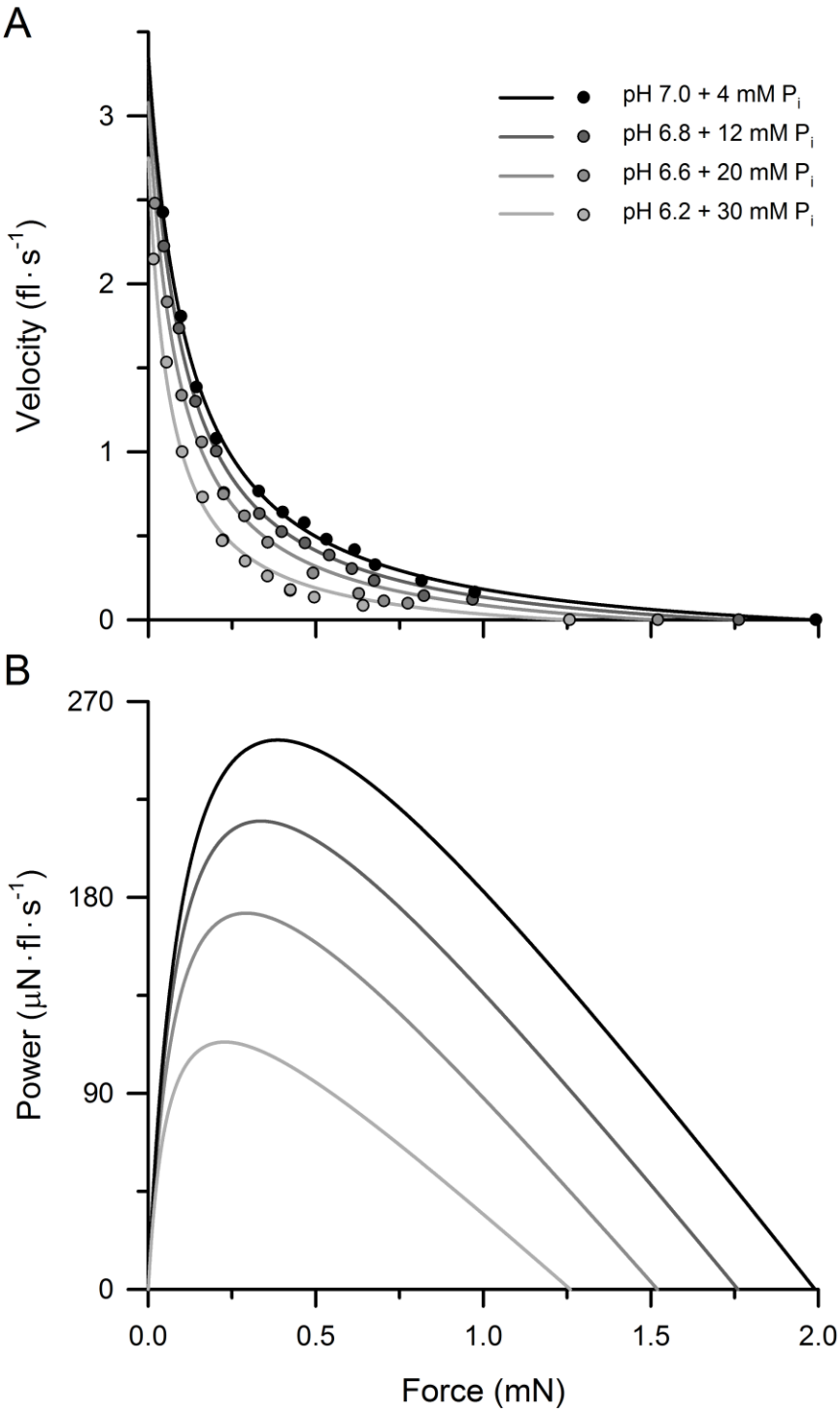

Figure 4.1. Representative force-velocity and force-power curves from a fast MHC IIa fiber at 15°C. An individual fiber was activated 4-6 times in each condition to obtain the fiber shortening velocities from a minimum of 12 different isotonic loads for all 4 activating conditions. Force-velocity plots were fit with the hyperbolic Hill equation (1938) for each condition (A). The force-power curves (B) were constructed by calculating the power values for each force level from the force-velocity curves. Data are from a 32 yr old male.

Peak isometric force (P_o): The P_o of MHC I fibers from young and old men and women progressively decreased with increasing concentrations of P_i and H^+ (Fig. 4.2) ($P < 0.001$). However, the P_i- and H^+-induced decrements in P_o did not differ between the cohorts in any of the conditions ($P > 0.05$). Independent of age and sex, the P_o of MHC I fibers was reduced by 17 ± 6%, 25 ± 8%, and 41 ± 8% in the mild-, moderate-, and severe-fatigue conditions compared to the 4 mM P_i condition, respectively ($P < 0.001$).

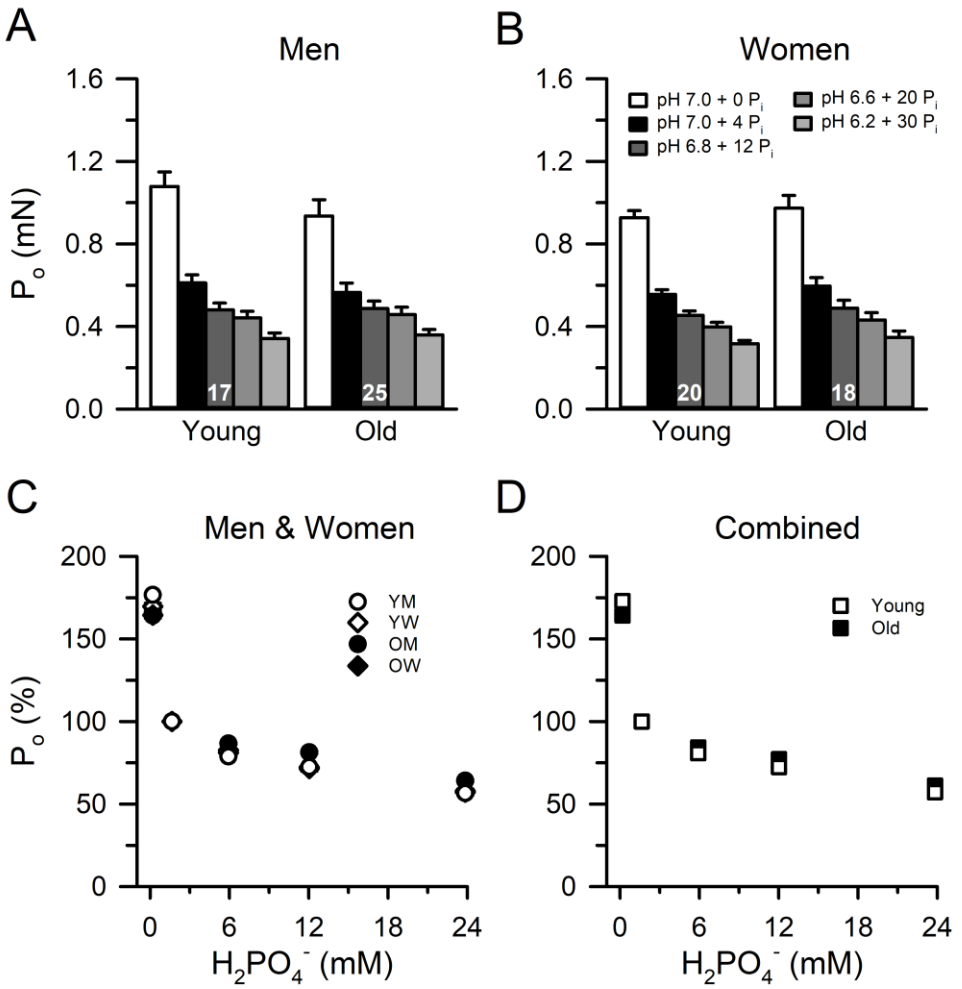

Figure 4.2. Peak isometric force (P_o) of MHC I fibers from young and old men and women. P_o progressively decreased with increasing concentrations of P_i and H^+ in the MHC I fibers from young and old men (A) and women (B). However, the cumulative effects of H^+ and P_i, which was represented as the concentration of dihydrogen phosphate ($H_2PO_4^-$), did not differ between any of the cohorts when analyzed separately (C) or when men and women were combined (D). Values are means ± SE, with the number of fibers (*n*) displayed within the bars. Error bars in panels C and D are obscured by the symbols.

Similar to the findings from MHC I fibers, the P_o of MHC IIa fibers progressively decreased with increasing concentrations of P_i and H^+ (Fig. 4.3) ($P < 0.001$). The P_i- and H^+-induced decrements in MHC IIa fiber P_o did not differ between the cohorts in any of the conditions ($P > 0.05$). Independent of age and sex, the P_o of MHC IIa fibers was reduced by 13 ± 4%, 24 ± 5%, and 40 ± 4% in the mild-, moderate-, and severe-fatigue conditions compared to the 4 mM P_i condition, respectively ($P < 0.001$).

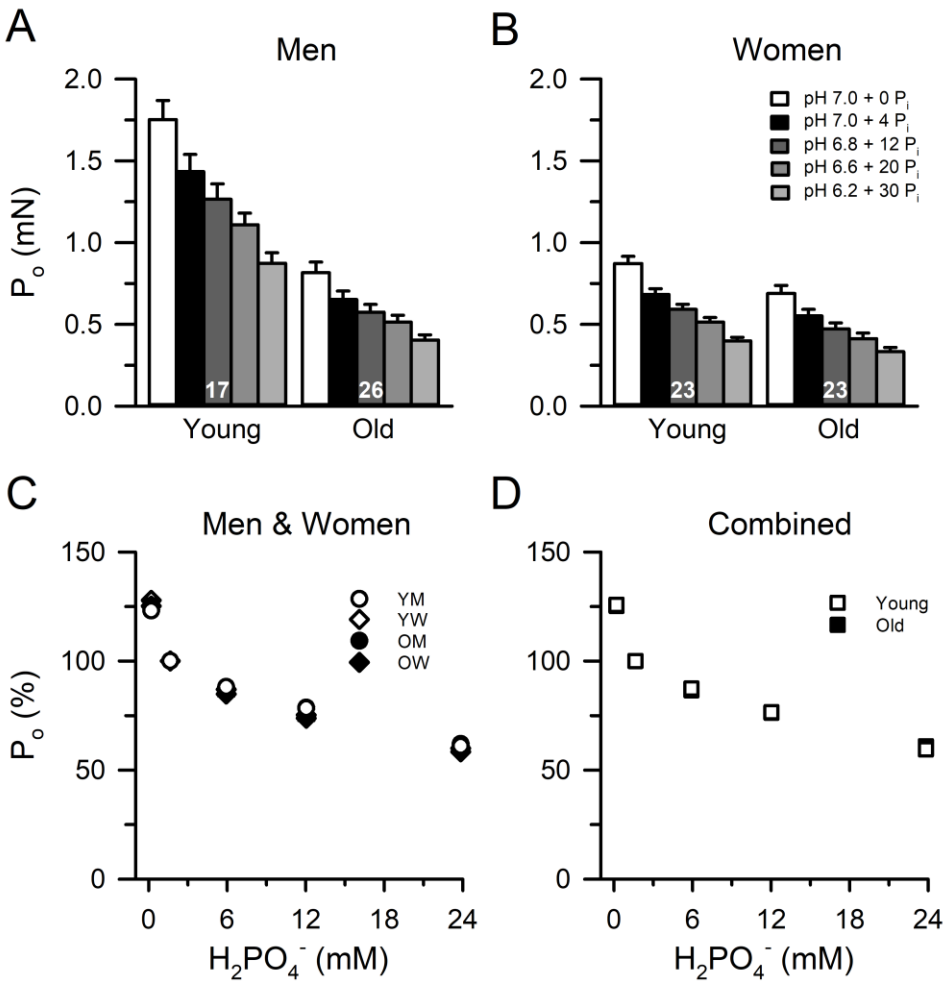

Figure 4.3. Peak isometric force (P_o) of MHC IIa fibers from young and old men and women. P_o progressively decreased with increasing concentrations of P_i and H^+ in the MHC IIa fibers from young and old men (A) and women (B). However, the cumulative effects of H^+ and P_i, represented by the $[H_2PO_4^-]$, did not differ between any of the cohorts when analyzed separately (C) or when men and women were combined (D). Values are means ± SE, with the number of fibers (*n*) displayed within the bars. Error bars in panels C and D are obscured by the symbols.

Force-velocity curves and peak power: There were no age or sex differences in the force-velocity parameters of MHC I fibers for any of the activating conditions (Table 4.3). Independent of age and sex, P_o, V_{max}, and peak power progressively decreased with increasing concentrations of P_i and H^+. The P_i- and H^+-induced changes in P_o, V_{max}, and a/P_o did not differ between the age groups or between men and women (Table 4.3). However, the P_i- and H^+-induced decrements in peak power (Fig. 4.4) were greater in women compared to men in the moderate- (women = -29 ± 8%, men = -20 ± 8%; *P* = 0.020) and severe-fatigue conditions (women = -54 ± 7%, men = -49 ± 5%; *P* = 0.020).

	Men		Women		Combined	
	Young (17)	Old (25)	Young (20)	Old (18)	Young (37)	Old (43)
Peak Power ($\mu N \cdot fl \cdot s^{-1}$)						
pH 7.0 + 4 mM P_i	23.8 ± 8.0	22.5 ± 8.1	22.2 ± 6.5	21.3 ± 6.0	22.9 ± 7.2	22.0 ± 7.3
pH 6.8 + 12 mM P_i	21.8 ± 7.6	20.5 ± 7.7	20.0 ± 6.1	18.9 ± 5.6	20.8 ± 6.8	19.8 ± 6.8
pH 6.6 + 20 mM P_i	19.0 ± 6.6	17.8 ± 6.8	15.7 ± 4.8	15.1 ± 4.6	17.2 ± 5.8	16.7 ± 6.1
pH 6.2 + 30 mM P_i	12.1 ± 4.0	11.5 ± 4.6	10.3 ± 3.4	9.7 ± 3.2	11.2 ± 3.7	10.7 ± 4.1
Peak Power ($W \cdot \Gamma^{1}$)						
pH 7.0 + 4 mM P_i	3.4 ± 0.8	4.6 ± 1.3	4.1 ± 1.1	4.5 ± 1.0	3.8 ± 1.0	4.5 ± 1.2
pH 6.8 + 12 mM P_i	3.1 ± 0.7	4.1 ± 1.1	3.7 ± 1.1	4.0 ± 0.9	3.4 ± 1.0	4.1 ± 1.0
pH 6.6 + 20 mM P_i	2.7 ± 0.5	3.6 ± 0.9	2.9 ± 0.9	3.2 ± 0.7	2.8 ± 0.7	3.4 ± 0.8
pH 6.2 + 30 mM P_i	1.7 ± 0.4	2.3 ± 0.6	1.9 ± 0.6	2.0 ± 0.6	1.8 ± 0.5	2.2 ± 0.6
V_{max} ($fl \cdot s^{-1}$)						
pH 7.0 + 4 mM P_i	1.50 ± 0.19	1.56 ± 0.18	1.57 ± 0.19	1.45 ± 0.42	1.54 ± 0.19	1.52 ± 0.31
pH 6.8 + 12 mM P_i	1.43 ± 0.18	1.47 ± 0.17	1.48 ± 0.17	1.34 ± 0.25	1.45 ± 0.17	1.42 ± 0.22
pH 6.6 + 20 mM P_i	1.33 ± 0.18	1.40 ± 0.14	1.36 ± 0.18	1.22 ± 0.23	1.35 ± 0.18	1.32 ± 0.20
pH 6.2 + 30 mM P_i	1.20 ± 0.15	1.24 ± 0.15	1.25 ± 0.18	1.11 ± 0.19	1.23 ± 0.17	1.19 ± 0.18
a/P_o						
pH 7.0 + 4 mM P_i	0.038 ± 0.008	0.038 ± 0.005	0.037 ± 0.007	0.038 ± 0.008	0.037 ± 0.006	0.038 ± 0.007
pH 6.8 + 12 mM P_i	0.048 ± 0.007	0.043 ± 0.005	0.045 ± 0.011	0.046 ± 0.012	0.047 ± 0.010	0.044 ± 0.009
pH 6.6 + 20 mM P_i	0.050 ± 0.011	0.042 ± 0.005	0.044 ± 0.010	0.046 ± 0.013	0.047 ± 0.011	0.043 ± 0.009
pH 6.2 + 30 mM P_i	0.049 ± 0.016	0.037 ± 0.007	0.038 ± 0.009	0.039 ± 0.012	0.043 ± 0.014	0.038 ± 0.009

Table 4.3. Force-velocity parameters and peak power of slow MHC I fibers from young and old men and women. Absolute ($\mu N \cdot fl \cdot s^{-1}$) and size specific ($W \cdot l^{-1}$) peak power were calculated with the fitted-parameters from the force-velocity curves. The maximal shortening velocity (V_{max}) was calculated using the Hill equation (1938), and the a/P_o ratio is a unitless parameter describing the curvature of the force-velocity relationship. The number of fibers (*n*) for each cohort is reported in parentheses. Values are means ± SD.

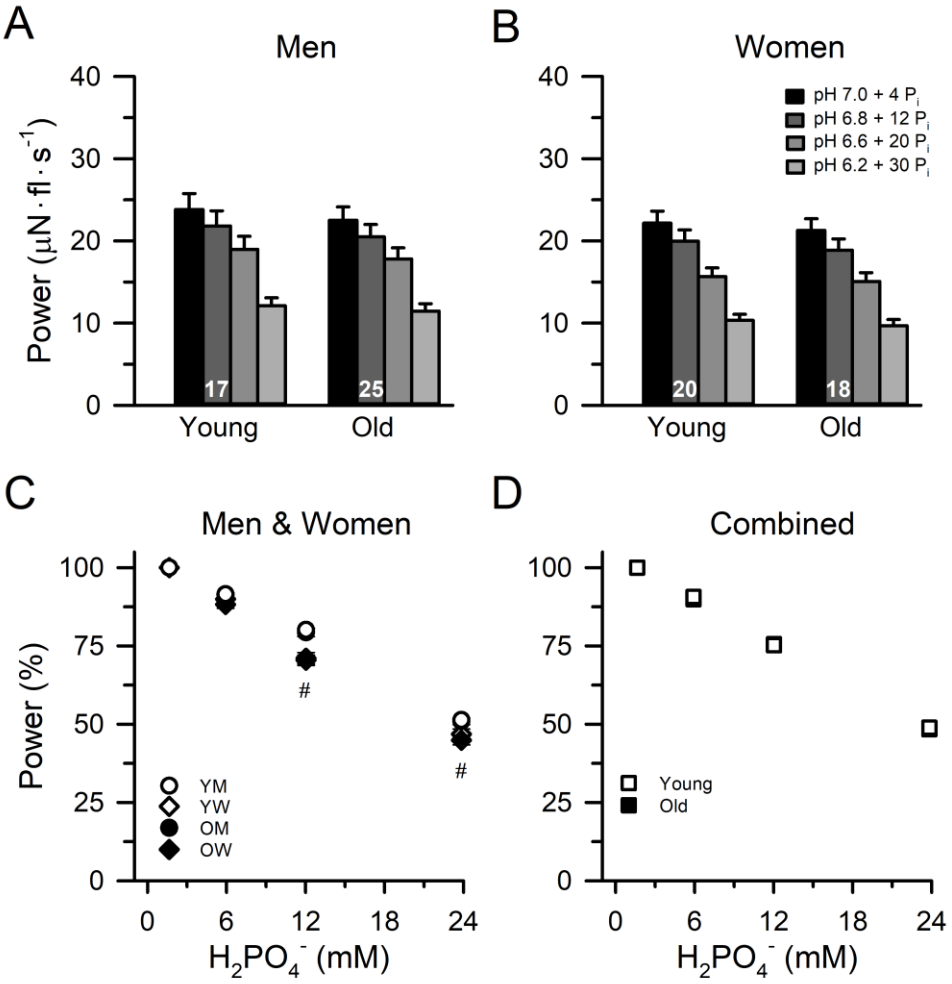

Figure 4.4. Peak power of slow MHC I fibers from young and old men and women. Peak power progressively decreased with increasing concentrations of P_i and H^+ in MHC I fibers from young and old men (A) and women (B). The H^+- and P_i-induced decrements in power were greater in women compared to men in the moderate- and severe-fatigue conditions (C) but did not differ between fibers from young and old adults (D). Values are means ± SE, with the number of fibers (*n*) displayed within the bars. Error bars in panels C and D are obscured by the symbols. # significantly different from men ($P < 0.05$).

Peak power of MHC IIa fibers from young and old men and women are shown in Figure 4.5, with the key force-velocity parameters reported in Table 4.4. Peak absolute power outputs were 41-44% lower in old compared to young adults ($P < 0.05$) and 37-43% lower in women compared to men in all 4 activating conditions ($P < 0.05$). The differences in absolute power were explained entirely by the differences in fiber CSA as

indicated by the lack of age or sex differences in the size specific peak power in any of the conditions (Table 4.4). Independent of age and sex, P_o, V_{max}, and peak power of MHC IIa fibers progressively decreased with increasing concentrations of P_i and H^+. Similar to the findings on MHC I fibers, the P_i- and H^+-induced changes in P_o, V_{max}, and a/P_o did not differ between the age groups or between men and women (Table 4.4). However, the P_i- and H^+-induced decrements in peak power (Fig. 4.5) were greater in women compared to men in the severe-fatigue condition (women = -54 ± 7%, men = -49 ± 5%; $P = 0.020$).

	Men		Women		Combined	
	Young (17)	Old (26)	Young (23)	Old (23)	Young (40)	Old (49)
Peak Power ($\mu N \cdot fl \cdot s^{-1}$)						
pH 7.0 + 4 mM P_i *#	173.6 ± 52.7	83.2 ± 25.2	89.1 ± 26.1	60.9 ± 24.2	125.0 ± 57.6	72.7 ± 26.9
pH 6.8 + 12 mM P_i *#	154.9 ± 49.1	72.9 ± 22.7	78.5 ± 24.9	51.8 ± 21.7	111.0 ± 53.0	63.0 ± 24.4
pH 6.6 + 20 mM P_i *#	128.1 ± 39.1	59.8 ± 17.8	63.8 ± 20.8	41.2 ± 17.8	91.1 ± 43.7	51.1 ± 20.0
pH 6.2 + 30 mM P_i *#	80.2 ± 23.7	39.6 ± 12.5	38.2 ± 12.4	25.3 ± 12.1	56.1 ± 27.6	32.9 ± 14.2
Peak Power ($W \cdot l^{-1}$)						
pH 7.0 + 4 mM P_i	20.5 ± 3.9	24.5 ± 6.2	21.4 ± 3.1	21.0 ± 5.8	21.1 ± 3.5	22.9 ± 6.2
pH 6.8 + 12 mM P_i	18.4 ± 3.8	21.5 ± 5.6	18.8 ± 2.9	17.8 ± 5.2	18.6 ± 3.3	19.8 ± 5.6
pH 6.6 + 20 mM P_i	15.3 ± 3.2	17.9 ± 5.1	15.3 ± 2.7	14.2 ± 4.3	15.3 ± 2.9	16.1 ± 5.1
pH 6.2 + 30 mM P_i	9.6 ± 2.0	11.7 ± 2.9	9.2 ± 1.8	8.73 ± 3.3	9.4 ± 1.9	10.3 ± 3.4
V_{max} ($fl \cdot s^{-1}$)						
pH 7.0 + 4 mM P_i	3.83 ± 0.47	3.88 ± 0.65	3.73 ± 0.47	3.05 ± 0.61	3.77 ± 0.47	3.49 ± 0.75
pH 6.8 + 12 mM P_i	3.60 ± 0.47	3.52 ± 0.42	3.47 ± 0.39	2.85 ± 0.62	3.53 ± 0.43	3.20 ± 0.62
pH 6.6 + 20 mM P_i	3.41 ± 0.43	3.32 ± 0.34	3.34 ± 0.35	2.72 ± 0.68	3.37 ± 0.38	3.03 ± 0.60
pH 6.2 + 30 mM P_i	3.04 ± 0.39	2.82 ± 0.43	2.91 ± 0.28	2.35 ± 0.69	2.97 ± 0.33	2.60 ± 0.61
a/P_o						
pH 7.0 + 4 mM P_i	0.049 ± 0.007	0.056 ± 0.016	0.056 ± 0.008	0.058 ± 0.010	0.053 ± 0.008	0.057 ± 0.013
pH 6.8 + 12 mM P_i	0.054 ± 0.007	0.063 ± 0.017	0.062 ± 0.011	0.063 ± 0.011	0.059 ± 0.010	0.063 ± 0.014
pH 6.6 + 20 mM P_i	0.053 ± 0.008	0.061 ± 0.017	0.060 ± 0.011	0.061 ± 0.013	0.057 ± 0.010	0.061 ± 0.015
pH 6.2 + 30 mM P_i	0.047 ± 0.007	0.060 ± 0.017	0.051 ± 0.010	0.049 ± 0.011	0.049 ± 0.009	0.055 ± 0.015

Table 4.4. Force-velocity parameters and peak power of fast MHC IIa fibers from young and old men and women. Absolute ($\mu N \cdot fl \cdot s^{-1}$) and size specific ($W \cdot l^{-1}$) peak power were calculated with the fitted-parameters from the force-velocity curves. The maximal shortening velocity (V_{max}) was calculated using the Hill equation (1938), and the a/P_o ratio is a unitless parameter describing the curvature of the force-velocity relationship. The number of fibers (*n*) for each cohort is reported in parentheses. Symbols next to the activating condition indicate a main effect of *age and #sex at $P < 0.05$. Values are means ± SD.

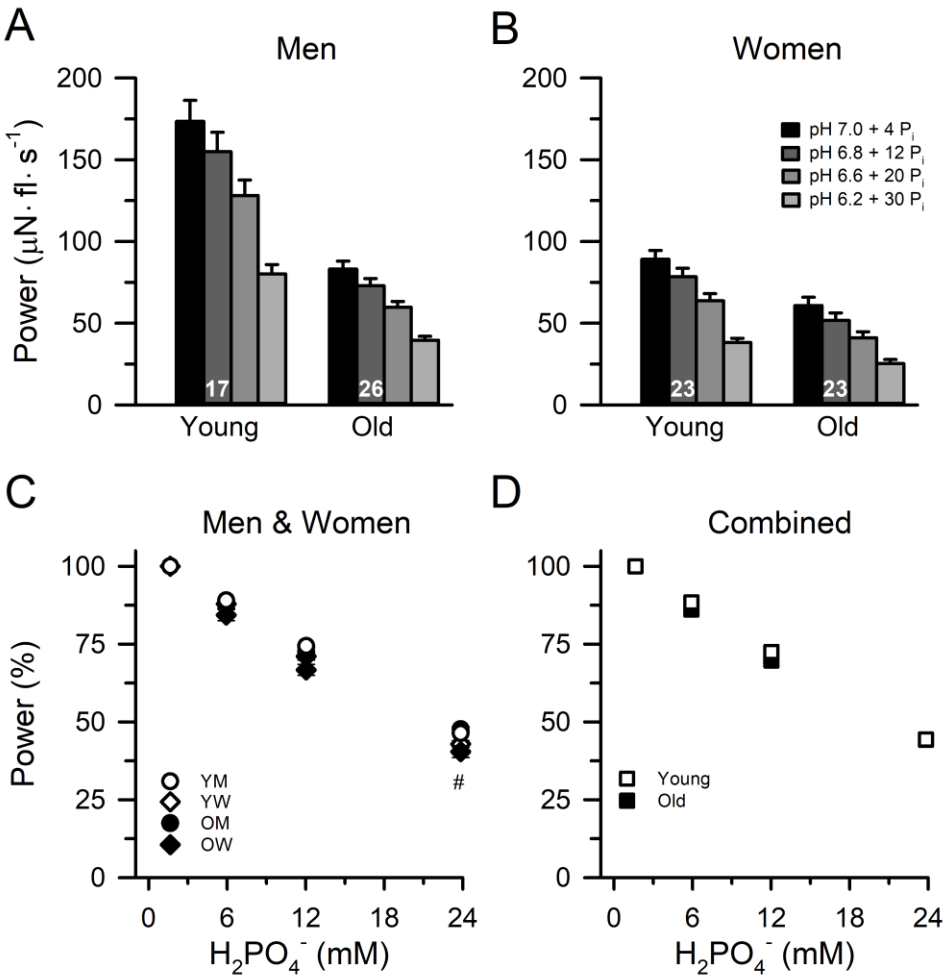

Figure 4.5. Peak power of fast MHC IIa fibers from young and old men and women. Peak power progressively decreased with increasing concentrations of P_i and H^+ in MHC IIa fibers from young and old men (A) and women (B). The H^+- and P_i-induced decrements in power were greater in women compared to men in the severe-fatigue conditions (C) but did not differ between fibers from young and old adults (D). Values are means ± SE, with the number of fibers (*n*) displayed within the bars. Error bars in panels C and D are obscured by the symbols. # significantly different from men ($P < 0.05$).

Fiber Type Differences for the Cumulative Effects of P_i and H^+ Independent of Age & Sex

Peak isometric force (P_o): The fiber type differences in P_o doubled when [P_i] was increased from ~0 to 4 mM (Fig. 4.6A), whereby the size specific P_o was 39% lower in MHC I (108 ± 25 kN·m^{-2}) compared to MHC IIa fibers in the pH 7.0 + 4 mM P_i condition (177 ± 31 kN·m^{-2}) ($P < 0.001$). The increase in the fiber type difference in size specific P_o

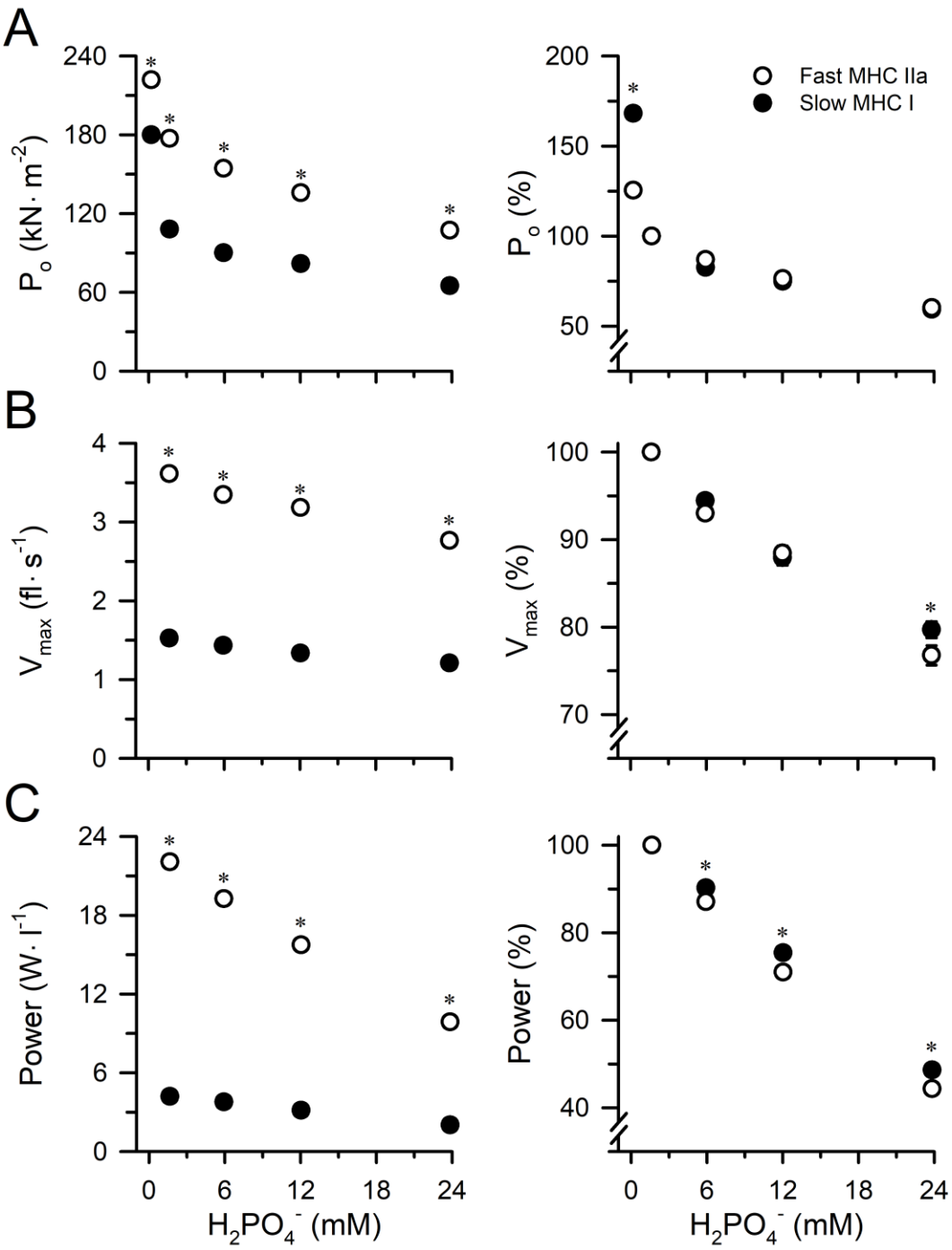

Figure 4.6. Cumulative effects of H^+ and P_i on force, velocity, and power in fast MHC IIa and slow MHC I fibers. Peak isometric force (P_o), maximal shortening velocity (V_{max}) and peak power progressively decreased with increasing concentrations of P_i and H^+ in both MHC IIa and MHC I fibers from young and old men and women. Decreasing the [P_i] from 4 to ~0 mM increased P_o more in slow compared to fast fibers (A). The reductions in V_{max} were greater in MHC IIa compared to MHC I fibers in the severe fatigue condition (B), whereas, the reductions in peak power were greater in MHC IIa fibers in all 3 fatigue-mimicking conditions (C). Values are means ± SE. Error bars are obscured by the symbols. * significant difference between slow and fast fibers ($P < 0.05$).

with the small increase in [P_i] was due to a greater sensitivity of MHC I fibers to P_i ($P < 0.001$). However, the H^+- and P_i-induced decrements in P_o in the mild, moderate, and severe-fatigue mimicking conditions did not differ between the fiber types when expressed as a percentage of P_o in the 4 mM P_i condition (Fig. 4.6A).

Maximal shortening velocity (V_{max}): V_{max} in all 4 activating conditions was ~2.4-fold greater in fast MHC IIa compared to slow MHC I fibers (Fig. 4.6B). The V_{max} progressively decreased in both fiber types with the increase in the concentrations of H^+ and P_i. However, the reduction in V_{max} was greater in MHC IIa compared to MHC I fibers in the severe-fatigue condition ($P < 0.05$), with no fiber type differences for the reductions in V_{max} in the mild- and moderate-fatigue conditions ($P > 0.05$).

Peak power: The size specific peak power in all 4 activating conditions was ~5-fold greater in fast MHC IIa compared to slow MHC I fibers (Fig. 4.6C). The higher peak power in MHC IIa fibers was primarily explained by the ~1.7-fold greater size specific P_o and ~2.4-fold greater V_{max} in MHC IIa compared to MHC I fibers, but was also partially due to the lower curvature (i.e., higher a/P_o ratio) of the force-velocity relationship in MHC IIa compared to MHC I fibers (Tables 4.3 and 4.4). Consistent with the effects of P_i and H^+ on P_o and V_{max}, peak power progressively decreased in both fiber types with the increase in the concentrations of H^+ and P_i. However, the P_i- and H^+-induced decrements in power were 3-5% greater in MHC IIa compared to MHC I fibers for all 3 fatigue-mimicking conditions (Fig. 4.6C).

DISCUSSION

The purpose of this study was to determine the cumulative effects of H^+ and P_i on the force-velocity relationship of skeletal muscle fibers from young and old adults across

a range of metabolite concentrations that regularly occur *in vivo*. In agreement with the first hypothesis, there was a hyperbolic relationship between the decrements in peak isometric force and the increase in the concentrations of H^+ and P_i for both slow MHC I and fast MHC IIa fibers (Figs. 4.2 and 4.3). However, when the analysis was restricted to only include the concentrations of these ions observed *in vivo* (Kemp *et al.*, 2007), the relationship between the decrements in isometric force and the increased concentration of these ions was linear. Similarly, the shortening velocity and peak power decreased linearly with the increase in the concentrations H^+ and P_i (Fig. 4.6). Contrary to the second hypothesis, the depressive effects of these ions were similar in fibers from young and old adults across all conditions. These data support the conclusion from chapter 3 that the age-related increase in fatigability cannot be attributed to an increased sensitivity of the cross-bridge to H^+ and P_i.

Cumulative effects of H^+ and P_i on cross-bridge function: important mediators of human muscle fatigue

Studies on the effects of H^+ and P_i on cross-bridge function have focused on either the individual effects of these ions or tested their effects under extreme concentrations (Metzger & Moss, 1987; Chase & Kushmerick, 1988; Pate & Cooke, 1989; Metzger & Moss, 1990b; Fryer *et al.*, 1995; Pate *et al.*, 1995; Potma *et al.*, 1995; Debold *et al.*, 2004; Debold *et al.*, 2006; Knuth *et al.*, 2006; Nelson *et al.*, 2014; Nelson & Fitts, 2014). In addition, no studies have tested the effects of H^+ and P_i on human skeletal muscle, which differ markedly in their contractile kinetics, fiber type distribution, and metabolic properties compared to muscles from smaller mammalian or amphibious species (Shirokova *et al.*, 1996; Edman, 2005; Schiaffino, 2010; Schiaffino & Reggiani, 2011). In

this chapter, it was observed that isometric force, shortening velocity, and peak power of human skeletal muscle fibers all decreased linearly with the increase in the concentrations of H^+ and P_i, and that the detrimental effects of these ions on cross-bridge function showed no signs of saturating at the higher concentrations. These novel findings have important implications for human skeletal muscle performance, because the accumulation of H^+ and P_i within the myoplasm occur at the onset of high-intensity contractile activity and continue to accumulate until the individual can no longer perform the task (Hogan *et al.*, 1999; Jones *et al.*, 2008; Chidnok *et al.*, 2013; Broxterman *et al.*, 2017). The detrimental effects of these ions may be particularly important to the physical performance of older adults, because they already have an impaired strength and power generating capacity compared to younger adults (Doherty, 2003; Reid & Fielding, 2012; Hunter *et al.*, 2016).

Similar to the findings on the effects of P_i on isometric force (Fryer *et al.*, 1995; Wang & Kawai, 1997; Coupland *et al.*, 2001; Tesi *et al.*, 2002; Pathare *et al.*, 2005), the relationship between the decrements in isometric force and the increase in the concentrations of both H^+ and P_i was hyperbolic. However, the hyperbolic relationship was only observed when the data from the pH 7.0 + 0 mM P_i condition were included – a condition that does not occur in human skeletal muscle *in vivo* (Kemp *et al.*, 2007). In contrast, when the data from the ~0 mM P_i condition were excluded, there was a linear relationship between the decrements in isometric force and the increase in the concentrations of H^+ and P_i. This finding is in close agreement with the linear relationship observed between the concentrations of dihydrogen phosphate ($H_2PO_4^-$) and the reductions in force in both young and old adults during a fatiguing isometric exercise

(Kent-Braun *et al.*, 2002; Lanza *et al.*, 2007). Collectively, these results provide strong evidence that H^+ and P_i are important mediators of human muscle fatigue by directly impairing the ability of the cross-bridge to generate force. Whether dihydrogen phosphate is the primary phosphate species to inhibit isometric force is unknown (Nosek *et al.*, 1987); however, it does provide an accurate marker to quantify the changes occurring in both H^+ and P_i because $H_2PO_4^-$ becomes the predominant species with the decrease in pH ($H_2PO_4^-$ pKa = 6.75 at 38˚C) (Lawson & Veech, 1979).

Surprisingly, the decrements in the maximal shortening velocity also showed a linear relationship with the increase in the concentrations of H^+ and P_i for both fast MHC IIa and slow MHC I fibers. There are a large number of animal studies demonstrating that P_i has little-to-no effect on shortening velocity, and that H^+ is the primary ion that inhibits velocity (Metzger & Moss, 1987; Chase & Kushmerick, 1988; Cooke *et al.*, 1988; Widrick, 2002; Debold *et al.*, 2004; Karatzaferi *et al.*, 2008; Nelson *et al.*, 2014; Debold *et al.*, 2016). However, controversy still exists as to the relative importance of decreased pH in inhibiting velocity (Pate *et al.*, 1995; Westerblad *et al.*, 1997; Knuth *et al.*, 2006; Karatzaferi *et al.*, 2008; Fitts, 2016; Westerblad, 2016), which has led to the hypothesis that H^+ does not inhibit shortening velocity until pH drops below 6.7 (Fitts, 2008). In contrast, we observed that the maximal shortening velocity measured by extrapolation of the force-velocity relationship (V_{max}) was already significantly decreased in the pH 6.8 + 12 mM P_i condition, albeit only by ~6%, and continued to decrease with the increase in the concentrations of H^+ and P_i. The explanation for the discrepancies between these findings compared with findings from animal studies is unclear, but perhaps is due to

differences in the contractile kinetics between mammalian species or that the pH 6.8 condition was studied in combination with 12 mM P_i.

It is notable that the fatigue-induced reductions in the maximal shortening velocity of the human adductor pollicis muscle *in vivo* (Jones *et al.*, 2006) has a time course that is generally similar to the changes in intracellular pH during fatiguing exercise (Fiedler *et al.*, 2016; Broxterman *et al.*, 2017). Specifically, during high-intensity exercise, intracellular pH initially becomes slightly more alkaline due to the predominance of ATP synthesized by the creatine kinase reaction (Adams *et al.*, 1990) followed by the precipitous decline in pH from the high rates of ATP hydrolysis and increased glycolytic flux (Robergs *et al.*, 2004). The delay in H^+ accumulation mirrors the delay in the fatigue-induced reduction in shortening velocity observed in the human adductor pollicis muscle *in vivo* (Jones *et al.*, 2006). These results interpreted together with the findings presented in this study suggest that H^+ is an important factor for the fatigue-induced reduction in shortening velocity of human skeletal muscle.

Although valuable mechanistic insight is gleaned from examining the effects of H^+ and P_i on peak isometric force and maximal shortening velocity, these parameters represent only two extremes of the force-velocity relationship. Thus, it is important from both a human performance and an aging perspective to examine how these ions influence the ability of skeletal muscle to shorten under submaximal loads and generate power. The combination of the P_i- and H^+-induced reductions in force and H^+ inhibition of shortening velocity resulted in marked decrements in peak power in both MHC I and IIa fibers in all three fatigue-mimicking conditions. Similar to the findings on isometric force and shortening velocity, there was a linear relationship between the decrements in peak power

and the increase in the concentrations of H^+ and P_i. The H^+- and P_i-induced reductions in peak power however, were 3-5% greater in MHC IIa compared with MHC I fibers (Fig. 4.6). The explanations for the fiber type dependence in the decrements in power are unclear but may be due, in part, to differences in the H^+- and P_i-induced changes in the curvature of the force-velocity relationship (a/P_o) in the fatigue-mimicking conditions.

Sex differences in single fiber contractile function

A surprising finding from these preliminary data was that, independent of age, the V_o of fast MHC IIa fibers from women was 15% lower than fibers from men (Table 4.2). Additionally, the H^+- and P_i-induced decrements in peak power were greater in both MHC I and IIa fibers from women compared to men (Figs. 4.4 and 4.5). These data are difficult to interpret in the context of the prevailing literature. For example, while there is evidence from one study that V_o in MHC I fibers from old women is reduced (Krivickas *et al.*, 2001), there is no evidence for a lower V_o in MHC IIa fibers from young or old women compared to men (Krivickas *et al.*, 2001; Trappe *et al.*, 2003). In addition, the fatigability and the associated mechanisms for both isolated limb exercise (Chapter 2) and whole-body dynamic exercise (Sundberg *et al.*, 2017) have been shown to be similar between men and women. In the few studies that have observed a sex difference in fatigability during dynamic exercise, most have found that women are less fatigable than men (Laurent *et al.*, 2010; Billaut & Bishop, 2012; Yoon *et al.*, 2015). In contrast, the single fiber data in this chapter reveal that both slow MHC I and fast MHC IIa fibers from women experience greater H^+- and P_i-induced decrements in power compared to fibers from men. The explanation for the sex differences in V_o and the sensitivity of the cross-bridge to elevated levels of H^+ and P_i is unclear. More data need to be collected

before a conclusion can be drawn regarding sex differences in single fiber contractile function, because currently data from only 2 old women and 3 young women have been collected.

CHAPTER 5

GENERAL DISCUSSION AND FUTURE DIRECTIONS

The purpose of this dissertation was to identify the mechanisms for the age-related increase in fatigability during dynamic contractions in both men and women. A highly-integrative approach was employed to study fatigue within both the intact neuromuscular system and in the isolated muscle cell with the aim of developing a comprehensive understanding of the fatigue process with aging. While the studies in this dissertation provide important advancements in the field, the mechanism responsible for the increased fatigability with aging remains elusive. This chapter provides a summary of the key findings from the dissertation and proposes future studies that may fill some of the voids in knowledge of the aging neuromuscular system and fatigue.

In chapter 2, non-invasive stimulation procedures were used to localize where along the motor pathway the primary mechanism of fatigue was originating in groups of young (≤35 yrs), old (60-79 yrs), and very old (≥80 yrs) men and women. This study was the first to 1) couple stimulations to both the motor cortex and the peripheral nervous system to identify the mechanisms of fatigue elicited by high-velocity dynamic exercise in old adults and 2) test whether the mechanisms for the age-related increase in fatigability differed between men and women. We found that aging of the neuromuscular system resulted in a progressive increase in fatigability of the knee extensors during high-velocity exercise that was more pronounced in very old adults (≥80 yrs) but occurred similarly in men and women in all age groups (Fig. 2.3). Importantly, the age-related increase in power loss could not be attributed to reduced neural drive from the motor cortex (Fig. 2.5) or impairments in neuromuscular propagation (Fig. 2.6), but was

strongly associated with changes in the electrically-evoked contractile properties in both men and women (Fig. 2.7). These data strongly suggest that the age-related increase in power loss during high-velocity fatiguing exercise is unaffected by biological sex and implicates mechanisms that disrupt excitation-contraction coupling and/or cross-bridge function as the primary mechanisms for the age-related increase in fatigability. Whether the same mechanisms are responsible for the age-related increase in fatigability in muscles of the upper limb (Senefeld *et al.*, 2017) or in mobility impaired older adults is unknown and worth further investigation.

It is important to note that although the fatiguing exercise is referred to as a 'high-velocity' exercise, the angular velocity of the knee joint at the end of the exercise was reduced to 157 ± 36 °/s and 121 ± 32 °/s in the old and very old adults, respectively, compared with 224 ± 26 °/s in the young adults. In addition, for the oldest participant studied in this dissertation (a 93 yr old man) the knee angular velocity decreased by 67% over the course of the fatiguing exercise, from 172 °/s at the beginning to 56 °/s by the end of the exercise. These knee extension velocities – performed against a relatively light load (i.e., ~20% MVC) – fall at-or-below the peak knee angular velocities used when older participants (~74 yrs) perform routine daily tasks such as rising from a chair (138 ± 25 °/s) or ascending a flight of stairs (141 ± 25 °/s) (Hortobagyi *et al.*, 2003). Thus, identifying the mechanisms for the age-related slowing of the neuromuscular system and the increased fatigability during dynamic exercise is important, not only from a basic science perspective, but to develop evidence-based countermeasures to improve physical function, mobility, and the quality of life in old adults.

The most reputed mechanism of fatigue is the accumulation of metabolic by-products (H^+, P_i, $H_2PO_4^-$) that act to impair muscle force and power production either indirectly via sensory afferent feedback to the central nervous system (Bigland-Ritchie *et al.*, 1986; Gandevia, 2001; Amann *et al.*, 2011) or directly by disrupting excitation-contraction coupling and cross-bridge function (Fitts, 1994; Allen *et al.*, 2008; Fitts, 2008; Allen *et al.*, 2011; Debold *et al.*, 2016). In chapter 2, it was found that, for the most part, the ability of the motor cortex to voluntarily drive the muscle and the excitability of the corticospinal tract (VL MEP amplitude) did not differ between young and old adults following the fatiguing dynamic exercise, and that the primary mechanism for the increased fatigability with aging was in the muscle. This led to the hypothesis that age-related changes within the muscle may cause either 1) an increased production of metabolic by-products or 2) an increased sensitivity of the muscle to a given concentration of metabolite accumulation during high-velocity exercise. Given the evidence that the decrease in pH and increase in intracellular [P_i] during a dynamic plantarflexor exercise did not differ or was blunted in old compared to young adults (Layec *et al.*, 2013; Layec *et al.*, 2014, 2015), the latter hypothesis seemed like the more plausible mechanism for the increased fatigability with aging.

In chapter 3, skeletal muscle fibers isolated from the vastus lateralis of young and old men were exposed to conditions mimicking quiescent human muscle (pH 7.0 + 4 mM P_i) and severe fatigue (pH 6.2 + 30 mM P_i) to test the hypothesis that the increased fatigability with aging was due an increased sensitivity of cross-bridge to H^+ and P_i. This study was the first to examine the effects of elevated levels of H^+ and P_i on the cross-bridge mechanics of human skeletal muscle. We confirmed the findings from non-human

studies (Cooke *et al.*, 1988; Karatzaferi *et al.*, 2008; Nelson *et al.*, 2014) that elevated levels of H^+ (pH 6.2) and P_i (30 mM) act synergistically to depress cross-bridge function by inhibiting isometric force (Fig. 3.3), shortening velocity (Fig. 3.5), peak power (Figs. 3.6-3.8) and the low-to high-force transition of the cross-bridge cycle (Fig. 3.4). These findings are important for human neuromuscular performance, because they provide evidence that H^+ and P_i are essential mediators of muscle fatigue in humans by directly inhibiting cross-bridge function. However, the depressive effects of these ions under saturating Ca^{2+} conditions were similar in fibers from old compared to young men, which suggests that the age-related increase in fatigability could not be attributed to an increased sensitivity of the cross-bridge to H^+ and P_i.

The studies in chapter 3 used a severe fatigue-mimicking condition, because it was anticipated that the age-differences in the sensitivity of the contractile proteins to elevated levels of H^+ and P_i, if present, would be most obvious under this condition. However, the effects of these ions on cross-bridge function may have been saturated in the severe fatigue-mimicking condition, potentially masking any age-related differences in the sensitivity of the cross-bridge to these ions. As a result, the purpose of chapter 4 was to test this hypothesis by exposing muscle fibers from young and old men and women to a range of elevated levels of H^+ and P_i that regularly occur *in vivo* (Wilson *et al.*, 1988; Cady *et al.*, 1989; Kemp *et al.*, 2007; Burnley *et al.*, 2010; Broxterman *et al.*, 2017). This study was the first to test the effects of varying levels of H^+ and P_i on cross-bridge function in human skeletal muscle, and revealed that there was a linear relationship between the increased concentrations of H^+ and P_i and the decrements in fiber force (Figs. 4.2 & 4.3), velocity (Fig. 4.6), and power (Figs. 4.4 & 4.5). However,

similar to the findings in chapter 3 and contrary to the hypotheses, the H^+- and P_i-induced decrements in fiber power and velocity were similar in fibers from old compared to young adults. These data confirm the results from chapter 3 that the age-related increase in fatigability during dynamic exerciser cannot be attributed to an increased sensitivity of the cross-bridge to these ions. This conclusion prompts the question: What is the cellular mechanism within the muscle that is responsible for the age-related increase in fatigability during moderate- to high-velocity exercise?

One possibility is that the fatigue-mimicking conditions used in chapters 3 and 4 did not adequately mimic the intracellular milieu of the whole-muscle *in vivo*. For example, during high-intensity contractile activity proteins, such as myosin binding protein-C and myosin regulatory light chain (RLC), are phosphorylated and modulate the binding kinetics of myosin to actin (Vandenboom & Houston, 1996; Rassier & Macintosh, 2000; Szczesna *et al.*, 2002; Ackermann & Kontrogianni-Konstantopoulos, 2011; Vandenboom, 2016). Importantly, it was found in rat fibers that the H^+- and P_i-induced decrements in fiber shortening velocity and peak power were exacerbated when RLC was phosphorylated (Karatzaferi *et al.*, 2008). Whether aging or biological sex affects the phosphorylation state of the regulatory proteins has received limited attention (Miller *et al.*, 2013; Brocca *et al.*, 2017), and no studies have examined how the phosphorylation of these proteins alters contractile function in human skeletal muscle. Future studies should test the effects of the phosphorylation state of regulatory proteins on contractile function in fibers from young and old men and women in conditions that mimic quiescent muscle and in the presence of elevated H^+ and P_i.

In addition to altering the phosphorylation state of regulatory proteins, high-intensity fatiguing exercise is also thought to reduce the amount of Ca^{2+} released from the sarcoplasmic reticulum (SR) (Fitts, 1994; Allen *et al.*, 2008; Allen *et al.*, 2011). Because H^+ and P_i decrease myofibrillar Ca^{2+} sensitivity, the reduced Ca^{2+} release into the myoplasm exacerbates the effects of these ions on cross-bridge function (Palmer & Kentish, 1994; Debold *et al.*, 2006; Allen *et al.*, 2011; Allen & Trajanovska, 2012; Nelson & Fitts, 2014; Debold, 2016; Debold *et al.*, 2016). Thus, studies that test the effects of H^+ and P_i on force, velocity, and peak power at submaximal Ca^{2+} compared to the saturating levels used in chapters 3 and 4 are likely more representative of the fatigue environment *in vivo.* In addition, recent studies have found that compared with young men, fibers from old men have lower endogenous and maximal releasable SR Ca^{2+} (Lamboley *et al.*, 2015) and increased Ca^{2+} leakage from the SR (Lamboley *et al.*, 2016). Although controversial, there are some studies that have also reported an age-related decrease in Ca^{2+} sensitivity in either MHC II fibers (Lamboley *et al.*, 2015) or both MHC I and II fibers (Straight *et al.*, 2018), with other studies showing no age differences in Ca^{2+} sensitivity (Hvid *et al.*, 2011; Hvid *et al.*, 2013). Thus, it is plausible that the age-related increase in fatigability during dynamic exercise is due to greater impairments in Ca^{2+} handling and/or the sensitivity of the myofilaments to Ca^{2+} in old compared to young adults and is worth further investigation.

Along with the studies on Ca^{2+} handling and phosphorylation of the regulatory proteins, future studies could quantify the changes in the intracellular milieu in young and old men and women during high-velocity fatiguing exercise. To my knowledge, the only studies that have measured the intracellular milieu during dynamic exercise in young and

old adults have been on the plantarflexor muscles and report that the decrease in pH and increase in intracellular [P_i] did not differ or was blunted in the old adults (Layec *et al.*, 2013; Layec *et al.*, 2014, 2015). However, it is unclear how an age-related increase of ~37% in the amount of ATP necessary to generate a given amount of mechanical power output (Layec *et al.*, 2015) could lead to a blunted accumulation of metabolic by-products. One possible explanation is that these investigators did not directly measure the force or velocity during the dynamic exercise, but rather, they predicted the power outputs based on the load applied and an assumed displacement (Layec *et al.*, 2013; Layec *et al.*, 2014, 2015). An additional explanation for the blunted accumulation of metabolic by-products with aging might be that the dynamic exercise was performed at slow velocities. It is known that the fatigability of old adults is either similar (Callahan *et al.*, 2009; Dalton *et al.*, 2012; Yoon *et al.*, 2013; Yoon *et al.*, 2015) or less than that of young adults (Lanza *et al.*, 2004) when the contractions are performed at slow velocities, but is greater when the dynamic exercise is performed at high-velocities (Chapter 2) (McNeil & Rice, 2007; Dalton *et al.*, 2010; Callahan & Kent-Braun, 2011; Dalton *et al.*, 2012; Senefeld *et al.*, 2017). Thus, it is plausible that the increased energetic demand during high-velocity concentric contractions (Ryschon *et al.*, 1997; He *et al.*, 2000; Barclay *et al.*, 2010) coupled with the age-related decrease in muscle oxidative capacity and mitochondrial content (Conley *et al.*, 2000; Larsen *et al.*, 2012; Kent & Fitzgerald, 2016; Murgia *et al.*, 2017) is responsible for the increased fatigability with aging. This would manifest as a greater accumulation of metabolic by-products in old compared to young adults during the high-velocity exercise due to an increased reliance on anaerobic metabolic pathways to synthesize ATP. We are currently testing this hypothesis by

measuring the accumulation of metabolic by-products (H^+, P_i, $H_2PO_4^-$) with ^{31}P-MRS in the quadriceps of young and old men and women performing a high-velocity knee extension exercise inside the magnet.

In summary, this dissertation showed that the fatigability of the knee extensor muscles during a high-velocity exercise progressively increased with age and was determined primarily by mechanisms originating within the muscle for both men and women (Chapter 2). It was also shown for the first time that elevated H^+ and P_i are essential mediators of human muscle fatigue by directly inhibiting cross-bridge function. However, the effects of the fatigue-mimicking conditions on cross-bridge function with either a severe (Chapter 3) or a range of elevated levels of H^+ and P_i (Chapter 4) did not differ with age. Future studies that continue investigating the mechanisms for the accelerated loss in power and increased fatigability with aging are necessary to develop evidence-based treatments to improve physical function, mobility, and quality of life in our aging society.

BIBLIOGRAPHY

Ackermann MA & Kontrogianni-Konstantopoulos A. (2011). Myosin binding protein-C: a regulator of actomyosin interaction in striated muscle. *J Biomed Biotechnol* **2011,** 636403.

Adams GR, Foley JM & Meyer RA. (1990). Muscle buffer capacity estimated from pH changes during rest-to-work transitions. *J Appl Physiol (1985)* **69,** 968-972.

Allen DG, Clugston E, Petersen Y, Roder IV, Chapman B & Rudolf R. (2011). Interactions between intracellular calcium and phosphate in intact mouse muscle during fatigue. *J Appl Physiol (1985)* **111,** 358-366.

Allen DG, Lamb GD & Westerblad H. (2008). Skeletal muscle fatigue: Cellular mechanisms. *Physiol Rev* **88,** 287-332.

Allen DG & Trajanovska S. (2012). The multiple roles of phosphate in muscle fatigue. *Front Physiol* **3,** 463.

Amann M, Blain GM, Proctor LT, Sebranek JJ, Pegelow DF & Dempsey JA. (2011). Implications of group III and IV muscle afferents for high-intensity endurance exercise performance in humans. *J Physiol* **589,** 5299-5309.

Barclay CJ, Woledge RC & Curtin NA. (2010). Is the efficiency of mammalian (mouse) skeletal muscle temperature dependent? *J Physiol* **588,** 3819-3831.

Barnes WS. (1980). The relationship between maximum isometric strength and intramuscular circulatory occlusion. *Ergonomics* **23,** 351-357.

Bassey EJ, Fiatarone MA, O'Neill EF, Kelly M, Evans WJ & Lipsitz LA. (1992). Leg extensor power and functional performance in very old men and women. *Clin Sci (Lond)* **82,** 321-327.

Bergstrom J. (1962). Muscle electrolytes in man. *Scand J Clin Lab Invest* **68,** 1–110.

Bigland-Ritchie BR, Dawson NJ, Johansson RS & Lippold OCJ. (1986). Reflex origin for the slowing of motoneuron firing rates in fatigue of human voluntary contractions. *J Physiol* **379,** 451-459.

Billaut F & Bishop DJ. (2012). Mechanical work accounts for sex differences in fatigue during repeated sprints. *Eur J Appl Physiol* **112,** 1429-1436.

Bilodeau M, Henderson TK, Nolta BE, Pursley PJ & Sandfort GL. (2001). Effect of aging on fatigue characteristics of elbow flexor muscles during sustained submaximal contraction. *J Appl Physiol (1985)* **91,** 2654-2664.

Brenner B & Eisenberg E. (1986). Rate of force generation in muscle: correlation with actomyosin ATPase activity in solution. *Proc Natl Acad Sci U S A* **83,** 3542-3546.

Brocca L, McPhee JS, Longa E, Canepari M, Seynnes O, De Vito G, Pellegrino MA, Narici M & Bottinelli R. (2017). Structure and function of human muscle fibres and muscle proteome in physically active older men. *J Physiol* **595,** 4823-4844.

Broxterman RM, Ade CJ, Wilcox SL, Schlup SJ, Craig JC & Barstow TJ. (2014). Influence of duty cycle on the power-duration relationship: observations and potential mechanisms. *Respir Physiol Neurobiol* **192,** 102-111.

Broxterman RM, Layec G, Hureau TJ, Amann M & Richardson RS. (2017). Skeletal muscle bioenergetics during all-out exercise: mechanistic insight into the oxygen uptake slow component and neuromuscular fatigue. *J Appl Physiol (1985)* **122,** 1208-1217.

Burnley M, Vanhatalo A, Fulford J & Jones AM. (2010). Similar metabolic perturbations during all-out and constant force exhaustive exercise in humans: a (31)P magnetic resonance spectroscopy study. *Exp Physiol* **95,** 798-807.

Cady EB, Jones DA, Lynn J & Newham DJ. (1989). Changes in force and intracellular metabolites during fatigue of human skeletal muscle. *J Physiol* **418,** 311-325.

Callahan DM, Foulis SA & Kent-Braun JA. (2009). Age-related fatigue resistance in the knee extensor muscles is specific to contraction mode. *Muscle Nerve* **39,** 692-702.

Callahan DM & Kent-Braun JA. (2011). Effect of old age on human skeletal muscle force-velocity and fatigue properties. *J Appl Physiol (1985)* **111,** 1345-1352.

Callahan DM, Umberger BR & Kent JA. (2016). Mechanisms of in vivo muscle fatigue in humans: investigating age-related fatigue resistance with a computational model. *J Physiol* **594,** 3407-3421.

Campbell MJ, McComas AJ & Petito F. (1973). Physiological changes in ageing muscles. *J Neurol Neurosurg Psychiatry* **36,** 174-182.

Candow DG & Chilibeck PD. (2005). Differences in size, strength, and power of upper and lower body muscle groups in young and older men. *J Gerontol A Biol Sci Med Sci* **60,** 148-156.

Caremani M, Melli L, Dolfi M, Lombardi V & Linari M. (2013). The working stroke of the myosin II motor in muscle is not tightly coupled to release of orthophosphate from its active site. *J Physiol* **591,** 5187-5205.

Caremani M, Melli L, Dolfi M, Lombardi V & Linari M. (2015). Force and number of myosin motors during muscle shortening and the coupling with the release of the ATP hydrolysis products. *J Physiol* **593,** 3313-3332.

Chase PB & Kushmerick MJ. (1988). Effects of pH on contraction of rabbit fast and slow skeletal muscle fibers. *Biophys J* **53,** 935-946.

Chidnok W, Fulford J, Bailey SJ, Dimenna FJ, Skiba PF, Vanhatalo A & Jones AM. (2013). Muscle metabolic determinants of exercise tolerance following exhaustion: relationship to the "critical power". *J Appl Physiol (1985)* **115,** 243-250.

Christie A, Snook EM & Kent-Braun JA. (2011). Systematic review and meta-analysis of skeletal muscle fatigue in old age. *Med Sci Sports Exerc* **43,** 568-577.

Chung LH, Callahan DM & Kent-Braun JA. (2007). Age-related resistance to skeletal muscle fatigue is preserved during ischemia. *J Appl Physiol (1985)* **103,** 1628-1635.

Clark BC & Taylor JL. (2011). Age-related changes in motor cortical properties and voluntary activation of skeletal muscle. *Curr Aging Sci* **4,** 192-199.

Coggan AR, Spina RJ, King DS, Rogers MA, Brown M, Nemeth PM & Holloszy JO. (1992). Histochemical and enzymatic comparison of the gastrocnemius muscle of young and elderly men and women. *J Gerontol* **47,** B71-76.

Conley KE, Jubrias SA, Amara CE & Marcinek DJ. (2007). Mitochondrial dysfunction: impact on exercise performance and cellular aging. *Exerc Sport Sci Rev* **35,** 43-49.

Conley KE, Jubrias SA & Esselman PC. (2000). Oxidative capacity and ageing in human muscle. *J Physiol* **526 Pt 1,** 203-210.

Cooke R, Franks K, Luciani GB & Pate E. (1988). The inhibition of rabbit skeletal muscle contraction by hydrogen ions and phosphate. *J Physiol* **395,** 77-97.

Coupland ME, Puchert E & Ranatunga KW. (2001). Temperature dependence of active tension in mammalian (rabbit psoas) muscle fibres: effect of inorganic phosphate. *J Physiol* **536,** 879-891.

D'Antona G, Pellegrino MA, Adami R, Rossi R, Carlizzi CN, Canepari M, Saltin B & Bottinelli R. (2003). The effect of ageing and immobilization on structure and function of human skeletal muscle fibres. *J Physiol* **552,** 499-511.

Dalton BH, Power GA, Vandervoort AA & Rice CL. (2010). Power loss is greater in old men than young men during fast plantar flexion contractions. *J Appl Physiol (1985)* **109,** 1441-1447.

Dalton BH, Power GA, Vandervoort AA & Rice CL. (2012). The age-related slowing of voluntary shortening velocity exacerbates power loss during repeated fast knee extensions. *Exp Gerontol* **47,** 85-92.

Dantzig JA, Goldman YE, Millar NC, Lacktis J & Homsher E. (1992). Reversal of the cross-bridge force-generating transition by photogeneration of phosphate in rabbit psoas muscle fibres. *J Physiol* **451,** 247-278.

De Ruiter CJ, Didden WJ, Jones DA & Haan AD. (2000). The force-velocity relationship of human adductor pollicis muscle during stretch and the effects of fatigue. *J Physiol* **526 Pt 3,** 671-681.

Debold EP. (2016). Decreased Myofilament Calcium Sensitivity Plays a Significant Role in Muscle Fatigue. *Exerc Sport Sci Rev* **44,** 144-149.

Debold EP, Dave H & Fitts RH. (2004). Fiber type and temperature dependence of inorganic phosphate: implications for fatigue. *Am J Physiol Cell Physiol* **287,** C673-681.

Debold EP, Fitts RH, Sundberg CW & Nosek TM. (2016). Muscle fatigue from the perspective of a single crossbridge. *Med Sci Sports Exerc* **48,** 2270-2280.

Debold EP, Longyear TJ & Turner MA. (2012). The effects of phosphate and acidosis on regulated thin-filament velocity in an in vitro motility assay. *J Appl Physiol (1985)* **113,** 1413-1422.

Debold EP, Romatowski J & Fitts RH. (2006). The depressive effect of Pi on the force-pCa relationship in skinned single muscle fibers is temperature dependent. *Am J Physiol Cell Physiol* **290,** C1041-1050.

Debold EP, Walcott S, Woodward M & Turner MA. (2013). Direct observation of phosphate inhibiting the force-generating capacity of a miniensemble of Myosin molecules. *Biophys J* **105,** 2374-2384.

Di Lazzaro V, Restuccia D, Oliviero A, Profice P, Ferrara L, Insola A, Mazzone P, Tonali P & Rothwell JC. (1998). Effects of voluntary contraction on descending volleys evoked by transcranial stimulation in conscious humans. *J Physiol* **508 (Pt 2),** 625-633.

Ditor DS & Hicks AL. (2000). The effect of age and gender on the relative fatigability of the human adductor pollicis muscle. *Can J Physiol Pharmacol* **78,** 781-790.

Doherty TJ. (2003). Invited review: Aging and sarcopenia. *J Appl Physiol (1985)* **95,** 1717-1727.

Doherty TJ, Vandervoort AA, Taylor AW & Brown WF. (1993). Effects of motor unit losses on strength in older men and women. *J Appl Physiol (1985)* **74,** 868-874.

Drake JC & Yan Z. (2017). Mitophagy in maintaining skeletal muscle mitochondrial proteostasis and metabolic health with ageing. *J Physiol* **595,** 6391-6399.

Edman KA. (1979). The velocity of unloaded shortening and its relation to sarcomere length and isometric force in vertebrate muscle fibres. *J Physiol* **291,** 143-159.

Edman KA. (2005). Contractile properties of mouse single muscle fibers, a comparison with amphibian muscle fibers. *J Exp Biol* **208,** 1905-1913.

Fabiato A. (1988). Computer programs for calculating total from specified free or free from specified total ionic concentrations in aqueous solutions containing multiple metals and ligands. *Methods Enzymol* **157,** 378-417.

Fabiato A & Fabiato F. (1979). Calculator programs for computing the composition of the solutions containing multiple metals and ligands used for experiments in skinned muscle cells. *J Physiol (Paris)* **75,** 463-505.

Fiedler GB, Schmid AI, Goluch S, Schewzow K, Laistler E, Niess F, Unger E, Wolzt M, Mirzahosseini A, Kemp GJ, Moser E & Meyerspeer M. (2016). Skeletal muscle ATP synthesis and cellular H(+) handling measured by localized (31)P-MRS during exercise and recovery. *Sci Rep* **6,** 32037.

Fitts RH. (1994). Cellular mechanisms of muscle fatigue. *Physiol Rev* **74,** 49-94.

Fitts RH. (2008). The cross-bridge cycle and skeletal muscle fatigue. *J Appl Physiol (1985)* **104,** 551-558.

Fitts RH. (2016). The Role of Acidosis in Fatigue: Pro Perspective. *Med Sci Sports Exerc* **48,** 2335-2338.

Folstein MF, Folstein SE & McHugh PR. (1975). "Mini-mental state". A practical method for grading the cognitive state of patients for the clinician. *J Psychiatr Res* **12,** 189-198.

Foulis SA, Jones SL, van Emmerik RE & Kent JA. (2017). Post-fatigue recovery of power, postural control and physical function in older women. *PLoS One* **12,** e0183483.

Frontera WR, Hughes VA, Fielding RA, Fiatarone MA, Evans WJ & Roubenoff R. (2000a). Aging of skeletal muscle: a 12-yr longitudinal study. *J Appl Physiol (1985)* **88,** 1321-1326.

Frontera WR, Reid KF, Phillips EM, Krivickas LS, Hughes VA, Roubenoff R & Fielding RA. (2008). Muscle fiber size and function in elderly humans: a longitudinal study. *J Appl Physiol (1985)* **105,** 637-642.

Frontera WR, Suh D, Krivickas LS, Hughes VA, Goldstein R & Roubenoff R. (2000b). Skeletal muscle fiber quality in older men and women. *Am J Physiol Cell Physiol* **279,** C611-618.

Fryer MW, Owen VJ, Lamb GD & Stephenson DG. (1995). Effects of creatine phosphate and P(i) on Ca2+ movements and tension development in rat skinned skeletal muscle fibres. *J Physiol* **482 (Pt 1),** 123-140.

Fuglevand AJ, Zackowski KM, Huey KA & Enoka RM. (1993). Impairment of neuromuscular propagation during human fatiguing contractions at submaximal forces. *J Physiol* **460,** 549-572.

Gandevia SC. (2001). Spinal and supraspinal factors in human muscle fatigue. *Physiol Rev* **81,** 1725-1789.

Geeves MA, Fedorov R & Manstein DJ. (2005). Molecular mechanism of actomyosin-based motility. *Cell Mol Life Sci* **62,** 1462-1477.

Giulian GG, Moss RL & Greaser M. (1983). Improved methodology for analysis and quantitation of proteins on one-dimensional silver-stained slab gels. *Anal Biochem* **129,** 277-287.

Godt RE & Nosek TM. (1989). Changes of intracellular milieu with fatigue or hypoxia depress contraction of skinned rabbit skeletal and cardiac muscle. *J Physiol* **412,** 155-180.

Grosicki GJ, Standley RA, Murach KA, Raue U, Minchev K, Coen PM, Newman AB, Cummings S, Harris T, Kritchevsky S, Goodpaster BH & Trappe S. (2016). Improved single muscle fiber quality in the oldest-old. *J Appl Physiol (1985)* **121,** 878-884.

Hart TL, Swartz AM, Cashin SE & Strath SJ. (2011). How many days of monitoring predict physical activity and sedentary behaviour in older adults? *Int J Behav Nutr Phys Act* **8,** 62.

Hassanlouei H, Sundberg CW, Smith AE, Kuplic A & Hunter SK. (2017). Physical activity modulates corticospinal excitability of the lower limb in young and old adults. *J Appl Physiol (1985)* **123,** 364-374.

He ZH, Bottinelli R, Pellegrino MA, Ferenczi MA & Reggiani C. (2000). ATP consumption and efficiency of human single muscle fibers with different myosin isoform composition. *Biophys J* **79,** 945-961.

Hepple RT & Rice CL. (2016). Innervation and neuromuscular control in ageing skeletal muscle. *J Physiol* **594,** 1965-1978.

Hermansen L & Osnes JB. (1972). Blood and muscle pH after maximal exercise in man. *J Appl Physiol* **32,** 304-308.

Hill AV. (1938). The heat of shortening and the dynamic constants of muscle. *Proc R Soc Lond B Biol Sci* **126,** 136-195.

Hogan MC, Richardson RS & Haseler LJ. (1999). Human muscle performance and PCr hydrolysis with varied inspired oxygen fractions: a P-31-MRS study. *J Appl Physiol (1985)* **86,** 1367-1373.

Hortobagyi T, Mizelle C, Beam S & DeVita P. (2003). Old adults perform activities of daily living near their maximal capabilities. *J Gerontol A Biol Sci Med Sci* **58,** M453-460.

Hunter SK. (2017). Performance Fatigability: Mechanisms and Task Specificity. *Cold Spring Harb Perspect Med*.

Hunter SK, Butler JE, Todd G, Gandevia SC & Taylor JL. (2006). Supraspinal fatigue does not explain the sex difference in muscle fatigue of maximal contractions. *J Appl Physiol (1985)* **101,** 1036-1044.

Hunter SK, Critchlow A & Enoka RM. (2004). Influence of aging on sex differences in muscle fatigability. *J Appl Physiol (1985)* **97,** 1723-1732.

Hunter SK, Critchlow A & Enoka RM. (2005). Muscle endurance is greater for old men compared with strength-matched young men. *J Appl Physiol (1985)* **99,** 890-897.

Hunter SK, Pereira HM & Keenan KG. (2016). The aging neuromuscular system and motor performance. *J Appl Physiol (1985)* **121,** 982-995.

Hunter SK, Thompson MW & Adams RD. (2000). Relationships among age-associated strength changes and physical activity level, limb dominance, and muscle group in women. *J Gerontol A Biol Sci Med Sci* **55,** B264-273.

Hunter SK, Thompson MW, Ruell PA, Harmer AR, Thom JM, Gwinn TH & Adams RD. (1999). Human skeletal sarcoplasmic reticulum Ca2+ uptake and muscle function with aging and strength training. *J Appl Physiol (1985)* **86,** 1858-1865.

Hunter SK, Todd G, Butler JE, Gandevia SC & Taylor JL. (2008). Recovery from supraspinal fatigue is slowed in old adults after fatiguing maximal isometric contractions. *J Appl Physiol (1985)* **105,** 1199-1209.

Hvid LG, Ortenblad N, Aagaard P, Kjaer M & Suetta C. (2011). Effects of ageing on single muscle fibre contractile function following short-term immobilisation. *J Physiol* **589,** 4745-4757.

Hvid LG, Suetta C, Aagaard P, Kjaer M, Frandsen U & Ortenblad N. (2013). Four days of muscle disuse impairs single fiber contractile function in young and old healthy men. *Exp Gerontol* **48,** 154-161.

Jacobsen LA, Mather M, Lee M, Kent M. (2011). America's aging population. *Population Bulletin* **66,** 2-16.

Jakobsson F, Borg K & Edstrom L. (1990). Fibre-type composition, structure and cytoskeletal protein location of fibres in anterior tibial muscle. Comparison between young adults and physically active aged humans. *Acta Neuropathol* **80,** 459-468.

Jones AM, Wilkerson DP, DiMenna F, Fulford J & Poole DC. (2008). Muscle metabolic responses to exercise above and below the "critical power" assessed using 31P-MRS. *Am J Physiol Regul Integr Comp Physiol* **294,** R585-593.

Jones DA. (2010). Changes in the force-velocity relationship of fatigued muscle: implications for power production and possible causes. *J Physiol* **588,** 2977-2986.

Jones DA, de Ruiter CJ & de Haan A. (2006). Change in contractile properties of human muscle in relationship to the loss of power and slowing of relaxation seen with fatigue. *J Physiol* **576,** 913-922.

Justice JN, Mani D, Pierpoint LA & Enoka RM. (2014). Fatigability of the dorsiflexors and associations among multiple domains of motor function in young and old adults. *Exp Gerontol* **55,** 92-101.

Karatzaferi C, Franks-Skiba K & Cooke R. (2008). Inhibition of shortening velocity of skinned skeletal muscle fibers in conditions that mimic fatigue. *Am J Physiol Regul Integr Comp Physiol* **294,** R948-955.

Kemp GJ, Meyerspeer M & Moser E. (2007). Absolute quantification of phosphorus metabolite concentrations in human muscle in vivo by 31P MRS: a quantitative review. *NMR Biomed* **20,** 555-565.

Kennedy DS, McNeil CJ, Gandevia SC & Taylor JL. (2016). Effects of fatigue on corticospinal excitability of the human knee extensors. *Exp Physiol* **101,** 1552-1564.

Kent JA & Fitzgerald LF. (2016). In vivo mitochondrial function in aging skeletal muscle: capacity, flux, and patterns of use. *J Appl Physiol (1985)* **121,** 996-1003.

Kent-Braun JA. (2009). Skeletal muscle fatigue in old age: whose advantage? *Exerc Sport Sci Rev* **37,** 3-9.

Kent-Braun JA, Fitts RH & Christie A. (2012). Skeletal Muscle Fatigue. *Compr Physiol* **2,** 997-1044.

Kent-Braun JA, Ng AV, Doyle JW & Towse TF. (2002). Human skeletal muscle responses vary with age and gender during fatigue due to incremental isometric exercise. *J Appl Physiol (1985)* **93,** 1813-1823.

Kent-Braun JA, Ng AV & Young K. (2000). Skeletal muscle contractile and noncontractile components in young and older women and men. *J Appl Physiol (1985)* **88,** 662-668.

Klass M, Baudry S & Duchateau J. (2007). Voluntary activation during maximal contraction with advancing age: a brief review. *Eur J Appl Physiol* **100,** 543-551.

Klein CS, Marsh GD, Petrella RJ & Rice CL. (2003). Muscle fiber number in the biceps brachii muscle of young and old men. *Muscle Nerve* **28,** 62-68.

Klitgaard H, Mantoni M, Schiaffino S, Ausoni S, Gorza L, Laurent-Winter C, Schnohr P & Saltin B. (1990). Function, morphology and protein expression of ageing skeletal muscle: a cross-sectional study of elderly men with different training backgrounds. *Acta Physiol Scand* **140,** 41-54.

Knuth ST, Dave H, Peters JR & Fitts RH. (2006). Low cell pH depresses peak power in rat skeletal muscle fibres at both 30 degrees C and 15 degrees C: implications for muscle fatigue. *J Physiol* **575,** 887-899.

Korhonen MT, Cristea A, Alen M, Hakkinen K, Sipila S, Mero A, Viitasalo JT, Larsson L & Suominen H. (2006). Aging, muscle fiber type, and contractile function in sprint-trained athletes. *J Appl Physiol (1985)* **101,** 906-917.

Kosek DJ, Kim JS, Petrella JK, Cross JM & Bamman MM. (2006). Efficacy of 3 days/wk resistance training on myofiber hypertrophy and myogenic mechanisms in young vs. older adults. *J Appl Physiol (1985)* **101,** 531-544.

Krivickas LS, Suh D, Wilkins J, Hughes VA, Roubenoff R & Frontera WR. (2001). Age- and gender-related differences in maximum shortening velocity of skeletal muscle fibers. *Am J Phys Med Rehabil* **80,** 447-455; quiz 456-447.

Lamboley CR, Wyckelsma VL, Dutka TL, McKenna MJ, Murphy RM & Lamb GD. (2015). Contractile properties and sarcoplasmic reticulum calcium content in type I and type II skeletal muscle fibres in active aged humans. *J Physiol* **593,** 2499-2514.

Lamboley CR, Wyckelsma VL, McKenna MJ, Murphy RM & Lamb GD. (2016). Ca(2+) leakage out of the sarcoplasmic reticulum is increased in type I skeletal muscle fibres in aged humans. *J Physiol* **594,** 469-481.

Lanza IR, Befroy DE & Kent-Braun JA. (2005). Age-related changes in ATP-producing pathways in human skeletal muscle in vivo. *Journal of Applied Physiology* **99,** 1736-1744.

Lanza IR, Larsen RG & Kent-Braun JA. (2007). Effects of old age on human skeletal muscle energetics during fatiguing contractions with and without blood flow. *J Physiol* **583,** 1093-1105.

Lanza IR, Russ DW & Kent-Braun JA. (2004). Age-related enhancement of fatigue resistance is evident in men during both isometric and dynamic tasks. *J Appl Physiol (1985)* **97,** 967-975.

Lanza IR, Towse TF, Caldwell GE, Wigmore DM & Kent-Braun JA. (2003). Effects of age on human muscle torque, velocity, and power in two muscle groups. *J Appl Physiol (1985)* **95,** 2361-2369.

Larsen RG, Callahan DM, Foulis SA & Kent-Braun JA. (2012). Age-related changes in oxidative capacity differ between locomotory muscles and are associated with physical activity behavior. *Appl Physiol Nutr Metab* **37,** 88-99.

Larsson L, Li X & Frontera WR. (1997). Effects of aging on shortening velocity and myosin isoform composition in single human skeletal muscle cells. *Am J Physiol* **272,** C638-649.

Laurent CM, Green JM, Bishop PA, Sjokvist J, Schumacker RE, Richardson MT & Curtner-Smith M. (2010). Effect of gender on fatigue and recovery following maximal intensity repeated sprint performance. *J Sports Med Phys Fitness* **50,** 243-253.

Law TD, Clark LA & Clark BC. (2016). Resistance Exercise to Prevent and Manage Sarcopenia and Dynapenia. *Annu Rev Gerontol Geriatr* **36,** 205-228.

Lawson JW & Veech RL. (1979). Effects of pH and free Mg2+ on the Keq of the creatine kinase reaction and other phosphate hydrolyses and phosphate transfer reactions. *J Biol Chem* **254,** 6528-6537.

Layec G, Haseler LJ & Richardson RS. (2013). Reduced muscle oxidative capacity is independent of O2 availability in elderly people. *Age (Dordr)* **35,** 1183-1192.

Layec G, Trinity JD, Hart CR, Kim SE, Groot HJ, Le Fur Y, Sorensen JR, Jeong EK & Richardson RS. (2014). In vivo evidence of an age-related increase in ATP cost of contraction in the plantar flexor muscles. *Clin Sci (Lond)* **126,** 581-592.

Layec G, Trinity JD, Hart CR, Kim SE, Groot HJ, Le Fur Y, Sorensen JR, Jeong EK & Richardson RS. (2015). Impact of age on exercise-induced ATP supply during

supramaximal plantar flexion in humans. *Am J Physiol Regul Integr Comp Physiol* **309,** R378-388.

Lexell J. (1995). Human aging, muscle mass, and fiber type composition. *J Gerontol A Biol Sci Med Sci* **50 Spec No,** 11-16.

Lexell J & Downham D. (1992). What is the effect of ageing on type 2 muscle fibres? In *J Neurol Sci*, pp. 250-251. Netherlands.

Lexell J, Henriksson-Larsen K, Winblad B & Sjostrom M. (1983). Distribution of different fiber types in human skeletal muscles: effects of aging studied in whole muscle cross sections. *Muscle Nerve* **6,** 588-595.

Lexell J & Taylor CC. (1991). Variability in muscle fibre areas in whole human quadriceps muscle: effects of increasing age. *J Anat* **174,** 239-249.

Lexell J, Taylor CC & Sjostrom M. (1988). What is the cause of the ageing atrophy? Total number, size and proportion of different fiber types studied in whole vastus lateralis muscle from 15- to 83-year-old men. *J Neurol Sci* **84,** 275-294.

Linari M, Caremani M & Lombardi V. (2010). A kinetic model that explains the effect of inorganic phosphate on the mechanics and energetics of isometric contraction of fast skeletal muscle. *Proc Biol Sci* **277,** 19-27.

Maden-Wilkinson TM, Degens H, Jones DA & McPhee JS. (2013). Comparison of MRI and DXA to measure muscle size and age-related atrophy in thigh muscles. *J Musculoskelet Neuronal Interact* **13,** 320-328.

Marner L, Nyengaard JR, Tang Y & Pakkenberg B. (2003). Marked loss of myelinated nerve fibers in the human brain with age. *J Comp Neurol* **462,** 144-152.

Martin KR, Koster A, Murphy RA, Van Domelen DR, Hung MY, Brychta RJ, Chen KY & Harris TB. (2014). Changes in daily activity patterns with age in U.S. men and women: National Health and Nutrition Examination Survey 2003-04 and 2005-06. *J Am Geriatr Soc* **62,** 1263-1271.

McNeil CJ, Butler JE, Taylor JL & Gandevia SC. (2013). Testing the excitability of human motoneurons. *Front Hum Neurosci* **7,** 152.

McNeil CJ & Rice CL. (2007). Fatigability is increased with age during velocity-dependent contractions of the dorsiflexors. *J Gerontol A Biol Sci Med Sci* **62,** 624-629.

Metzger JM, Greaser ML & Moss RL. (1989). Variations in cross-bridge attachment rate and tension with phosphorylation of myosin in mammalian skinned skeletal muscle

fibers. Implications for twitch potentiation in intact muscle. *J Gen Physiol* **93,** 855-883.

Metzger JM & Moss RL. (1987). Greater hydrogen ion-induced depression of tension and velocity in skinned single fibres of rat fast than slow muscles. *J Physiol* **393,** 727-742.

Metzger JM & Moss RL. (1990a). Calcium-sensitive cross-bridge transitions in mammalian fast and slow skeletal muscle fibers. *Science* **247,** 1088-1090.

Metzger JM & Moss RL. (1990b). pH modulation of the kinetics of a Ca2(+)-sensitive cross-bridge state transition in mammalian single skeletal muscle fibres. *J Physiol* **428,** 751-764.

Miller MS, Bedrin NG, Ades PA, Palmer BM & Toth MJ. (2015). Molecular determinants of force production in human skeletal muscle fibers: effects of myosin isoform expression and cross-sectional area. *Am J Physiol Cell Physiol* **308,** C473-484.

Miller MS, Bedrin NG, Callahan DM, Previs MJ, Jennings ME, 2nd, Ades PA, Maughan DW, Palmer BM & Toth MJ. (2013). Age-related slowing of myosin actin cross-bridge kinetics is sex specific and predicts decrements in whole skeletal muscle performance in humans. *J Appl Physiol (1985)* **115,** 1004-1014.

Miller MS & Toth MJ. (2013). Myofilament protein alterations promote physical disability in aging and disease. *Exerc Sport Sci Rev* **41,** 93-99.

Moss RL. (1979). Sarcomere length-tension relations of frog skinned muscle fibres during calcium activation at short lengths. *J Physiol* **292,** 177-192.

Murgia M, Toniolo L, Nagaraj N, Ciciliot S, Vindigni V, Schiaffino S, Reggiani C & Mann M. (2017). Single Muscle Fiber Proteomics Reveals Fiber-Type-Specific Features of Human Muscle Aging. *Cell Rep* **19,** 2396-2409.

Nelson CR, Debold EP & Fitts RH. (2014). Phosphate and acidosis act synergistically to depress peak power in rat muscle fibers. *Am J Physiol Cell Physiol* **307,** C939-C950.

Nelson CR & Fitts RH. (2014). Effects of low cell pH and elevated inorganic phosphate on the pCa-force relationship in single muscle fibers at near-physiological temperatures. *Am J Physiol Cell Physiol* **306,** C670-678.

Nosek TM, Fender KY & Godt RE. (1987). It is diprotonated inorganic phosphate that depresses force in skinned skeletal muscle fibers. *Science* **236,** 191-193.

Palmer S & Kentish JC. (1994). The role of troponin C in modulating the Ca2+ sensitivity of mammalian skinned cardiac and skeletal muscle fibres. *J Physiol* **480 (Pt 1),** 45-60.

Parsons B, Szczesna D, Zhao J, Van Slooten G, Kerrick WG, Putkey JA & Potter JD. (1997). The effect of pH on the Ca2+ affinity of the Ca2+ regulatory sites of skeletal and cardiac troponin C in skinned muscle fibres. *J Muscle Res Cell Motil* **18,** 599-609.

Pate E, Bhimani M, Franks-Skiba K & Cooke R. (1995). Reduced effect of pH on skinned rabbit psoas muscle mechanics at high temperatures: implications for fatigue. *J Physiol* **486 (Pt 3),** 689-694.

Pate E & Cooke R. (1989). Addition of phosphate to active muscle fibers probes actomyosin states within the powerstroke. *Pflugers Arch* **414,** 73-81.

Pathare N, Walter GA, Stevens JE, Yang Z, Okerke E, Gibbs JD, Esterhai JL, Scarborough MT, Gibbs CP, Sweeney HL & Vandenborne K. (2005). Changes in inorganic phosphate and force production in human skeletal muscle after cast immobilization. *J Appl Physiol (1985)* **98,** 307-314.

Petrella JK, Kim JS, Tuggle SC, Hall SR & Bamman MM. (2005). Age differences in knee extension power, contractile velocity, and fatigability. *J Appl Physiol (1985)* **98,** 211-220.

Potma EJ, van Graas IA & Stienen GJ. (1995). Influence of inorganic phosphate and pH on ATP utilization in fast and slow skeletal muscle fibers. *Biophys J* **69,** 2580-2589.

Power GA, Minozzo FC, Spendiff S, Filion ME, Konokhova Y, Purves-Smith MF, Pion C, Aubertin-Leheudre M, Morais JA, Herzog W, Hepple RT, Taivassalo T & Rassier DE. (2016). Reduction in single muscle fiber rate of force development with aging is not attenuated in world class older masters athletes. *Am J Physiol Cell Physiol* **310,** C318-327.

Purves-Smith FM, Sgarioto N & Hepple RT. (2014). Fiber typing in aging muscle. *Exerc Sport Sci Rev* **42,** 45-52.

Rassier DE & Macintosh BR. (2000). Coexistence of potentiation and fatigue in skeletal muscle. *Braz J Med Biol Res* **33,** 499-508.

Raue U, Slivka D, Minchev K & Trappe S. (2009). Improvements in whole muscle and myocellular function are limited with high-intensity resistance training in octogenarian women. *J Appl Physiol (1985)* **106,** 1611-1617.

Reid KF & Fielding RA. (2012). Skeletal muscle power: a critical determinant of physical functioning in older adults. *Exerc Sport Sci Rev* **40,** 4-12.

Robergs RA, Ghiasvand F & Parker D. (2004). Biochemistry of exercise-induced metabolic acidosis. *Am J Physiol Regul Integr Comp Physiol* **287,** R502-516.

Rodriguez-Falces J & Place N. (2017). Determinants, analysis and interpretation of the muscle compound action potential (M wave) in humans: implications for the study of muscle fatigue. *Eur J Appl Physiol*.

Round JM, Jones DA, Chapman SJ, Edwards RH, Ward PS & Fodden DL. (1984). The anatomy and fibre type composition of the human adductor pollicis in relation to its contractile properties. *J Neurol Sci* **66,** 263-272.

Rozand V, Senefeld JW, Hassanlouei H & Hunter SK. (2017). Voluntary activation and variability during maximal dynamic contractions with aging. *Eur J Appl Physiol* **117,** 2493-2507.

Russ DW, Gregg-Cornell K, Conaway MJ & Clark BC. (2012). Evolving concepts on the age-related changes in "muscle quality". *J Cachexia Sarcopenia Muscle* **3,** 95-109.

Ryschon TW, Fowler MD, Wysong RE, Anthony A & Balaban RS. (1997). Efficiency of human skeletal muscle in vivo: comparison of isometric, concentric, and eccentric muscle action. *J Appl Physiol (1985)* **83,** 867-874.

Sadamoto T, Bonde-Petersen F & Suzuki Y. (1983). Skeletal muscle tension, flow, pressure, and EMG during sustained isometric contractions in humans. *Eur J Appl Physiol Occup Physiol* **51,** 395-408.

Sahlin K, Tonkonogi M & Soderlund K. (1998). Energy supply and muscle fatigue in humans. *Acta Physiologica Scandinavica* **162,** 261-266.

Salat DH, Buckner RL, Snyder AZ, Greve DN, Desikan RS, Busa E, Morris JC, Dale AM & Fischl B. (2004). Thinning of the cerebral cortex in aging. *Cereb Cortex* **14,** 721-730.

Schiaffino S. (2010). Fibre types in skeletal muscle: a personal account. *Acta Physiol (Oxf)* **199,** 451-463.

Schiaffino S & Reggiani C. (2011). Fiber types in mammalian skeletal muscles. *Physiol Rev* **91,** 1447-1531.

Schluter JM & Fitts RH. (1994). Shortening velocity and ATPase activity of rat skeletal muscle fibers: effects of endurance exercise training. *Am J Physiol* **266,** C1699-1673.

Seals DR. (2014). Edward F. Adolph Distinguished Lecture: The remarkable anti-aging effects of aerobic exercise on systemic arteries. *Journal of Applied Physiology* **117,** 425-439.

Seals DR, Justice JN & LaRocca TJ. (2016). Physiological geroscience: targeting function to increase healthspan and achieve optimal longevity. *J Physiol* **594,** 2001-2024.

Segovia G, Porras A, Del Arco A & Mora F. (2001). Glutamatergic neurotransmission in aging: a critical perspective. *Mech Ageing Dev* **122,** 1-29.

Senefeld J, Yoon T & Hunter SK. (2017). Age differences in dynamic fatigability and variability of arm and leg muscles: Associations with physical function. *Exp Gerontol* **87,** 74-83.

Shirokova N, Garcia J, Pizarro G & Rios E. (1996). Ca2+ release from the sarcoplasmic reticulum compared in amphibian and mammalian skeletal muscle. *J Gen Physiol* **107,** 1-18.

Sidhu SK, Bentley DJ & Carroll TJ. (2009). Cortical voluntary activation of the human knee extensors can be reliably estimated using transcranial magnetic stimulation. *Muscle Nerve* **39,** 186-196.

Sjogaard G, Jensen BR, Hargens AR & Sogaard K. (2004). Intramuscular pressure and EMG relate during static contractions but dissociate with movement and fatigue. *J Appl Physiol (1985)* **96,** 1522-1529; discussion.

Sjogaard G, Kiens B, Jorgensen K & Saltin B. (1986). Intramuscular pressure, EMG and blood flow during low-level prolonged static contraction in man. *Acta Physiol Scand* **128,** 475-484.

Sjogaard G, Savard G & Juel C. (1988). Muscle blood flow during isometric activity and its relation to muscle fatigue. *Eur J Appl Physiol Occup Physiol* **57,** 327-335.

Slivka D, Raue U, Hollon C, Minchev K & Trappe S. (2008). Single muscle fiber adaptations to resistance training in old (>80 yr) men: evidence for limited skeletal muscle plasticity. *Am J Physiol Regul Integr Comp Physiol* **295,** R273-280.

Spendiff S, Vuda M, Gouspillou G, Aare S, Perez A, Morais JA, Jagoe RT, Filion ME, Glicksman R, Kapchinsky S, MacMillan NJ, Pion CH, Aubertin-Leheudre M, Hettwer S, Correa JA, Taivassalo T & Hepple RT. (2016). Denervation drives mitochondrial dysfunction in skeletal muscle of octogenarians. *J Physiol* **594,** 7361-7379.

Straight CR, Ades PA, Toth MJ & Miller MS. (2018). Age-related reduction in single muscle fiber calcium sensitivity is associated with decreased muscle power in men and women. *Exp Gerontol* **102,** 84-92.

Sundberg CW & Bundle MW. (2015). Influence of duty cycle on the time course of muscle fatigue and the onset of neuromuscular compensation during exhaustive dynamic isolated limb exercise. *Am J Physiol Regul Integr Comp Physiol* **309,** R51-61.

Sundberg CW, Hunter SK & Bundle MW. (2017). Rates of performance loss and neuromuscular activity in men and women during cycling: evidence for a common metabolic basis of muscle fatigue. *J Appl Physiol (1985)* **122,** 130-141.

Sundberg CW, Kuplic A, Hassanlouei H & Hunter SK. (2018). Mechanisms for the age-related increase in fatigability of the knee extensors in old and very old adults. *J Appl Physiol (1985).*

Szczesna D, Zhao J, Jones M, Zhi G, Stull J & Potter JD. (2002). Phosphorylation of the regulatory light chains of myosin affects Ca2+ sensitivity of skeletal muscle contraction. *J Appl Physiol (1985)* **92,** 1661-1670.

Tesi C, Colomo F, Piroddi N & Poggesi C. (2002). Characterization of the cross-bridge force-generating step using inorganic phosphate and BDM in myofibrils from rabbit skeletal muscles. *J Physiol* **541,** 187-199.

Tevald MA, Foulis SA, Lanza IR & Kent-Braun JA. (2010). Lower energy cost of skeletal muscle contractions in older humans. *Am J Physiol Regul Integr Comp Physiol* **298,** R729-739.

Todd G, Taylor JL, Butler JE, Martin PG, Gorman RB & Gandevia SC. (2007). Use of motor cortex stimulation to measure simultaneously the changes in dynamic muscle properties and voluntary activation in human muscles. *J Appl Physiol (1985)* **102,** 1756-1766.

Todd G, Taylor JL & Gandevia SC. (2003). Measurement of voluntary activation of fresh and fatigued human muscles using transcranial magnetic stimulation. *J Physiol* **551,** 661-671.

Todd G, Taylor JL & Gandevia SC. (2016). Measurement of voluntary activation based on transcranial magnetic stimulation over the motor cortex. *J Appl Physiol (1985)* **121,** 678-686.

Trappe S, Gallagher P, Harber M, Carrithers J, Fluckey J & Trappe T. (2003). Single muscle fibre contractile properties in young and old men and women. *J Physiol* **552,** 47-58.

United Nations. (2017). World Population Ageing 2017 - Highlights (ST/ESA/SER.A/397), ed. Department of Economic and Social Affairs PD.

Vandenboom R. (2016). Modulation of Skeletal Muscle Contraction by Myosin Phosphorylation. *Compr Physiol* **7,** 171-212.

Vandenboom R & Houston ME. (1996). Phosphorylation of myosin and twitch potentiation in fatigued skeletal muscle. *Can J Physiol Pharmacol* **74,** 1315-1321.

Venturelli M, Saggin P, Muti E, Naro F, Cancellara L, Toniolo L, Tarperi C, Calabria E, Richardson RS, Reggiani C & Schena F. (2015). In vivo and in vitro evidence that intrinsic upper- and lower-limb skeletal muscle function is unaffected by ageing and disuse in oldest-old humans. *Acta Physiol (Oxf)* **215,** 58-71.

Wahr PA, Cantor HC & Metzger JM. (1997). Nucleotide-dependent contractile properties of Ca(2+)-activated fast and slow skeletal muscle fibers. *Biophys J* **72,** 822-834.

Wang G & Kawai M. (1997). Force generation and phosphate release steps in skinned rabbit soleus slow-twitch muscle fibers. *Biophys J* **73,** 878-894.

Westerblad H. (2016). Acidosis Is Not a Significant Cause of Skeletal Muscle Fatigue. *Med Sci Sports Exerc* **48,** 2339-2342.

Westerblad H, Bruton JD & Lannergren J. (1997). The effect of intracellular pH on contractile function of intact, single fibres of mouse muscle declines with increasing temperature. *J Physiol* **500 (Pt 1),** 193-204.

Widrick JJ. (2002). Effect of P(i) on unloaded shortening velocity of slow and fast mammalian muscle fibers. *Am J Physiol Cell Physiol* **282,** C647-653.

Widrick JJ, Trappe SW, Costill DL & Fitts RH. (1996). Force-velocity and force-power properties of single muscle fibers from elite master runners and sedentary men. *Am J Physiol* **271,** C676-683.

Wilson JR, McCully KK, Mancini DM, Boden B & Chance B. (1988). Relationship of muscular fatigue to pH and diprotonated Pi in humans: a 31P-NMR study. *J Appl Physiol (1985)* **64,** 2333-2339.

Yoon T, Doyel R, Widule C & Hunter SK. (2015). Sex differences with aging in the fatigability of dynamic contractions. *Exp Gerontol* **70,** 1-10.

Yoon T, Schlinder-Delap B & Hunter SK. (2013). Fatigability and recovery of arm muscles with advanced age for dynamic and isometric contractions. *Exp Gerontol* **48,** 259-268.

Yoon T, Schlinder-Delap B, Keller ML & Hunter SK. (2012). Supraspinal fatigue impedes recovery from a low-intensity sustained contraction in old adults. *J Appl Physiol (1985)* **112,** 849-858.